TITLE PAGE

IDENTIFICATION OF NOVEL PATHWAYS THAT PROMOTE ANOIKIS THROUGH GENOME-WIDE SCREENS

A Dissertation Presented

By

VICTORIA ELIZABETH PEDANOU

Submitted to the Faculty of the
University of Massachusetts Graduate School of Biomedical Sciences, Worcester
in partial fulfillment of the requirements for the degree of

DOCTOR OF PHILOSOPHY

OCTOBER 14TH, 2016

CANCER BIOLOGY

SIGNATURE PAGE

IDENTIFICATION OF NOVEL PATHWAYS THAT PROMOTE ANOIKIS THROUGH GENOME-WIDE SCREENS

A Dissertation Presented
By
VICTORIA ELIZABETH PEDANOU

This work was undertaken in the Graduate School of Biomedical Sciences
Cancer Biology

The signature of the Thesis Advisor signifies validation of Dissertation content

_____
Michael R. Green, Thesis Advisor

The signatures of the Dissertation Defense Committee signify completion and approval as to style and content of the Dissertation

_____
Eric H. Baehrecke, Member of Committee

_____
Sharon B. Cantor, Member of Committee

_____
Brian C. Lewis, Member of Committee

_____
Joan S. Brugge External Member of Committee

The signature of the Chair of the Committee signifies that the written dissertation meets the requirements of the Dissertation Committee

_____
Arthur M. Mercurio, Chair of Committee

The signature of the Dean of the Graduate School of Biomedical Sciences signifies that the student has met all graduation requirements of the School.

_____
Anthony Carruthers, Ph.D., Dean of the Graduate School of Biomedical Sciences
October 14th, 2016

DEDICATION

This thesis is dedicated to my family and friends who have unconditionally supported me through my 8 years of graduate school and to my son, Macaire. Especially to my parents, Joe and Kristy Ruhl, who have supported me through my 30+ years of education, I would not be where I am today without them. I also specifically dedicate this thesis to my Nana, Dana Shouse, who takes the time to understand my research and read every article about science that I show her. Finally, for my husband Bo who has been my main support group since my first year of graduate school. I would be lost without him.

ACKNOWLEDGEMENTS

First and foremost, I must acknowledge my thesis advisor, Michael R. Green. Michael has provided me with advice and support on my research projects for the last 8 years and has allowed me to develop my scientific and research skills. I am the scientist I am today because of Michael's mentorship. When I joined the lab as a rotation student a post doc in the lab, Stephane Gobeil, was my direct mentor. I learned much of what I based my research on from Stephane and I am grateful for his help and advice. He also started the work on anoikis in the lab, which I continued when he took a faculty job at the University of Lavalle, Quebec.

Other members of the Green lab have been great mentors and co-workers over the years and have helped me with protocols, reagents, and scientific advise – all of which I am forever grateful. The helpful insight and suggestions I receive from my fellow lab members at both our weekly meetings and scientific discussions within the lab have proved to be a vital part of my development as a scientist.

I would also like to acknowledge our collaborators at McGill University, Peter Siegel and his post doc Sebastien Tabaries. They assisted us with metastasis assays that we do not have the expertise for, which made a significant contribution to our KDM3A manuscript.

I would like to acknowledge my thesis research advisory committee, Arthur Mercurio, Eric Baehrecke, Sharon Cantor, and Brian Lewis, has helped me with scientific and career advise over the years. And my external committee member, Joan Brugge, who has taken the time to come out the Worcester for my defense and whose research formed the basis of much of my investigations.

Finally, I have to send a special thanks to Sara Deibler who has provided invaluable editorial assistance over the years. Her comments and edits on my writing and data have taught me a great amount about scientific writing that will stick with me for years to come.

ABSTRACT

Epithelial cells that lose attachment to the extracellular matrix (ECM) undergo a specialized form of apoptosis called anoikis. Anoikis has an important role in preventing oncogenesis, particularly metastasis, by eliminating cells that lack proper ECM cues. The basis of anoikis resistance remains to be determined and to date has not been linked to alterations in expression or activity of previously identified anoikis effector genes. Here, I utilized two different screening strategies to identify novel anoikis effector genes and miRNAs in order to gain a deeper understanding of anoikis and the potential mechanisms of anoikis resistance in cancer.

Using large-scale RNA interference (RNAi) screening, I found that KDM3A, a histone H3 lysine 9 (H3K9) mono- and di-demethylase plays a pivotal role in anoikis induction. In attached breast epithelial cells, *KDM3A* expression is maintained at low levels by integrin signaling. Following detachment, integrin signaling is decreased resulting in increased *KDM3A* expression. RNAi-mediated knockdown of *KDM3A* substantially reduces apoptosis following detachment and, conversely, ectopic expression of *KDM3A* induces cell death in attached cells. I found that KDM3A promotes anoikis through transcriptional activation of *BNIP3* and *BNIP3L*, which encode pro-apoptotic proteins. Using mouse models of breast cancer metastasis I show that knockdown of *Kdm3a* enhances metastatic potential. Finally, I find defective *KDM3A* expression in human breast cancer cell

lines and tumors. Collectively, my results reveal a novel transcriptional regulatory program that mediates anoikis.

Next, I sought to discover miRNAs involved in anoikis by investigated changes in miRNA expression during anoikis using small RNA sequencing technology. Through this approach I discovered that miR-203 is an anoikis effector miRNA that is also highly down-regulated in invasive breast cancer cells. In breast epithelial cells, miR-203 is induced upon the loss of ECM attachment and inhibition of miR-203 activity leads to a resistance to anoikis. I utilized a dual functional- and expression- based RNA sequencing approach and found that miR-203 directly targets a network of pro-survival genes to induce cell death upon detachment. Finally, I found that the loss of miR-203 in invasive breast cancer leads to the elevation of several anoikis-related pro-survival target genes to contribute to anoikis resistance. Taken together, my studies reveal novel pathways through which cell death is induced upon detachment from the ECM and provide insight into potential mechanisms of anoikis resistance in cancer.

TABLE OF CONTENTS

LIST OF TABLES

LIST OF FIGURES

LIST OF PUBLICATIONS

The histone H3K9 demethylase KDM3A promotes anoikis by transcriptionally activating pro-apoptotic genes BNIP3 and BNIP3L.
Pedanou, V.E., Gobeil, S., Tabaries, S., Simone, T.M., Zhu, L.J., Siegel, P.M., and Green, M.R. (2016). Elife *5*.

CHAPTER I: INTRODUCTION

Cancer Background and History

The disease of cancer is, at its core, a genetic disease rising from acquired mutations and alterations in the genome over time that cause an uncontrolled growth of cells. Over the last few decades significant advances in cancer research have allowed us to have a better understanding of how cancer develops and the genetic events that are required to result in tumorigenesis. Although most of the knowledge we now have about cancer has been discovered in the last few decades, cancer itself is not a new disease. The first known description of cancer comes from ancient Egypt where they described breast tumors that were removed by cauterization and it was also stated back then that "there is no treatment" for these tumors. (History of Cancer, ACS, pg 1)

Genetic alterations that contribute to cancer development can occur by a multitude of mechanisms. One method is by DNA mutation, which happens at a constant rate in human cells but occasionally a mutation occurs in a gene that contributes to tumorigenesis. Another method of genetic alteration is by epigenetic changes, which are modifications made to DNA that do not alter the DNA sequence but do affect gene expression. Finally, chromosome alterations such as deletions, translocations, or duplications can dramatically alter gene

expression and lead to tumor development (Hsu and Moorhead, 1956; Stich and Emson, 1959). These types of genomic instability give rise to the heterogeneous traits of cancers.

In the past decade, with the complete sequencing of the human genome and the significant advances in massive sequencing technology we have been able to identify traits of cancer including gene expression profiles, mutations across cancer genomes, chromosomal abnormalities and microRNA (miRNA) expression profiles (Consortium, 2001). These methods have identified multiple genetic and epigenetic changes within the cancer cells themselves and within the tumor microenvironment that lead to the development of cancer and subsequent metastasis of some cancers.

In addition to the genetic components of cancer development, recent work has shown that the tumor microenvironment is also an important aspect of cancer biology (Hofmann et al., 2003; Kaur et al., 2016; Lizotte et al., 2016). The tumor microenvironment of a solid tumor includes multiple different types of cells and the extra cellular matrix (ECM), all of which evolve as the tumor progresses. Cancer stem cells, cancer cells, cancer associated fibroblasts, endothelial cells, pericytes, and immune inflammatory cells all make up the tumor microenvironment and each cell type contributes to the development of the tumor (the immune inflammatory cells can be either tumor-promoting or tumor-killing

cells). All of these components play a significant role in tumorigenesis and add a layer of complexity to the study of cancer biology (Hanahan and Weinberg, 2011).

One widely accepted hypothesis of how genetic alterations lead to tumorigenesis is the “two hit” hypothesis which states that a cell must acquire two cancer driving mutations in order for that cell to begin uncontrolled proliferation and subsequent tumor growth (Tomlinson et al., 2001). Alfred Knudson suggested the Two Hit Hypothesis in 1971 after studying children with heritable and sporadic retinoblastoma. Knudson found that heritable retinoblastoma always presented in both eyes and occurred earlier than sporadic retinoblastoma. From these results Knudson hypothesized that multiple genetic alterations are required for the development of tumors and that the children with heritable retinoblastoma were already born with one “hit” and had a higher chance of acquiring a second “hit” than normal children (Knudson, 1971). This hypothesis was later confirmed by the finding that the Retinoblastoma (Rb) tumor suppressor gene is inactivated in children with heritable retinoblastoma and is commonly inactivated in a variety of other cancers (Horowitz et al., 1990).

It has been proposed that genomic instability leads to eight biological capabilities of cancer cells termed, “hallmarks” of cancer, that are acquired during the development of human tumors. Resisting cell death is counted as one

of these hallmarks of cancer (Hanahan and Weinberg, 2000, 2011). Cell death or apoptosis was first identified as a barrier to cancer development in hormone-dependent tumors. When the hormone is present, the cancer cells thrive and proliferate uncontrolled but when the hormones were withdrawn from these tumors it resulted in massive apoptosis in the tumor cells (Kerr et al., 1972). Additionally, the overexpression of the activated MYC oncogene in primary human cells resulted in apoptosis, suggesting that apoptosis is a mechanism of ridding the body of cells with mutations that activate oncogenes (Evan et al., 1992).

Death from cancer is not caused by the primary tumor in most cases but is eventually caused by metastasis, a greek word meaning “displacement”, to distant organs, which then result in organ failure. In 1889 Stephen Paget proposed that the “seed and soil” theory of metastasis where certain cells from the primary tumor, the “seeds”, are able to form secondary tumors in specific organ microenvironments, the “soil” (Fidler, 2003). The general principle behind the “seed and soil” hypothesis remains true today and the multiple steps that lead the “seed” to the “soil” has been defined and is termed the “metastatic cascade” (Colombano and Reese, 1980).

The metastatic cascade involves multiple steps that primary tumor cells must go through to establish a tumor in a secondary site. In the first step of the

metastatic cascade, cells detach from the primary tumor and invade and intravasate into the circulatory system where the tumor cells are able to travel through the bloodstream. Next, metastatic cells must extravasate and invade into secondary tumor sites, usually specific organs that depend on the primary cancer. Finally, the metastatic cells must interact with the microenvironment of the secondary organ site and initiate tumor growth (Chambers et al., 2002). As with the primary tumor, the tumor microenviroment plays a significant role in metastatic tumor development, when the primary tumor cells reach a secondary site a supportive microenvironment is developed to facilitate tumor growth (Hanahan and Weinberg, 2011). While the metastatic cascade has been delineated and there has been a great deal of research on metastatic cancers in recent times, there remains a vast amount of unknowns and further studies on the genetic alterations and changes in the tumor microenvironment that contribute to metastasis are needed.

Anoikis

Epithelial cells that lose attachment to the extracellular matrix (ECM), or attach to an inappropriate ECM, undergo a specialized form of apoptosis called anoikis meaning “the state of being without a home” (Frisch and Francis, 1994a; Frisch and Francis, 1994b). Anoikis was first identified in Madin-Darby canine kidney epithelial (MDCK) cells through the observation that disruption of the cell-matrix interactions by forcing the cells to grow in suspension, resulted in

apoptosis. The result was confirmed by the addition of integrin blocking antibodies to the media of attached cells, which also led to apoptosis due to the loss of integrin signaling. This initial study on anoikis also found that both the overexpression of BCL-2 and the transformation of cells with activated RAS or SRC conferred resistance to anoikis, suggesting early on that anoikis resistance might be an important aspect of cancer biology and might contribute to the cancer hallmark of avoiding apoptosis (Frisch and Francis, 1994b).

Several signaling pathways have been shown to regulate anoikis. In particular, anoikis is suppressed by integrin signaling, which functions through focal adhesion kinase (FAK), a non-receptor tyrosine kinase and an activator of the RAF/MEK/ERK pathway (King et al., 1997). Upon interactions of integrins with ECM proteins, FAK is auto-phosphorylated and activated. The auto-phosphorylation of FAK leads to activation and recruitment of SRC, which then further phosphorylates FAK leading to the fully active form of FAK. Activated FAK leads to downstream pro-survival signals through the PI3K pathway and the RAF/MEK/ERK pathway (Calalb et al., 1995; Lietha et al., 2007). Following detachment and loss of integrin signaling, FAK is inactivated and the downstream pro-survival signals are lost (Frisch et al., 1996). Ectopic expression of a constitutively active form of FAK causes resistance to anoikis in two different epithelial cells lines, MDCK and HaCat cells (Frisch et al., 1996), similarly, FAK

blocking antibodies or a dominant-negative FAK mutant leads to increased sensitivity to anoikis (Bouchard et al., 2007).

Upstream of FAK are integrins, which directly contact ECM proteins to initiate downstream pro-survival signaling. Integrins consist of two subunits, the α and β subunits, and each integrin is defined depending on the specific subunits. There are 4 integrins that are known to play a role in cell survival signaling, α5β1, αvβ3, α1β1 and α6β1, all of which result in different downstream signaling consequences (Brassard et al., 1999; Matter et al., 1998; O'Brien et al., 1996; Zhang et al., 1995). The interactions between integrins and the ECM act through a pro-survival signaling pathway within cells to promote survival, growth and proliferation. When the integrin-ECM interactions are lost or disrupted or when a cell interacts with an ECM that is not ideal for the cell-specific integrins, the pro-survival signals are lost leading to cell death.

Anoikis is also suppressed by integrin-mediated, ligand independent activation of the epidermal growth factor receptor (EGFR) signaling pathway, which, like FAK, also stimulates pro-survival RAF/MEK/ERK activity. Integrin-ECM interactions lead to the production of reactive oxygen species (ROS), which activate SRC. SRC activation leads to the ligand independent phosphorylation and activation of EGFR leading to the activation of the pro-survival MAPK and Akt pathways (Moro et al., 1998). Upon detachment of cells from the ECM,

EGFR expression is lost which leads to accumulation of the pro-apoptotic protein BIM and subsequent anoikis, however ectopic expression of EGFR causes resistance to anoikis in detached cells (Reginato et al., 2003).

The FAK and EGFR cell signaling pathways have been found to regulate the levels of BIM (also called BCL2L11) and BMF, two pro-apoptotic members of the BCL2 family of apoptosis regulators that are known to contribute to anoikis (Reginato et al., 2003; Schmelzle et al., 2007). Specifically, activated EGFR and ERK suppress BIM activity through phosphorylation and ubiquitin-mediated degradation of BIM when cells are attached to the ECM (Collins et al., 2005). However, depletion of BIM or BMF diminishes but does not completely prevent anoikis (Reginato et al., 2003; Schmelzle et al., 2007), suggesting the existence of other pro-apoptotic factors and regulatory pathways that can promote anoikis. The basis of anoikis resistance remains to be determined and to date has not been linked to alterations in expression or activity of BIM or BMF.

While the major signaling pathways involved in anoikis have been identified, to date there have been many groups that have identified downstream novel anoikis effector genes. The previously discussed BIM and BMF were identified by specifically looking at the expression of a subset of BCL2 pro-apoptotic proteins and microarray analysis, respectively (Reginato et al., 2003; Schmelzle et al.,

2007), other studies have utilized multiple approaches to identify other anoikis effector genes.

Previous unbiased screening approaches have identified several other novel anoikis effector genes. A genome wide retroviral cDNA library was the first screening approach used to discover anoikis effectors in rat intestinal epithelial (RIE-1) cells. The screen identified a neurotrophic tyrosine kinase receptor, TrkB, that activates downstream PI3K signaling to suppress anoikis and enhance metastasis (Douma et al., 2004). A more recent genome wide shRNA loss of function screen in RWPE-1 prostate cells found that alpha/beta hydrolase domain containing 4 (ABHD4) promotes anoikis through cleavage of PARP and Caspase-3 (Simpson et al., 2012).

Additional studies have taken more directed approaches to identifying anoikis effector genes such as studying genes already known to play a role in apoptosis. One such study identified IGF-1 as an anoikis suppressor in mouse embryonic fibroblast cells (MEF) that acts through activation of Ras (Valentinis et al., 1999). Another directed study found that angiopoietin-like 4 (ANGPTL4) promotes cell survival upon detachment by elevating levels of reactive oxygen species (ROS), which then activate the pro-survial ERK and PI3K pathways (Zhu et al., 2011).

Anoikis is studied in cell culture by detaching cells from adherent conditions and plating the cells on poly-hydroxyethylmethacrylate (polyHEMA) coated or ultra low attachment plates to force the cells to grow in suspension. The polyHEMA coating prevents cell attachment by preventing the deposition of ECM because of its non-ionic nature, thereby forcing cells to grow in suspension (Frisch and Francis, 1994b). While there are now standard experiments to model anoikis *in vitro*, *in vivo* anoikis experiments are less straightforward. Cells require specific ECM attachments from their native environment, therefore when cells enter a foreign environment anoikis should occur. Sensitivity to anoikis *in vivo* was observed in one study that found that tumor cells show enhanced metastasis when the primary tumor is orthotopically grown as compared to ectopic tumors, which proved the importance of tumor cell and ECM interactions (Glinskii et al., 2003).

Anoikis Resistance and Metastasis

Throughout the metastatic cascade, cells need the ability to survive without attachment to neighboring cells and the original ECM and thus need to acquire resistance to anoikis (Frisch and Ruoslahti, 1997). Metastatic cells need to bypass anoikis both when the tumor cell detaches from the primary tumor, and therefore from the ECM, and enters the bloodstream and then when the tumor cell arrives at a secondary site where there is a different ECM composition and therefore different signaling from the primary tumor microenvironment.

Anoikis plays an important role in preventing oncogenesis, particularly metastasis, by eliminating cells that lack proper ECM cues (Simpson et al., 2008; Zhu et al., 2001). Previous studies have shown that when malignant cells lose contact with both neighboring tumor cells and their ECM, the cells will normally undergo apoptosis (Glinskii et al., 2003). However, metastatic cells must bypass this cell death in order to detach from the primary tumor and enter the circulatory system and finally extravasate into a secondary site and form a tumor in that secondary site. Since the secondary tumor site most often contains a different ECM than the primary site, the metastatic cells also need to bypass anoikis after the last step of metastasis (Berezovskaya et al., 2005; Howard et al., 2008).

In addition to the role anoikis plays in preventing metastasis, there is also evidence to suggest that anoikis functions to prevent the invasion of tumor cells into the luminal space, which is a characteristic of epithelial tumors (Debnath et al., 2002). In general, epithelial-derived cancers, such as breast cancer, develop resistance to anoikis which results in the filling of the luminal space or ductal carcinoma in situ (DCIS), an early stage in breast cancer tumorigenesis (Schwartz, 1997).

While multiple anoikis pathways and effectors have been discovered and studied since anoikis was first identified, there are likely many other factors

involved in anoikis. Anoikis is proving to be a complex biological process that has a link to tumorigenesis and metastasis that has yet to be fully defined. The mechanism of resistance to anoikis in cancer remains largely unknown. It is likely that critical anoikis effectors are genetically altered in cancer so it is important to relate anoikis research back to human cancer in order to understand the mechanism by which cancer cells, specifically metastatic cells, bypass anoikis. This knowledge would lead to a greater understanding of metastasis and potentially new avenues for therapeutics.

Epigenetics and Cancer

Epigenetics, DNA modifications that do not change the DNA sequence, affect gene expression through chromatin associated proteins and post-translational modifications of histones. Specific mechanisms of epigenetic regulation include DNA methylation, post-translational modifications of histones (methylation, acetylation, sumoylation, ubiquitination), and nucleosome remodeling. The mysregulation of epigenetic mechanisms has been shown to contribute to human disease and many defects in epigenetic mechanisms have been linked to cancer development (Bracken et al., 2003; Lin and Nelson, 2003; Sato et al., 2003). Identification of epigenetic alterations in cancer has led to the development of various therapies that target epigenetic mechanisms that promote cancer. Two drugs that target DNA methyl transferases (5-azacytidine and decitabine) were some of the first epigenetic-based drugs to be approved to treat human disease

(SAIKI et al., 1978; van Groeningen et al., 1986). Rapid advances in the field of epigenetics and cancer have led to the development of several potent inhibitors of histone methyltransferases (Kubicek et al., 2007), histone demethylases (Feng et al., 2016), and chromodomain proteins (Ren et al., 2015). Because the epigenetic landscape and mechanisms are complex we likely do not have a full understanding of the involvement of all epigenetic regulating proteins in cancer development and further studies and developments are needed to create a clearer picture.

Histone Methylation

One major aspect of epigenetic control of gene expression and source of aberrant gene expression in cancer is changes in chromatin modifications. In general, histone modifications change the structure and function of chromatin, subsequently leading to changes in gene expression. Transcription can either be activated or repressed by histone modifications based on the modifications that are present on a specific gene (Liu et al., 2005; Pokholok et al., 2005). Lysine acetylation on histones is associated with transcriptional activation whereas lysine methylation can be associated with either transcriptional activation or transcriptional repression depending on which lysine residue is methylated. The differing effects on transcription by methylated lysines occur from the formation of differing binding sites for chromo-domain proteins that have different effector functions (Vakoc et al., 2005). Histone modifications can be altered in cancer

through the differing expression of histone modifying enzymes. This can lead to aberrant changes in gene expression that can promote tumor growth and metastasis (Van Rechem et al., 2015; Xiang et al., 2007; Yamane et al., 2007).

Methylation is a post-translational modification of lysine and arginine residues on histones that affects gene expression. It has been demonstrated that histone lysine methylation can occur in the mono-, di-, or tri-methyl state and arginine methylation can occur in the mono- or di-methylated state. Histone methylation affects gene expression through the recruitment of “reader” proteins, which then recruit protein complexes that can either repress or enhance transcription (reviewed in (Musselman et al., 2012)). Histone methylation was found to be a reversible modification with the discovery of the first histone demethylase, KDM1A/LSD1 (Shi et al., 2004). Since the discovery of LSD1, a family of proteins that contain homologous JmjC domains have been identified and each member of the family has been shown to demethylate specific histone lysine residues, some specifically demethylate mono- di- or tri-methylated lysines, while one member of the JmjC family has been shown to demethylate histone arginine residues (Chang et al., 2007).

KDM3A is a member of the JmjC domain-containing protein family of histone demethylases. Proteins in this family have a catalytic JmjC domain that demethylates lysine and arginine residues on histones in an oxidative reaction

that requires Fe(II) and alpha-ketoglutarate as cofactors (Tsukada et al., 2006). KDM3A (also called JMJD1A or JHDM2A) is a histone demethylase that has been shown to specifically demethylate mono- and di-methyl histone H3 lysine 9 (H3K9me1 and H3K9me2) but not tri-methyl Histone H3 lysine 9 (H3K9me3) (Yamane et al., 2006). Both H3K9me1 and H3K9me2 have been identified as transcriptionally repressive marks, although H3K9me2 has also been discovered to be present on several actively transcribed genes (Lienert et al., 2011; Snowden et al., 2002). As suggested by its function, KDM3A has been implicated as an activator of transcription and acts as a coactivator for androgen receptor (AR) (Yamane et al., 2006) and hypoxia-inducible factor (HIF) (Beyer et al., 2008). In addition to the JmjC domain, KDM3A also contains a Zinc Finger domain that likely contributes to DNA binding and transcriptional activation of specific target genes (Yamane et al., 2006).

While the exact mechanism by which KDM3A controls gene expression is known, the role KDM3A plays in cancer is not well understood and has so far been controversial. There have been differing studies suggesting that KDM3A is both anti-oncogenic (Du et al., 2011) and pro-oncogenic (Krieg et al., 2010), suggesting that the role of KDM3A is likely dependent on other factors and could differ among tissue types. Further research is needed to determine the factors that influence the tissue or cancer type specific role that KDM3A plays in cancer progression.

microRNA

microRNAs (miRNAs) are short RNA molecules (~22 nucleotides) that regulate gene expression through translational repression and mRNA decay (Djuranovic et al., 2012), recent evidence even suggests that mRNA degradation by miRNAs is the predominant reason for reduced protein levels in mammals (Guo et al., 2010). The first miRNA (lin-4) was discovered in C. elegans in 1993 and in the more than two decades since the discovery of miRNAs, over a thousand miRNAs have been identified in the human genome (Griffiths-Jones et al., 2008; Lee et al., 1993

). The discovery that miR-15 and miR-16 are frequently downregulated in chronic lymphocytic leukemia (CLL) marked the first implication of miRNA involvement in cancer (Calin et al., 2002). In the time since the CLL study, there have been thousands of other published studies that aim to define the relationship between miRNAs and cancer.

The genes encoding miRNAs are transcribed by RNA polymerase II into long transcripts, which are then processed by the RNAse III protein, DROSHA, into a ~60 nucleotide precursor miRNA hairpin (pre-miRNA) (Zeng et al., 2005). Exportin5 then transports the pre-miRNA into the nucleus where it is further processed by another RNAse III protein, DICER (Zhang et al., 2002), which generates a mature ~22 nucleotide mature miRNA. The mature miRNA is then loaded into an Argonaute (Ago) protein in the RNA-induced silencing complex

(RISC), which is then directed to specific target mRNAs. While mature miRNAs can interact with Ago1-4, Ago2 is the Argonaute responsible for targeted mRNA degradation by miRNAs (Meister et al., 2004).

miRNAs control the expression of target genes through specificity in the seed sequence region (7 nucleotides) of the miRNA that binds to the complementary sequence in the 3' untranslated region (3'UTR) of transcripts to inhibit translation of the mRNA and inhibit transcription by causing the deadenylation and decay of the target mRNA (Guo et al., 2010). Classicaly, it was thought that the major mechanism of miRNA repression was through inhibition of translation, however recent data suggests that the main mechanism of mammalian miRNA repression is by mRNA degradation (Guo et al., 2010). Several databases (including Targetscan and miRDB) exist to predict the target mRNAs of miRNAs based on matching the seed sequence of the miRNA to a complementary sequence in the 3'UTR of known genes (Agarwal et al., 2015).

The expression of miRNAs themselves is regulated by two different methods— transcriptional changes that can affect the levels of pri-miRNA transcripts or post-transcriptional changes in processing of the pre-miRNA or the mature miRNA. One method by which the transcription of pri-miRNAs is controlled is through transcription factors. For example, E2F7 (a member of the E2F family of transcription factors) directly binds to the promoters of miR-25,

miR-92a, and miR-7 to repress the transcription of the corresponding pri-miRNAs (Mitxelena et al., 2016). Another mechanism of transcriptional control of miRNAs is by DNA methylation. Previous studies have identified miR-31 (Augoff et al., 2012), the miR-200 cluster (Wee et al., 2012) , and miR-33b (Yin et al., 2016) as just a few of the miRNAs that are aberrantly expressed in cancer due to DNA hypermethylation.

The processing of all miRNAs requires the same large protein complex machinery (i.e. DROSHA and DICER), however recent studies have started to uncover regulatory factors that influence the processing of specific miRNAs or specific groups of miRNAS. On a global level, mutations in both DROSHA and DICER have been discovered to effect miRNA processing in cancer (Heravi-Moussavi et al., 2012; Rakheja et al., 2014). Recent discoveries provide examples of how specific miRNA expression can be regulated by DICER regulatory factors that influence the processing of that specific miRNA. One example of miRNA-specific altered processing occurs when RNA editing of the pri-miR-151 completely blocks DICER cleavage of pre-miR-151 (Kawahara et al., 2007). The processing of specific miRNAs can also be regulated uridylation, mediated by Lin28 and TUT4, of the pre-miR, which also blocks DICER cleavage of the pre-miR (Heo et al., 2009). The study of factors affecting miRNA processing is a relatively new field of research and knowledge on miRNA processing will likely grow over the coming years.

Previous studies have established that miRNAs are widely dysregulated in cancers (Zhang et al., 2006), however few miRNAs have been implicated in promoting or suppressing anoikis. Because miRNAs have not been widely studied in the context of anoikis, the role of miRNAs in anoikis remains to be determined. Previous studies have suggested that the miR-200 family both enhances anoikis sensitivity (Howe et al., 2012) and promotes anoikis resistance and metastasis (Yu et al., 2013). Given the critical role that miRNAs play in gene expression, it is likely that miRNAs play a yet to be determined role in anoikis, revealing that further studies should be done to fully delineate the role of miRNAs during anoikis.

While many miRNAs can be grouped into families or clusters, there is a subset that do not cluster with any other miRNAs, miR-203 falls into this category. miR-203 was identified in multiple genome wide miRNA profiling studies but a group that studied the role of miR-203 in primary keratinocyte differentiation was the first to identify a function of miR-203 when they showed that miR-203 suppressed the “stemness” of skin stem cells (Lena et al., 2008). Since the first miR-203-specific study in 2008, research has mostly been focused on the role miR-203 plays in cancer.

Several groups have implicated miR-203 as a tumor suppressor and anti-invasion miRNA specifically. Since 2008 there have been similar studies performed in multiple different tissues that suggest miR-203 is universally an anti-proliferative miRNA (Ding et al., 2013; Furuta et al., 2010; Noguchi et al., 2012; Saini et al., 2011; Viticchie et al., 2011), while the exact mechanism of proliferation and invasion suppression likely differs between cancer types. Further investigation showed that miR-203 is epigenetically silenced by promoter methylation in some cancers including ovarian carcinoma (Iorio et al., 2007) and rhabdomyosarcoma (Diao et al., 2014). Expression analysis of several miRNAs in breast cancer cells lines revealed that miR-203 is highly downregulated in invasive breast cancer cell lines compared to both normal breast epithelial (MCF10A cells) and less invasive breast cancer cell lines (Luo et al., 2013) and is significantly downregulated in human triple negative breast cancer samples (Yu et al., 2012). Furthermore, ectopic expression of miR-203 in cancer cell lines inhibits proliferation, migration, and invasion (Noguchi et al., 2012). To date, miR-203 has not been implicated in anoikis and the exact role miR-203 plays in inhibiting breast cancer invasion and metastasis has yet to be determined.

As stated above, the main mechanism by which miRNAs control cellular processes is by targeting one or more specific mRNAs resulting in decreased protein output of those targets. There are several hundred predicted miR-203 target genes based on the seed sequence of miR-203 and the sequences of the

3'UTR of target mRNAs. However, only a few of these predicted targets have been confirmed as *bona fide* miR-203 targets including p63 (Yi et al., 2008), ABL1 (Bueno et al., 2008), BMI1 (Chen et al., 2015), BIRC5, LASP1 (Wang et al., 2012), Survivin (Bian et al., 2012), E2F3 (Noguchi et al., 2012), SNAI2 (Zhang et al., 2011) and RUNX2 (Taipaleenmaki et al., 2015). Interestingly, most of the *bona fide* target genes have been identified across different tissues and the targets do not seem to overlap between tissue types, with the exception of p63 which has been confirmed in multiple cell types (Lena et al., 2008; Yi et al., 2008; Yuan et al., 2011) This suggests that tissue type could play an important role in determining the specific miR-203 target genes.

RNAi screens

RNA interference (RNAi) is a cellular process that involves degradation of mRNAs through sequence specific binding of small interfering RNAs (siRNAs) that was first discovered in *Caenorhabditis elegans (C. elegans)* (Fire et al., 1998). For more than a decade, scientists have utilized RNAi as a research tool to deplete specific mRNA transcripts by inserting sequence specific RNAi reagents into cell culture or whole organisms in order to delineate the function of specific genes. In addition to targeted gene depletion, libraries consisting of small hairpin RNAs (shRNAs) designed to target the whole genome have been used to perform genome wide screens with phenotypic readouts. shRNA libraries are designed using microRNA (miRNA) and small interfering RNA (siRNA)

technology, where a hairpin similar to the structure of pre-miRNA transcripts are ligated into lentiviral or retroviral plasmids. Once the plasmid is inside the cell, the hairpin is loaded into the endogenous small RNA processing machinery, which results in small RNAs that inhibit the transcription of its target gene in a siRNA-like mechanism. The genome wide shRNA libraries contain multiple different shRNAs to target each gene in the genome and are normally used in a pool format. This has proven to be a successful unbiased approach that has allowed scientists to identify novel genes that are involved in biological processes from immunology (Ng et al., 2007) to cancer biology (Gazin et al., 2007).

shRNA screens (both whole genome and directed smaller scale screens) have proven to be useful research tools in cancer research. The most common form of RNAi screening used to study cancer biology are cell culture based loss of function screens with a phenotypic readout (e.g. (Wajapeyee et al., 2008) and (Kessler et al., 2012)). More recently, *in vivo* shRNA screens have been successful in identifying novel oncogenes and tumor suppressors in mouse models of cancer because of the long-term stable suppression of mRNA transcripts by shRNAs (Gargiulo et al., 2014). The research in the Green lab in recent years has been focused on utilizing shRNA genome wide screens to identify novel factors in multiple aspects of transcription and cancer biology. Specifically, our lab has used RNAi screens to identify new genes involved in oncogene induced senescence (Wajapeyee et al., 2008), genome integrity (Fang

et al., 2015), chemotherapy resistance (Ma et al., 2014), lung cancer progression (Lin et al., 2014), aberrant oncogenic methylation (Fang et al., 2014), and glioma progression (Sheng et al., 2010). We use a genome wide small hairpin RNA (shRNA) library that contains ~62,400 shRNAs directed against ~28,000 genes (Silva et al., 2003; Silva et al., 2005).

Small RNA Profiling

After the discovery of miRNA and subsequent identification of multiple miRNAs that are dysregulated in cancer, the field was seeking to study the expression of multiple miRNAs in cancers but in the early 2000's northern blotting was the only technique available to determine the expression of a miRNA. Northern blots had many limitations for detecting multiple miRNAs in a study, including the high amount of RNA needed for one northern blot and the need to use radioactive labels to detect the miRNA. Thus, a miRNA microarray was developed to profile the expression of all known miRNAs in human and mouse tissues (Liu et al., 2004). Not long after the development of the miRNA microarray multiple groups started using high throughput sequencing as a direct method of profiling small RNA expression, this method has allowed for both determining the expression of known miRNAs in the genome and identifying novel miRNAs (Lu et al., 2006; Ruby et al., 2006).

Small RNA profiling has become a standard, unbiased method for identifying miRNAs that are involved in cellular processes and diseases. The advantages of using the small RNA sequencing method of profiling miRNAs include the high sequence accuracy, which has the potential of identifying novel miRNAs. While there have been a plethora of miRNA profiling studies done in human cancers there has yet to be any study of miRNA changes during the process of anoikis—there has even been very few directed miRNA studies in anoikis research.

Focus of this dissertation

While there are several known anoikis effector genes reviewed above, in the first part of my thesis research, I chose to use a genome wide RNAi screen to identify novel anoikis effector genes. With this approach, I sought to identify novel anoikis pathways by performing the unbiased genome wide shRNA screen in breast epithelial cells to identify novel anoikis effector genes. The screen identified multiple novel factors as anoikis effector genes, including KDM3A, ZCCHC24, ZNF345, METAP1D, and PIH1D3. I chose to focus my investigation on the histone demethylase, KDM3A, because of the intriguing possibility that epigenetics and transcription play a major role in the control of anoikis. In this study, I identify KDM3A as an anoikis effector that is induced upon detachment of cells from the ECM. I further delineated the mechanism by which KDM3A functions to promote anoikis in human breast epithelial cells and showed that the

activation of KDM3A upon detachment from the ECM causes transcriptional activation of two pro-apoptotic BH3-only proteins, BNIP3 and BNIP3L resulting in anoikis. Also, knockdown of KDM3A causes a non-metastatic breast cancer cell line to become metastatic, implicating the loss of KDM3A in anoikis resistance and enhanced metastasis.

In the second part of my thesis research, I sought to identify changes in miRNA expression during anoikis to discover miRNAs that could be implicated in anoikis resistance during cancer development. To date there have been a wide array of whole genome miRNA studies completed in cancers (Iorio et al., 2007; Mi et al., 2007; Wölfl et al., 2011) including breast cancers (Fassan et al., 2009; Luo et al., 2013) and even profiling miRNAs at different stages of breast cancer (Dadiani et al., 2016). However, there have not yet been any anoikis-related genome wide miRNA studies completed, only directed miRNA investigations into how a few single miRNAs play a role in anoikis have been done (as discussed above), leaving the possibility that there are other miRNAs involved in anoikis that have yet to be identified. I completed genome wide miRNA profiling during the early stages of anoikis by using small RNA sequencing. Through these miRNA profiling experiments, I found a group of miRNAs that are upregulated during anoikis and a separate group that are downregulated during anoikis. From these two group of miRNAs, I chose to focus on the most highly upregulated miRNA, miR-203, because miR-203 had already been implicated as a tumor-

supressive miRNA (as discussed above). I found that miR-203 is significantly upregulated during anoikis and promotes cell death. I also identified several pro-survival miR-203 target genes that are downregulated by miR-203 upon detachment of the cells from the ECM and therefore lead to cell death. My results show that miR-203 is a novel anoikis effector miRNA and in addition to previous studies, my results suggest that miR-203 is a tumor suppressor miRNA in triple negative and invasive breast cancers.

In conclusion, I have identified two novel factors that are critical anoikis effectors, KDM3A and miR-203. My research furthers the general understanding of the process of anoikis and provides insight into potential mechanisms of anoikis resistance in metastatic tumor cells.

CHAPTER II: MATERIALS AND METHODS

Cell lines and culture

T47D, MDA-MB-231, BT549, Hs578t, and CLS1 cells were obtained from ATCC (Manassas, VA) and grown as recommended by the supplier. MCF7 cells (National Cancer Institute, Bethesda, MD) were maintained in DMEM (GE Healthcare Life Sciences, Marlborough, MA) supplemented with 1X nonessential amino acids (NEAA; Thermo Scientific, Waltham, MA) and 10% fetal bovine serum (FBS; Atlanta Biologics, Norcross, GA). MCF10A cells (ATCC) were maintained in DMEM/F12 (GE Healthcare Life Sciences) supplemented with 5% donor horse serum (Thermo Scientific), 20 ng/ml epidermal growth factor (Peprotech, Rocky Hill, NJ), 10 µg/ml insulin (Life Technologies, Grand Island, NY), 1 ng/ml cholera toxin (Sigma-Aldrich, St. Louis, MO), 100 µg/ml hydrocortisone (Sigma-Aldrich), 50 U/ml penicillin (Thermo Scientific), and 50 µg/ml streptomycin (Invitrogen, Grand Island, NY). SUM149 cells were obtained from Dr. Donald Hnatowich (University of Massachusetts Medical School, Worcester, MA) and grown in RPMI (Invitrogen) supplemented with 10% FBS, 0.01% insulin, 50 U/ml penicillin, and 50 µg/ml streptomycin. 67NR and 4T07 cells were obtained from Dr. Fred Miller (Wayne State University School of Medicine, Detroit, MI) and were grown in high glucose DMEM (GE Healthcare Life Sciences) supplemented with 10% FBS, 50 U/ml penicillin, and 50 µg/ml streptomycin.

Ectopic expression

KDM3A and KDM3A(H1120G/D1122N) were PCR amplified from pCMV-JMJD1A and pCMV-JMJD1A(H1120G/D1122N), respectively, obtained from Dr. Peter Staller (Biotech Research and Innovation Centre, University of Copenhagen, Denmark), using primers (forward, 5'-CTCGAGCCGTTAAGGTTTGCCAAAAC-3' and reverse, 5'-ATCGTTAACAGGGAGATT AAGGTTTGCCA-3') engineered with XhoI and HpaI restriction sites and then cloned into pMSCVpuro (ClonTech Laboratories, Inc., Mountain View, CA). BNIP3L was PCR amplified from Bnip3L pcDNA3.1 (plasmid #17467, Addgene, Cambridge, MA) using primers (forward, 5'-AATCTCGAGCATGTCGTCCCACCTAGT-3' and reverse 5'-ATCGAATTCTTAATAGGT GCTGGCAGAGG-3') engineered with XhoI and EcoRI restriction sites and cloned into pMSCVhygro (ClonTech Laboratories, Inc.). BNIP3 was PCR amplified from MGC Human BNIP3 cDNA (Dharmacon, Marlborough, MA) using primers (forward, 5'-AATCTCGAGCAT GTCGCAGAACGGAGCG-3' and reverse 5'-ATCGAATTCACTAAATTAGGAACGCAGC AT-3') engineered with XhoI and EcoRI restriction sites and cloned into pMSCVpuro.

MCF10A cells stably expressing pMSCVpuro-JMJD1A, pMSCVpuro-JMJD1A-H1120G/D1122N, pMSCVpuro-BNIP3, pMSCVhygro-BNIP3L, pMSCVpuro-empty, pMSCVhygro-empty, pBABE-MEK2DD (obtained from Dr. Sylvain

Meloche, Universite de Montreal), pBABE-EGFR (Addgene), or pBABE-empty (Addgene) were generated by retroviral transduction as described previously (Santra et al., 2009). Twelve days after puromycin or hygromycin selection, cells were stained with 0.5% crystal violet.

RNA interference

The human shRNA^{mir} pSM2 library (Open Biosystems/Thermo Scientific, Pittsburgh, PA) was obtained through the University of Massachusetts Medical School RNAi Core Facility (Worcester, MA). Retroviral pools were generated and used to transduce MCF10A cells as described previously (Gazin et al., 2007). Following puromycin selection, transduced cells were divided into two populations: one was plated on poly-HEMA-coated tissue culture plates (plates were coated with poly-HEMA (20 mg/ml) (Sigma-Aldrich), dried at room temperature overnight, and washed with phosphate buffered saline (PBS) before use) and grown for 10 days, and the other was grown for 10 days under normal tissue culture conditions. Cells that survived 10 days in suspension (a time point at which >95% of cells transduced with the control NS shRNA were killed) were seeded under normal tissue culture conditions to expand the population. shRNAs present in the surviving suspension population and the attached population were identified by deep sequencing at the University of Massachusetts Medical School Deep Sequencing Core Facility (Worcester, MA). The frequency of individual shRNAs in each sample was determined as described previously (Xie et al.,

2012). The raw sequencing data have been uploaded to NCBI Gene Expression Omnibus with accession number GSE80144, and are accessible to reviewers through the following link: http://www.ncbi.nlm.nih.gov/geo/query/acc.cgi?token=inevskwqzxaprmb&acc=GSE80144.

For stable shRNA knockdowns, $1x10^5$ cells were seeded in a six-well plate to 50% confluency and subsequently transduced with 200 µl lentiviral particles expressing shRNAs (obtained from Open Biosystems/Thermo Scientific through the UMMS RNAi Core Facility, listed in Supplementary file 1) in a total volume of 1 ml of appropriate media supplemented with 6 µg/ml polybrene (Sigma-Aldrich). Media was replaced after overnight incubation to remove the polybrene, and viral particles and cells were subjected to puromycin selection (2 µg/ml) for 3 days.

qRT-PCR

Total RNA was isolated and reverse transcription was performed as described (Gazin et al., 2007), followed by qRT-PCR using Power SYBR Green PCR Master Mix (Applied Biosystems, Grand Island, NY). *RPL41* or *GAPDH* were used as internal reference genes for normalization. See Table 2.1 and 2.3 for primer sequences. Each sample was analyzed three independent times and the results from one representative experiment, with technical triplicates or quadruplicates, are shown.

Anoikis assays

Cells were placed in suspension in normal growth media in the presence of 0.5% methyl cellulose (Sigma Aldrich) (to avoid clumping of cells) on poly-HEMA-coated tissue culture plates. All anoikis assays were done at a cell density of $3x10^5$ cells/ml. Control cells were cultured under normal cell culture conditions. Cell death was measured by staining the cells with FITC-conjugated Annexin-V (ApoAlert, ClonTech) according to the manufacturer's instructions followed by analysis by flow cytometry (Flow Cytometry Core Facility, University of Massachusetts Medical School) at the indicated times. To restore integrin signaling in suspension, media was supplemented with 5% growth-factor-reduced Matrigel (BD Biosciences, San Diego, CA). Each sample was analyzed in biological triplicate

Immunoblot analysis

Cell extracts were prepared by lysis in Laemmli buffer in the presence of protease inhibitor cocktail (Roche, Indianapolis, IN). The following commercial antibodies were used: beta-ACTIN (Sigma-Aldrich); BNIP3, BNIP3L, KDM3A, H3K9me2 (all from Abcam, Cambridge, MA); cleaved Caspase 3, BIM, phospho-ERK1/2, total ERK1/2, phospho-EGFR, total EGFR, phospho-FAK (all from Cell Signaling Technology, Danvers, MA); total FAK (Millipore, Billerica, MA); GFP

(One World Lab, San Diego, CA); and α-tubulin (TUBA; Sigma-Aldrich).

Chemical Inhibitor Treatment

Cells were treated with dimethyl sulfoxide (DMSO), 1, 5 or 10 μM U0126 (Cell Signaling Technology), gefitinib (Santa Cruz Biotechnology, Inc., Dallas, TX), or FAK inhibitor 14 (CAS 4506-66-5, Santa Cruz Biotechnology, Inc.) for 48 hours prior to preparation of cell extracts or total RNA isolation, as described above.

ChIP assays

ChIP assays were performed as previously described (Gazin et al., 2007) using antibodies against KDM3A and H3K9me2 (both from Abcam) and H3K9me1 (Epigentek). ChIP products were analyzed by qPCR (see Table 2.2 for promoter-specific primer sequences). Samples were quantified as percentage of input, and then normalized to an irrelevant region in the genome (~3.2 kb upstream from the transcription start site of GCLC). Fold enrichment was calculated by setting the IgG control IP sample to a value of 1. Each ChIP experiment was performed three independent times and the results from one representative experiment, with technical duplicates, are shown.

Analysis of *KDM3A* expression in human breast cancer samples

This study was approved by the institutional review boards at the University of Massachusetts Medical School (UMMS) and the Mayo Clinic. Total RNA from 24 breast cancer patient samples were obtained from Fergus Couch (Mayo Clinic, Rochester, MN) and total RNA from five normal breast samples were obtained from the University of Massachusetts Medical School Tissue and Tumor Bank Facility. *KDM3A* expression was measured by qRT-PCR in technical triplicates of each patient sample. Statistical analysis (unequal variance t-test) was performed using R, a system for statistical computation and graphics (Ihaka and Gentleman, 1996). The Oncomine Cancer Profiling Database (Compendia Bioscience, Ann Arbor, MI) was queried using the cancer type Breast Cancer and a threshold p-value of 0.05 to access Finak (Finak et al., 2008), Sorlie (Sorlie et al., 2001), Zhao (Zhao et al., 2004) and TCGA (TCGA, 2011) datasets. Histograms depicting *KDM3A* gene expression in each sample, and the p value for the comparison of *KDM3A* expression between the groups, were obtained directly through the Oncomine software.

Animal experiments

All animal protocols were approved by the Institution Animal Care and Use Committee (IACUC). Animal sample sizes were selected based on precedent established from previous publications.

In vivo anoikis assays

CLS1 cells were stably transduced with either a NS or *Kdm3a* shRNA and selected with 2 µg/ml puromycin for 5 days. Stably transduced CLS1 cells ($2x10^5$) were injected into the tail vein of 4-6 week old female BALB/c mice (Taconic Biosciences) (n=4 mice per shRNA). Two weeks post injection the lungs were harvested, dissociated into single cell suspension, and plated onto tissue culture plates. Transduced CLS1 cells were selected for by treating the dissociated lung cells with 2 µg/ml puromycin. Surviving colonies were stained with crystal violet and quantified by counting. All experiments were performed in accordance with the Institutional Animal Care and Use Committee (IACUC) guidelines.

Pulmonary tumor assay

67NR cells were transduced with a NS or *Kdm3a* shRNA and selected with 2 µg/ml puromycin for 5 days. Stably transduced 67NR cells ($2x10^5$) were injected into the tail vein of 6-8 week old female BALB/c mice (n=3 mice per shRNA). Five weeks post injection, mice were given an intraperitoneal injection of D-Luciferin (100 mg/kg) (Gold Biotechnology, St. Louis, MO) and imaged on the Xenogen IVIS-100 (Caliper Life Sciences). Images were taken with Living Image software. All experiments were performed in accordance with the Institutional Animal Care and Use Committee (IACUC) guidelines.

Spontaneous metastasis assays

Female BALB/c mice (4-6 weeks) were purchased from Charles River Laboratories (Shrewsbury, MA). The mice were housed in facilities managed by the McGill University Animal Resources Centre (Montreal, Canada), and all animal experiments were conducted under a McGill University–approved Animal Use Protocol in accordance with guidelines established by the Canadian Council on Animal Care.

Spontaneous metastasis studies were carried out as previously described (Tabaries et al., 2011). Briefly, 4T07 cells expressing a NS or *Kdm3a* shRNA were harvested from subconfluent plates, washed once with PBS, and resuspended ($5x10^3$ cells) in 50 µl of a 50:50 solution of Matrigel (BD Biosciences) and PBS. This cell suspension was injected into the right abdominal mammary fat pad of BALB/c mice (n=10 mice per shRNA) and measurements were taken beginning on day 7 post-injection. Animals that did not develop a primary tumor were excluded from the study. Tumor volumes were calculated using the following formula: $\pi LW^2/6$, where L is the length and W is the width of the tumor. Tumors were surgically removed, using a cautery unit, once they reached a volume around 500 mm^3, approximately 3 weeks post injection. Lungs were collected 8 weeks post-injection. Tumor burden in the lungs was quantified from

four H&E stained step sections (200 µm/step). The number of lesions per section were counted using Imagescope software (Aperio, Vista, CA).

Small RNA Profiling

Total RNA was isolated with the mirVana kit (Thermo Fisher Scientific), then 18–24-nt-long RNA was gel purified. Size-selected RNA was derived from at least 50 µg total RNA for attached and detached (24 hours) MCF10A cells. Small RNA Library preparation was as described previously (Ghildiyal et al., 2008). Deep sequencing was performed at the Umass Medical School Deep Sequencing Core Facility. Reads were mapped to known human miRNAs using miRAnalyzer (Hackenberg et al., 2011).

Northern Blot Analysis

Total RNA was isolated with the mirVana kit (Thermo Fisher Scientific). At least 20 µg total RNA was loaded on a 15% denaturing urea-polyacrylamide gel. Semi-dry transfer was used to transfer the gel to a Hybond N+ nylon membrane (GE Healthcare Life Sciences). RNA was crosslinked to the membrane by irradiation with 254 nm UV light and the membrane was pre-hybridized with Church buffer at 37^{o}C. 5'end P^{32}-labeled Starfire probes (Integrated DNA Technologies) for miR-203 (TAGTGGTCCTAAACATTTCA) and U6 (CACGAATTTGCGTGTCATCCTTGCGCAGGGGCC) were added to the pre-

hybridization reaction and incubated overnight to detect miRNA. U6 RNA was used as a loading control.

miRNA-qRT-PCR

Total RNA was isolated with the mirVana kit (Thermo Fisher Scientific). At least 1 µg of RNA was used for cDNA reactions using the miScript II RT Kit (Qiagen) according to the manufacturer's protocol followed by qRT-PCR using the miScript SYBR Green kit (Qiagen) with the Universal Primer included in the kit and a forward primer specific to the miRNA of interest. U6 RNA was used as an internal control (see Table 2.4 for primer sequences). Each sample was analyzed three independent times and the results from one representative experiment, with technical triplicates or quadruplicates, are shown.

miRNA Ectopic Expression and Inhibition

For ectopic expression, the pre-miR-203 hairpin sequence was obtained from miRBase (mirbase.org). Pre-miR-203 was PCR amplified from MCF10A genomic DNA using primers (Forward 5'-AATCTCGAGCTCCTCTCTCCGCAGCTC-3′ and Reverse 5′- ATCGAATTCGCACCCCTGACTGTGACTCTG-3') engineered with restriction sites, EcoRI and XhoI, then cloned into pMSCVpuro (ClonTech Laboratories, Inc.). Cells stably expressing pMSCVpuro-pre-miR-203 or

pMSCVpuro-emtpy were generated by retroviral transduction as described previously (Santra et al., 2009).

For miRNA inhibition, a miArrest miRNA Inhibitor specific to miR-203 was obtained from Genecopoeia (Rockville, MD). The inhibitor was packaged into lentiviral particles and used to infect cells. The scrambled control inhibitor was also obtained from Genecopoeia.

AGO2 Immunoprecipitation

Cells were lysed for 30 minutes on ice in cell lysis buffer then centrifuged for 30 minutes at 14,000 rpm at 4°C. The supernatant was used as cell lysate for the IP. Mouse anti-AGO2 (Abcam) was coupled to Protein G Dynabeads (Thermo Fisher Scientific) then added to lysates. Antibody-lysate mixtures were rotated for 4 hours at 4°C to bind RISC in each sample. The beads were washed in IP wash buffer supplemented with a protease inhibitor cocktail then eluted in TriPure Reagent (Roche Life Sciences). mRNA was purified from immunoprecipitated protein complexes using the mirVana miRNA isolation kit (Thermo Fisher Scientific).

RNA sequencing and Data Analysis

Total RNA was extracted from MCF10A cells expressing a pMSCV-empty vector

control or a pMSCV-pre-miR-203 using the mirVana miRNA Isolation Kit (Thermo Fisher Scientific) and mRNA purification, cDNA synthesis, and amplification were carried out according to the TrueSeq RNA sample preparation guide (Illumina). Libraries were sequenced as 100-bp paired end using Illumina HiSeq 2000. All reads were mapped to the human genome using TopHat, followed by running Cufflinks to assemble and quantify the transcriptome (Trapnell et al., 2012). Empty Vector control and pMSCV-pre-miR-203 total RNA samples were run in duplicate. Ago2 IP RNA isolates were run in identical fashion. Relative abundances were measured in fragments per kilobase of exon per million fragments mapped (FPKM).

Statistics

All quantitative data were collected from experiments performed in at least triplicate, and expressed as mean ± standard deviation, with the exception of Figures 3.31 and 3.32, which are expressed as mean ± SEM. Differences between groups were assayed using two-tailed Student's t test, except where noted above. Significant differences were considered when $P<0.05$.

Gene	Forward primer sequence (5'->3')	Reverse primer sequence (5'->3')
BAD	aagactccagctctgcagag	Atgatggctgctgctggttg
BAK	tcgacttcatgctgcatcac	acaaactggcccaacagaac
BAX	actggacagtaacatggagctg	aaacatgtcagctgccactc
BID	tgttctgacaacagcttccg	atcagtctgcagctcatcgtag
BIK	tggctttcatctacgaccagac	gtggtgaaaccgtccatgaaac
BIM	tgcagacattttgcttgttcaa	Gaaccgctggctgcataataat
BMF	gaggtacagattgcccgaaa	Ttcaaagcaaggttgtgcag
BNIP3	Acgagcgtcatgaagaaagg	aatccgatggccagcaaatg
BNIP3L	tgcgaggaaaatgagcagtc	tgccattgctgctgttcatg
BOK	Acatctccctgcagtctgag	tgcctgcagagaagatgtgg
Gapdh	tgcaccaccaactgcttagc	Ggcatggactgtggtcatgag
HRK	caccagcgcaccatgtgg	cagccaaggccagtaggtg
JMJD1A	gagttcaaggctgggctattgt	ttcagccactttgatgcagcta
Jmjd1a	attcgagctgtttcccacac	tccaagactccccatcaaac
METAP1D	aacaacgtgctctgtcatgg	accacattcgtccacattgc
MULE	tcaccgcactgtgttaaacc	tgcgcttgacatcaaagtcg
NOXA	agagctggaagtcgagtgtg	gaagtttctgccggaagttcag
PIH1D3	tattcagacagcaggtgggaac	agccactagttcactgcaac
PUMA	acctcaacgcacagtacgag	acctaattgggctccatctcg
RPL41	cattaaatagccgtagacggaactt	gcgcagaggtttccaaaaaa
ZCCHC24	Tgccacatcaacgtgtatcca	ggccgtcgggcttctc
ZNF345	aaacagggatctcaggaaggac	ggatactgaaagtgggcatgtc

Table 2.1. qRT-PCR primer sequences for Chapter III.

Gene	Forward primer sequence (5' -> 3')	Reverse primer sequence (5' -> 3')
BNIP3	CACTAGCAGGATGGAAAGACG	ACTCTCTGGGCACTGGCTAC
BNIP3L	AGATACCCTGGGTAGCAGTAAC	ACCCGGTAAAGAACTAGCAGAG
JMJD1A	CGCTTGTAAAATGGGAGGCATG	TTGTGTGCTCTGGACCTGAAG
NCR (GCLC)	ATGGTTGCCACTGGGGATCT	TGCCAAAGCCTAGGGGAAGA

Table 2.2. ChIP-qRT-PCR primer sequences for Chapter III.

Gene	Forward primer sequence (5'->3')	Reverse primer sequence (5'->3')
AKAP7	acgctgaactagtaaggctcag	tgcttcggttttcacagagc
ANKH	ttcatggacgcaatggcatg	atctgagattgaggcacatccc
C4orf33	tgggaaggcaaagcttatctcc	tgtccttgctgcagttcatg
CSRNP2	ttaaatgccaggtggatcgc	attcaatgcgtcctgccatg
GMEB1	tttgcagttacagcctgtgc	tccgacccagcttcataaatcc
HBEGF	tttgaaagcccaaggtgctg	aaagctacaggcatggaagc
IFIT3	aagggcgaaggtgtgttttg	tacatcgcaattgccagtcc
IMPACT	accccaaatggacactttgc	taaatccgcacgttcttgcc
KIAA1430	tagcacccgggaaaaactactc	ttttgcttcccggcttttcc
KLC4	tgtacaggagtttgggtctgtg	tgccggcttttgctcatttc
LIN7C	tgaaagccgcacaaggaaag	ttgcctgcgttttgctgatc
LNX2	aaccgagcacacaaccattc	aatgccaagctgttcaccag
MAP4K3	aattgcatcagcgaggacac	ttaggctttggtggcaaagg
MSRB3	ttggccttcattccacgatg	aaaatgtgcccaaggtgagc
NEDD9	atcttggccatcaacaagcc	tgcgttggtgttgatggttg
NFIL3	aggccacgcaaaaactttcc	ttggggcactatgcttttcg
NIPAL3	acgccaacaacattgtcgtg	cccttgaatggacaagacaagc
PAPSS2	aaatatccgccggattgctg	attttgcgggcattctcacg
PARP11	ttgcaggaaaaaggctcagc	tgctggtaccatgaaacagc
PDE4D	tctgagcaacccaacaaagc	tttccacggaagcattgtgc
PDE6D	tggctttgtgatccctaactcc	ttaagacgcttgctggcatc
PPAP2B	aaatgacgctgtgctctgtg	agcagcccacttgcttatagag
PRKAB1	tctttgtggatggtcagtggac	acacatcggagcacttttgg
PRPS2	aggctgttgtcgtcacaaac	ttgcttcggccaagatcatg
PSMD5	tacggccattgcaaaccaac	agctttgtcatgctccacag
RAPGEF1	tgttgtactgcgaggcattc	tgacgcgcttcttgaatgtg
RASSF6	atcacagcaacaccctgaag	agctgcttcactcatggttc
RPRD2	tctcagcagagacccatttcac	atgggcgttttggtgcaaag
SEC24D	aatggctgccatcgattgtg	acactggattaaggctccactg
SEMA5A	aaggcctgttacagcaaagg	agacaggcgtgaatgcattg
SMG8	ttgctggaccaacttaggagtc	aaagttgttgtcggctgtgc
SOX13	tgccatgctgtttgagaagc	tgctgctgctttgcaatctg
TP63	tgcaggactcggacctgagt	tgttcaggagccccaggtt
TRPV4	ttttccgattcctgctcgtc	ttgcacaccttcatgttggc
TTC39A	aaaggcggcatcaaagttcg	ttgtgaggactgaacaaggc
USP8	gctgtcgaagaagctgaaagac	ttttgttgtagccgctgtgc
VAV3	tccaaaagtgctgggcattg	accagccatttgcactcatc
WDR69	tgcaactgcttcagctgatg	accttccagtttggcaatgc

ZNF281	ttgccaaagcctccttttgg	aggtgtcaactgctgatgtg
ZNF440	ttgtgtgtggagaagttggc	tgccttgtgtccaatgtcac
ZXDB	acacttggaaaagccgttgc	aaccatgtgcgtcttcatgc
pre-miR-203	gctgggtccagtggttctta	gccgggtctagtggtcctaa

Table 2.3. List of qRT-PCR primers for miR-203 candidate target genes (Chapter IV).

RNA	Forward primer sequence (5'->3')	Reverse primer sequence (5'->3')
miR-197	cgggtagagagggcagtgggagg	Universal Primer (Qiagen)
miR-203	gtgaaatgtttaggaccactag	Universal Primer (Qiagen)
miR-324	cgcatcccctagggcattggtgt	Universal Primer (Qiagen)
U6	ctcgcttcggcagcaca	aacgcttcacgaatttgcgt

Table 2.4. List of miRNA-qRT-PCR primer sequences (Chapter IV).

CHAPTER III: The histone H3K9 demethylase KDM3A promotes anoikis by transcriptionally activating pro-apoptotic genes *BNIP3* and *BNIP3L*

Preface

This research chapter derives from the work I started in my first year in Michael Green's lab, which was completed in the summer of 2016 when it was published in the journal *eLife* entitled "The histone H3K9 demethylase KDM3A promotes anoikis by transcriptionally activating pro-apoptotic genes *BNIP3* and *BNIP3L".* I am the first author of this publication with additional authors Stephane Gobeil, Sebastien Tabaries, Tessa Simone, Lihua (Julie) Zhu, Peter Siegel and Michael Green.

The project was initiated by Stephane Gobeil, a post doctoral associate in the Green lab who was my direct mentor for my first year in the lab. Stephane developed and performed the genome wide screen for anoikis effector genes and validated the candidates. Lihua (Julie) Zhu performed the bioinformatic analysis to identify the shRNAs in the deep sequencing of the genome wide screen. Stephane also helped perform the *in vivo* anoikis experiments. Michael Green and myself conceived all of the other experiments in this chapter. I performed and analyzed all of the subsequent experiments except for the *in vivo* spontaneous metastasis assays which were performed by Sebastien Tabaries in

the lab of Peter Siegel at McGill University, Sebastien and Peter also collected and analyzed the data from these experiments. Tessa Simone assisted with performing and analyzing the annexin-V FACS experiments and Lynn Chamberlain and Alysia Bryll provided experimental assistance. Michael Green and myself wrote the manuscript with editorial assistance from Sara Deibler. Douglas Green (St. Jude Hospital) provided valuable advice on the manuscript.

Abstract

Epithelial cells that lose attachment to the extracellular matrix undergo a specialized form of apoptosis called anoikis. Here, using large-scale RNA interference (RNAi) screening, we find that KDM3A, a histone H3 lysine 9 (H3K9) mono- and di-demethylase, plays a pivotal role in anoikis induction. In attached breast epithelial cells, KDM3A expression is maintained at low levels by integrin signaling. Following detachment, integrin signaling is decreased resulting in increased KDM3A expression. RNAi-mediated knockdown of KDM3A substantially reduces apoptosis following detachment and, conversely, ectopic expression of KDM3A induces cell death in attached cells. We find that KDM3A promotes anoikis through transcriptional activation of BNIP3 and BNIP3L, which encode pro-apoptotic proteins. Using mouse models of breast cancer metastasis we show that knockdown of Kdm3a enhances metastatic potential. Finally, we find defective KDM3A expression in human breast cancer cell lines and tumors. Collectively, our results reveal a novel transcriptional regulatory program that mediates anoikis.

Introduction

Epithelial cells that lose attachment to the extracellular matrix (ECM), or attach to an inappropriate ECM, undergo a specialized form of apoptosis called anoikis. Anoikis has an important role in preventing oncogenesis, particularly metastasis, by eliminating cells that lack proper ECM cues (Simpson et al., 2008; Zhu et al., 2001). Anoikis also functions to prevent the invasion of tumor cells into the luminal space, which is a hallmark of epithelial tumors (Debnath et al., 2002). In general, epithelial-derived cancers, such as breast cancer, develop resistance to anoikis (reviewed in (Schwartz, 1997). Several signaling pathways have been shown to regulate anoikis (reviewed in (Paoli et al., 2013). In particular, anoikis is suppressed by integrin signaling, which functions through focal adhesion kinase (FAK), an activator of the RAF/MEK/ERK pathway (King et al., 1997). FAK signaling is active in attached cells and is inactive following detachment (Frisch et al., 1996). Anoikis is also suppressed by integrin-mediated, ligand independent activation of the epidermal growth factor receptor (EGFR) signaling pathway (Moro et al., 1998), which, like FAK, also stimulates RAF/MEK/ERK activity.

These cell signaling pathways have been found to regulate the levels of BIM (also called BCL2L11) and BMF, two pro-apoptotic members of the BCL2 family of apoptosis regulators previously shown to contribute to anoikis (Reginato et al., 2003; Schmelzle et al., 2007). However, depletion of BIM or BMF diminishes but does not completely prevent anoikis (Reginato et al., 2003;

Schmelzle et al., 2007), suggesting the existence of other factors and regulatory pathways that can promote anoikis. Moreover, the basis of anoikis resistance remains to be determined and to date has not been linked to alterations in expression or activity of BIM or BMF.

Results

Identification of KDM3A as an anoikis effector in breast cancer epithelial cells.

To investigate the possibility that there are additional factors and regulatory pathways that promote anoikis, we performed a large-scale RNA interference (RNAi) screen for genes whose loss of expression confer anoikis resistance. The screen was performed in MCF10A cells, an immortalized but non-transformed human breast epithelial cell line that has been frequently used to study anoikis (see, for example, (Huang et al., 2010; Reginato et al., 2003; Schmelzle et al., 2007; Taube et al., 2006). A genome-wide human small hairpin RNA (shRNA) library comprising ~62,400 shRNAs directed against ~28,000 genes (Silva et al., 2003; Silva et al., 2005) was divided into 10 pools, which were packaged into retroviral particles and used to stably transduce MCF10A cells. Following selection, the cells were divided into two populations, one of which was plated on poly-2-hydroxyethylmethacrylate (HEMA)-coated plates for 10 days to inhibit cell attachment to matrix, and another that was cultured attached to matrix for 10 days as a control (Figure 3.1). Surviving cells were selected and shRNAs identified by deep sequencing. Bioinformatic analysis of the two populations identified 26 shRNAs whose abundance was significantly enriched >500-fold following detachment (Table 3.1); such shRNAs presumably

confer upon MCF10A cells a selective advantage by protecting them from undergoing anoikis.

To validate candidates isolated from the primary screen, we selected the top 20 most highly enriched shRNAs and analyzed them in an independent assay for their ability to confer resistance to anoikis. Briefly, MCF10A cells were transduced with a single shRNA, detached from matrix for 96 hours, and analysed for cell death by annexin V staining. As expected, knockdown of BIM, a positive control, decreased cell death following detachment compared to the control non-silencing (NS) shRNA (Figure 3.2). Of the 20 candidate shRNAs tested, five reduced the level of detachment-induced apoptosis compared to the NS shRNA, indicating they conferred anoikis resistance (Figure 3.2). Similar results were obtained using a second, unrelated shRNA directed against the same target gene (Figure 3.3). Quantitative RT-PCR (qRT-PCR) confirmed in all cases that expression of the target gene was decreased in the knockdown cell line (Figure 3.4).

One of the top scoring validated candidates was KDM3A (Table 3.1), a histone demethylase that specifically demethylates mono-methylated (me1) and di-methylated (me2) histone H3 lysine 9 (H3K9) (Yamane et al., 2006). H3K9 methylation is a transcriptional repressive mark, and the identification of KDM3A raised the intriguing possibility that induction of anoikis involves transcriptional

activation of specific genes through H3K9me1/2 demethylation. Therefore, our subsequent experiments focused on investigating the role of KDM3A in anoikis.

We asked whether ectopic expression of KDM3A was sufficient to promote cell death in attached cells. MCF10A cells were transduced with a retrovirus expressing wild-type KDM3A, a catalytically inactive KDM3A mutant [KDM3A(H1120G/D1122N)] (Beyer et al., 2008) or, as a control, empty vector (Figure 3.5), and then treated with puromycin for 10 days at which time viability was assessed by crystal violet staining. The results of Figure 3.5 show that ectopic expression of wild-type KDM3A but not KDM3A(H1120G/D1122N) greatly reduced MCF10A cell viability. Collectively, these results demonstrate that KDM3A is necessary and sufficient for efficient induction of anoikis in breast epithelial cells.

Detachment and loss of integrin and growth factor receptor signaling induces KDM3A expression.

We next examined the relationship between KDM3A expression and induction of anoikis. The immunoblot of Figure 3.6 shows that KDM3A protein levels were undetectable in attached MCF10A cells, but robustly increased in a time-dependent manner following detachment. The qRT-PCR analysis of Figure 3.6 shows that an increase in *KDM3A* expression following detachment was also detected at the mRNA level.

We next sought to understand the basis for the increase in KDM3A levels following detachment. As mentioned above, anoikis is suppressed by integrin signaling, which functions through FAK, a regulator of the RAF/MEK/ERK pathway (Frisch et al., 1996; King et al., 1997). Detachment causes a disruption in integrin–ECM contacts, resulting in a loss of FAK signaling in the detached cells (Frisch and Francis, 1994a; Frisch et al., 1996), which we observed have elevated KDM3A levels (see Figure 3.6). We therefore tested whether restoration of integrin signaling in detached cells would block the increase in KDM3A levels. The results of Figure 3.7 show that the addition of growth factor reduced Matrigel basement membrane-like matrix, which restores integrin signaling, to detached cells markedly blocked the elevated levels of the BIM isoform BIM_{EL}, as expected, and KDM3A. Treatment of MCF10A cells with a FAK inhibitor increased the levels of KDM3A protein and mRNA (Figure 3.8). Thus, the increase in KDM3A levels upon detachment of MCF10A cells is due, at least in part, to the loss of integrin/FAK signaling.

We next analyzed the relationship between the EGFR signaling pathway and KDM3A levels. In the first set of experiments, we ectopically expressed either EGFR or a constitutively active MEK mutant, MEK2(S222D/S226D) (MEK2DD) (Voisin et al., 2008), both of which have been previously shown to block anoikis in detached cells (Reginato et al., 2003). Consistent with these previous results, Figure 3.9 shows that in detached MCF10A cells, expression of

either EGFR or MEK2DD substantially decreased the level of BIM_{EL} (Reginato et al., 2003). Expression of either EGFR or MEK2DD also decreased the levels of KDM3A in detached MCF10A cells. Conversely, KDM3A protein levels were increased in attached MCF10A cells treated with the EGFR inhibitor gefitinib (Barker et al., 2001; Ward et al., 1994) (Figure 3.10) or the MEK inhibitor U0126 (Favata et al., 1998) (Figure 3.11). Both gefitinib and U0126 treatment also resulted in increased *KDM3A* mRNA levels (Figure 3.10 and 3.11).

KDM3A induces anoikis by transcriptionally activating *BNIP3* and *BNIP3L*.

The results described above suggest a model in which following detachment, the resulting increase in KDM3A demethylates H3K9me1/2 to stimulate expression of one or more pro-apoptotic genes. To test this model and identify pro-apoptotic KDM3A target genes, we took a candidate-based approach and analyzed expression of a panel of genes encoding pro-apoptotic BCL2 proteins (Boyd et al., 1994; Lomonosova and Chinnadurai, 2008; Matsushima et al., 1998) in attached MCF10A cells and detached cells expressing a NS or *KDM3A* shRNA. We sought to identify genes whose expression increased following detachment in control but not in *KDM3A* knockdown cells. We found that expression of the vast majority of genes encoding pro-apoptotic BCL2 proteins were unaffected by detachment in MCF10A cells (Figure 3.12). Consistent with previous results (Reginato et al., 2003; Schmelzle et al., 2007), expression of *BIM* and *BMF* were increased upon detachment. However,

knockdown of *KDM3A* did not decrease expression of either *BIM* or *BMF*. By contrast, following detachment, expression of *BNIP3* and *BNIP3L* increased, and were the only genes whose expression was diminished more than 2-fold by *KDM3A* knockdown (Figure 3.12). We therefore performed a series of experiments to determine whether *BNIP3* and *BNIP3L* are critical KDM3A target genes that mediate anoikis.

In the first set of experiments we analyzed BNIP3 and BNIP3L protein levels during anoikis induction. The immunoblot of Figure 3.13 shows that BNIP3 and BNIP3L levels were very low in attached cells and substantially increased following detachment, with a time course similar to that of detachment-induced KDM3A expression (see Figure 3.6). The chromatin immunoprecipitation (ChIP) experiment of Figure 3.14 shows that KDM3A was bound to the *BNIP3* and *BNIP3L* promoters in detached but not attached cells. Moreover, the levels of H3K9me2 and H3K9me1 (Figure 3.15) on the *BNIP3* and *BNIP3L* promoters were greatly diminished following detachment, which was counteracted by knockdown of *KDM3A*. Conversely, overexpression of KDM3A but not KDM3A(H1120G/D1122N) in attached MCF10A cells resulted in decreased levels of H3K9me1 and H3K9me2 on the *BNIP3* and *BNIP3L* promoters and increased expression of *BNIP3* and *BNIP3L* (Figure 3.16). Finally, knockdown of *BNIP3* or *BNIP3L* (Figure 3.17) resulted in decreased apoptosis following detachment (Figure 3.18). To further establish the pro-apoptotic role of BNIP3

and BNIP3L in MCF10A cells, we ectopically expressed BNIP3, BNIP3L or both in attached cells (Figure 3.19). Figure 3.19 shows that moderate cell death was observed upon ectopic expression of either BNIP3 or BNIP3L, but substantial cell death occurred in cells ectopically expressing both BNIP3 and BNIP3L. Collectively, these results establish *BNIP3* and *BNIP3L* as critical KDM3A target genes that mediate anoikis (Figure 3.20).

KDM3A **prevents metastasis and its expression is defective in human breast cancer cell lines and tumors.**

We considered the possibility that decreased *KDM3A* expression may contribute to anoikis resistance in breast cancer cells and performed a series of experiments to test this idea. We first analyzed a panel of human breast cancer cell lines (BT549, MDA-MB-231, MCF7, SUM149 and T47D) comparing, as a control, anoikis-sensitive MCF10A cells. As expected, detachment-induced apoptosis was significantly diminished in breast cancer cell lines compared to MCF10A cells, indicative of anoikis resistance (Figure 3.21). Moreover, following detachment of the breast cancer cell lines, induction of KDM3A at both the protein and mRNA (Figure 3.22) levels was much lower than that observed in MCF10A cells. However, ectopic expression of KDM3A was sufficient to induce apoptosis in each of the five breast cancer cell lines (Figure 3.23). Collectively,

these results indicate that anoikis-resistance of human breast cancer cells is due, at least in part, to inefficient induction of KDM3A following detachment.

We next analyzed *KDM3A* expression in human breast cancer patient samples. Interrogation of the Oncomine database (Rhodes et al., 2007) revealed decreased expression levels of *KDM3A* in several breast cancer datasets (Figure 3.24). To confirm these in silico results, we analyzed *KDM3A* expression by qRT-PCR in a series of human breast cancer patient samples. The results of Figure 3.25 show that compared to normal breast epithelium *KDM3A* expression was significantly decreased in a high percentage of breast cancers. Likewise, basal *KDM3A* expression levels were also diminished in most human breast cancer cell lines analyzed (Figure 3.26).

Finally, we performed a series of experiments to determine whether KDM3A affects metastatic potential. We first asked whether depletion of KDM3A would promote anoikis resistance *in vivo* using a mouse pulmonary survival assay. Briefly, immortalized but non-transformed mouse mammary epithelial CLS1 cells were stably transduced with an NS or *Kdm3a* shRNA (Figure 3.27) and injected into the tail vein of syngeneic mice. After 2 weeks, the lungs were harvested, dissociated into single cell suspensions, and plated in media containing puromycin to select for cells expressing the shRNA. The surviving colonies were visualized by crystal violet staining and quantified. The results of

Figure 3.27 show that *Kdm3a* knockdown significantly increased the number of cells that survived in the mouse lung relative to the control NS shRNA.

In a second set of experiments, we used a well-characterized mouse breast cancer carcinoma progression series comprising isogenic cell lines with increasing metastatic potential: (1) non-invasive and non-metastatic 67NR cells, which form primary tumors, (2) invasive and non-metastatic 4T07 cells, which enter the circulation but fail to establish secondary tumors, and (3) highly metastatic 4T1 cells, which disseminate widely and colonize distant organ sites (Aslakson and Miller, 1992). qRT-PCR analysis revealed decreased *Kdm3a* expression in cell lines with greater metastatic potential (Figure 3.28). We expressed either a control NS shRNA or a *Kdm3a* shRNA in 67NR cells containing a luciferase reporter gene (Figure 3.29). Cells were injected into the tail veins of three syngeneic mice and pulmonary metastases were visualized by live animal imaging after 5 weeks. The results of Figure 3.29 show, as expected, that control 67NR cells failed to form pulmonary metastases in any of the three mice analyzed. By contrast, *Kdm3a* knockdown 67NR cells formed substantial pulmonary metastases in all three mice.

Finally, in a more stringent metastasis experiment, control and *Kdm3a* knockdown 4T07 cells (Figure 3.30), a non-metastatic mouse breast cancer cell line, were injected in the mammary fat pad of ten syngeneic mice. After 22 days

the primary tumors were surgically removed and 8 weeks post-injection the animals were sacrificed and pulmonary tumors quantified. The growth of primary tumors formed by NS or *Kdm3a* knockdown cells was similar (Figure 3.31). However, *Kdm3a* knockdown cells caused significantly increased metastatic burden in the lungs compared to control 4T07 cells (Figure 3.32). Consistent with our results, knockdown of *Bnip3* has also been shown to cause increased metastasis in similar *in vivo* experiments (Manka et al., 2005). Collectively, these results show that KDM3A functions to prevent metastasis.

Figures

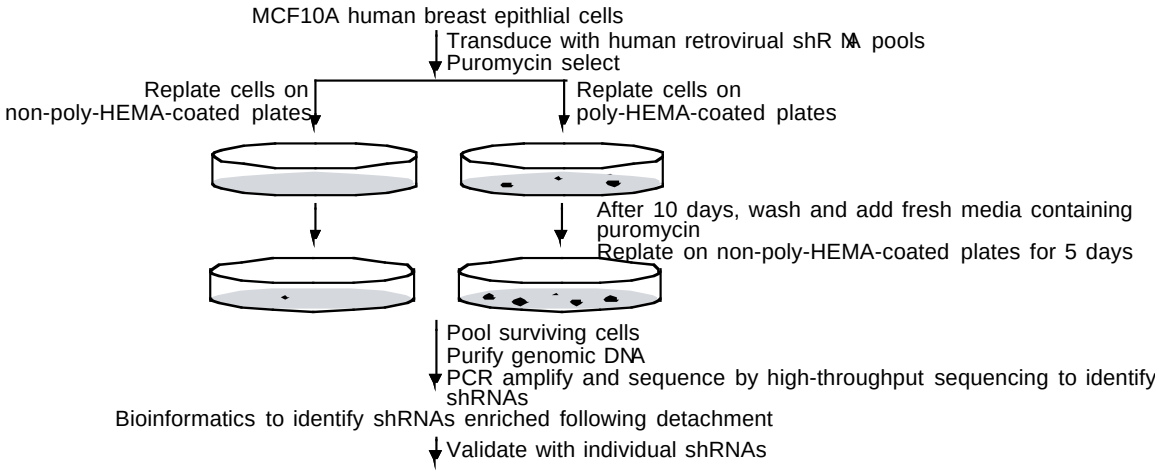

Figure 3.1. Schematic of the design of the large-scale RNAi screen to identify anoikis effectors.

Fold enrichment (detached vs. attached)	shRNA sequence	Gene symbol	Gene name
1620.792946	TAACACTTCACTGTAACTC	*ZCCHC24*	zinc finger CCHC-type containing 24
1324.931564	AAATGCTTCACAATCAAAG	*KDM3A*	lysine demethylase 3A
1139.789798	TAATCTTCAAATAAGCTGA	*RALBP1*	ralA binding protein 1
947.6848454	TCACTTACAAGTTTCTTTC	*RFC1*	Replication factor C subunit 1
848.4223889	AATATAAGGATTGCTATCG	*LRIG3*	leucine-rich repeats and immunoglobulin like domains 3
798.0503961	TTAAGTAGCTTAGAGAGGG	*PIH1D3*	PIH1 domain containing 3
720.0231915	TGTCATTCCAAGAGATCCT	*DKK1*	dickkopf WNT signaling pathway inhibitor 1
710.1463302	ATTTGCCGGAGGATCAAGG	*SENP6*	SUMO1/sentrin specific peptidase 6
681.0095893	AATCTAATACATTAATCTG	*PLEKHG1*	pleckstrin homology and RhoGEF domain containing G1
671.1327279	TTGGAGATGAGGCTCAGTG	*FGD5*	FYVE, RhoGEF and PH domain containing 5
665.2066111	TAATCCAATAATTCATTTC	*LOC339524*	
659.2804943	TTAAAATGGAGACACCATC	*METAP1D*	methionyl aminopeptidase type 1D (mitochondrial)
645.3541198	ATTCCTTCAAGATTTCAAG	*VMP1*	vacuole membrane protein 1
633.6006548	TCTCTGATGCTGAGTAAGG	*ZNF345*	zinc finger protein 345
619.2792059	TTCTATCGAATAAGCAATC	*FAM227B*	family with sequence similarity 227 member B
610.5022036	TTACGTTTCTGAATTTCTG	*PDE7A(variant 2)*	phosphodiesterase 7A
609.6640814	AACTTATAGACATTCAGAC	*GPC5*	glypican 5
605.9454431	TTCCCTCACATGTGGGATG	*AP4M1*	adaptor related protein complex 4 mu 1 subunit
598.4192748	ATTGAAATATTGAAACTTC	*SUSD1*	sushi domain containing 1
561.9934101	ATAGAGAAAGTCTTTATAC	*RBFOX3*	RNA binding protein, fox-1 homolog (C. elegans) 3
559.5241948	TAGAATAAGAACTACTGTC	*DNAJB9*	DnaJ heat shock protein family (Hsp40) member B9
543.6619555	TTAATCTTATCTTTGCCTG	*CYP39A1*	cytochrome P450 family 39 subfamily A member 1
527.4243955	TGAAAGACTTAACAATTGG	*CECR5-AS1*	CECR5 antisense RNA 1
526.4367093	TAACTTCAAAGGTGTATCC	*ADH7*	alcohol dehydrogenase 7 (class IV), mu or sigma polypeptide
518.5352203	ATAGATATATGCATTTAGG	*RNF125*	ring finger protein 125, E3 ubiquitin protein ligase
513.1029465	TATTAGGAATCTTAACCAC	*HOXA11*	homeobox A11

Table 3.1 List of 26 shRNAs, and the target genes, whose abundance was significantly enriched >500-fold following detachment of MCF10A cells.

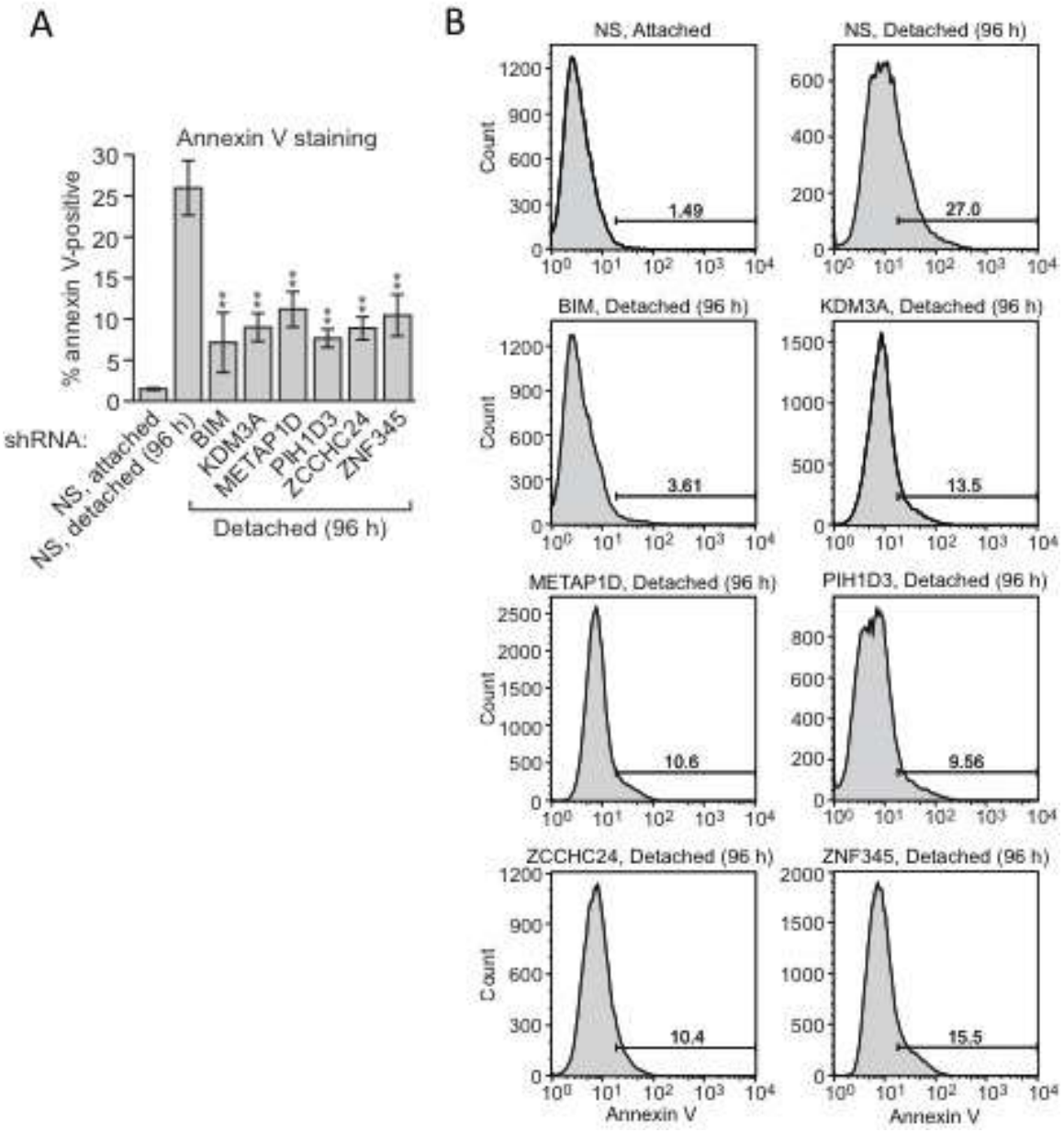

Figure 3.2. Knockdown of anoikis effector candidate genes causes a resistance to anoikis. (A) Cell death, monitored by annexin V staining, in MCF10A cells expressing a non-silencing (NS) shRNA and cultured attached to the matrix, or in detached cells (cultured in suspension for 96 h) expressing a NS shRNA or one of five candidate shRNAs. Error bars indicate SD. *P* value comparisons are made to the detached, NS shRNA control. ***P*<0.01. (B) FACS analysis. Representative FACS plots corresponding to the bar graph in A.

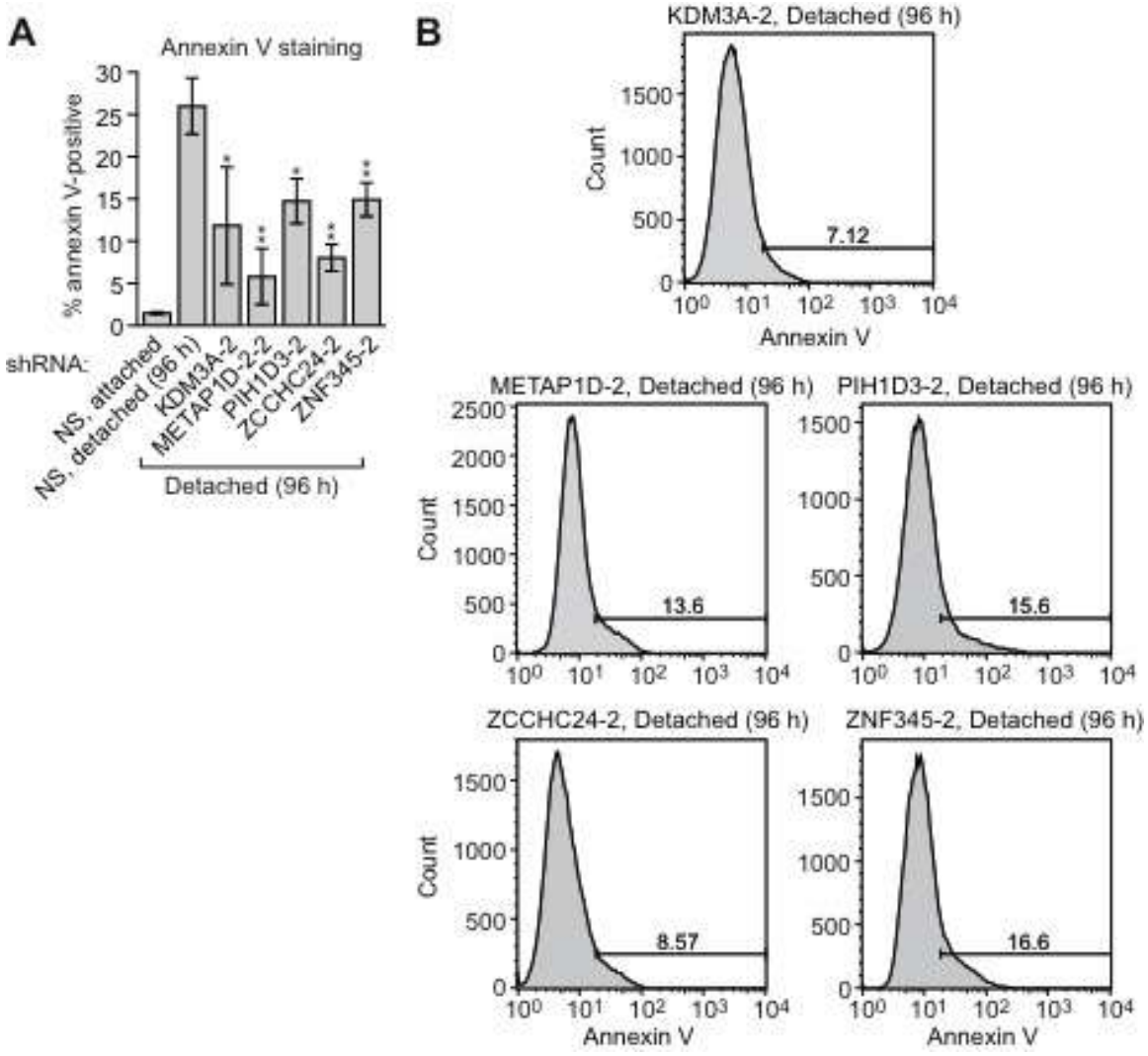

Figure 3.3. Knockdown of anoikis effector candidate genes with a second shRNA also causes a resistance to anoikis. (**A**) Cell death, monitored by annexin V staining, in MCF10A cells expressing a non-silencing (NS) shRNA and cultured attached to the matrix, or in detached cells (cultured in suspension for 96 h) expressing a NS shRNA or one of five candidate shRNAs unrelated to those used in Figure 3-2. Error bars indicate SD. ***P*<0.01. (**B**) Representative FACS plots corresponding to (A).

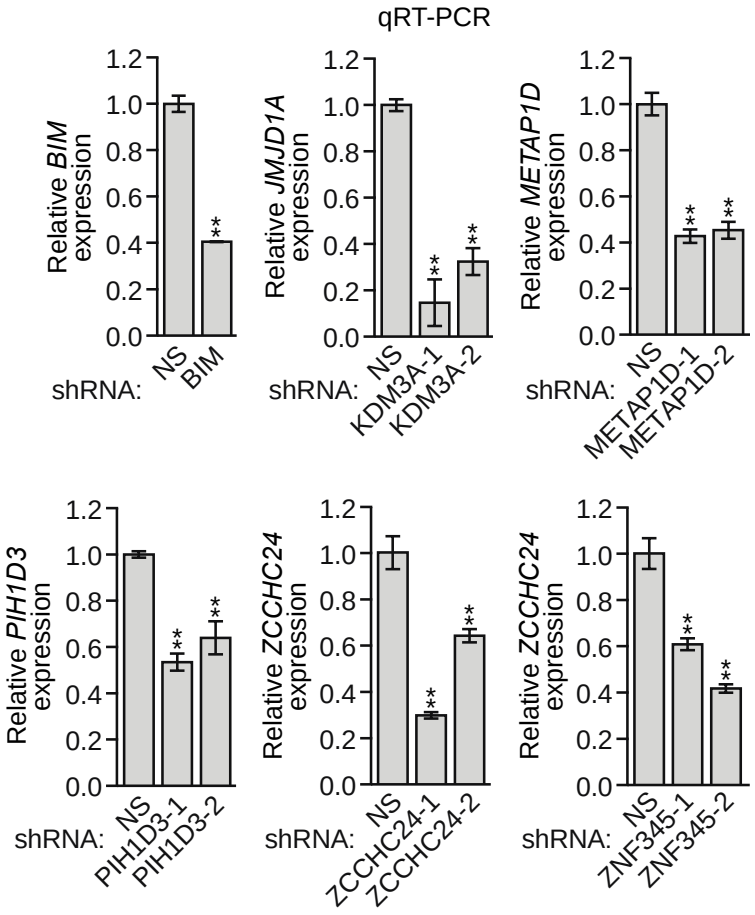

Figure 3.4. Analysis of *BIM* and candidate shRNA knockdown efficiencies. qRT-PCR analysis monitoring knockdown efficiencies of *BIM* and two unrelated shRNAs directed against the five candidate genes in MCF10A cells. Error bars indicate SD. **P*<0.05; ***P*<0.01.

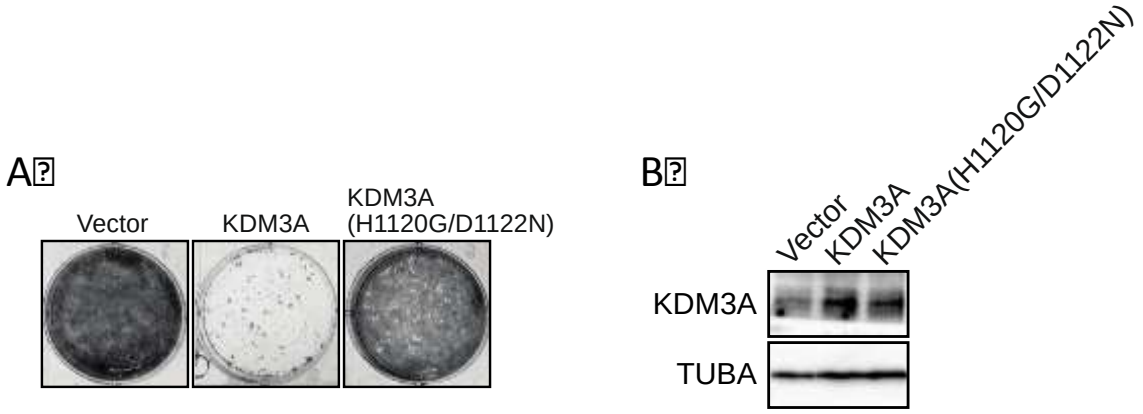

Figure 3.5. Ectopic expression of WT KDM3A but not a catalytic dead mutant causes cell death in MCF10A cells. (**A**) Crystal violet staining of MCF10A cells expressing vector, KDM3A or the catalytically-inactive KDM3A(H1120G/D1122N) mutant. (**B**) Immunoblot analysis monitoring levels of KDM3A in MCF10A cells expressing vector, KDM3A or KDM3A(H1120G/D1122N). The results confirm increased expression of KDM3A in cells transfected with KDM3A-expressing plasmids. α-tubulin (TUBA) was monitored as a loading control.

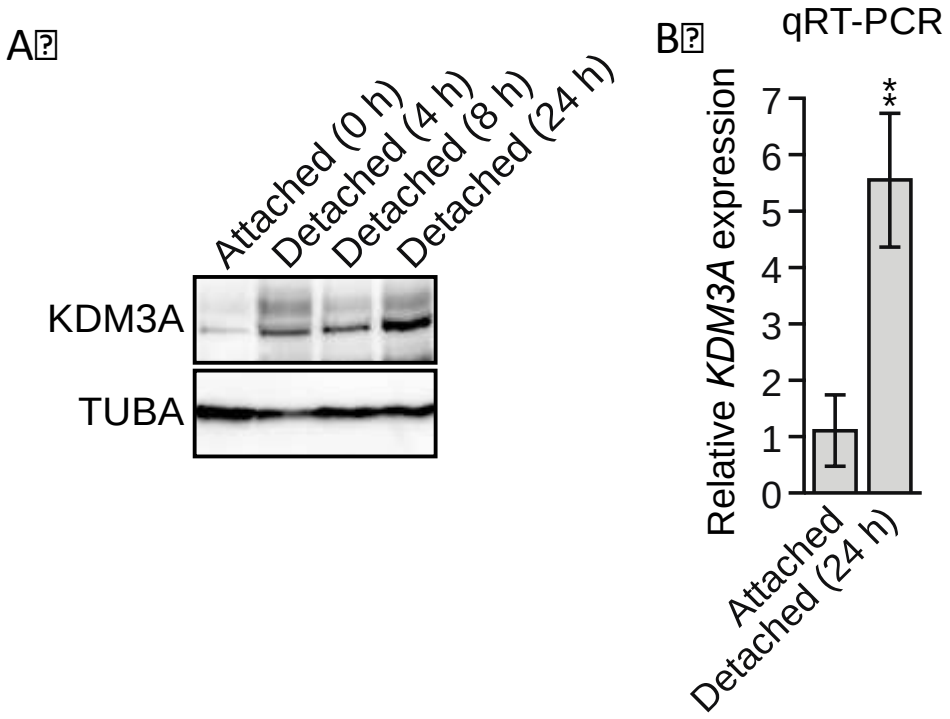

Figure 3.6. KDM3A is induced upon detachment from the ECM. (**A**) Immunoblot monitoring KDM3A levels in attached MCF10A cells, or detached cells cultured in suspension for 4, 8 or 24 h. β-actin (ACTB) was monitored as a loading control. (**B**) qRT-PCR analysis monitoring *KDM3A* mRNA levels in attached MCF10A cells, or detached cells cultured in suspension for 24 h. Error bars indicate SD. ***P*<0.01.

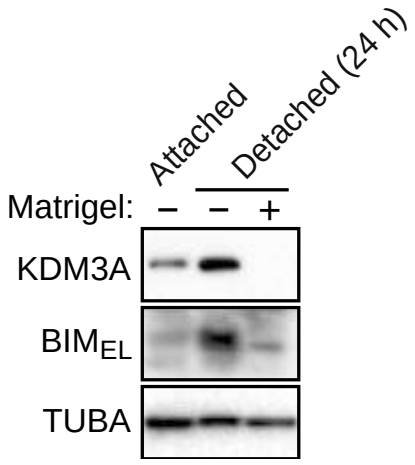

Figure 3.7. The induction of KDM3A upon detachment from the ECM is due to the loss of integrin signaling. Immunoblot monitoring levels of KDM3A and BIM_{EL} in attached MCF10A cells or detached MCF10A cells cultured in suspension for 24 h and treated in the presence or absence of Matrigel. α-tubulin (TUBA) was monitored as a loading control.

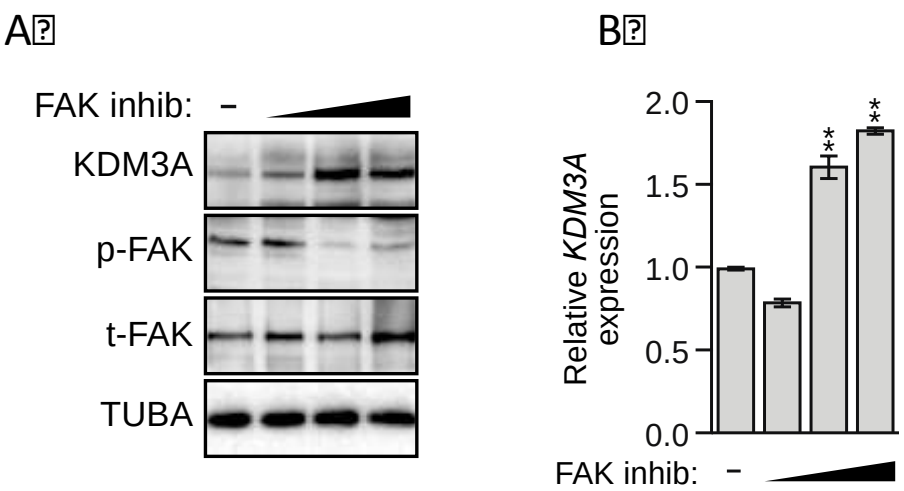

Figure 3.8. Inhibition of FAK in attached MCF10A cells causes induction of KDM3A. (**A**) Immunoblot monitoring levels of KDM3A, phosphorylated FAK (p-FAK) or total FAK (t-FAK) in MCF10A cells treated for 48 hours with 0, 1, 5 or 10 μM FAK inhibitor. (**B**) qRT-PCR analysis monitoring *KDM3A* expression in MCF10A cells treated for 48 hours with 0, 1, 5 or 10 μM FAK inhibitor.

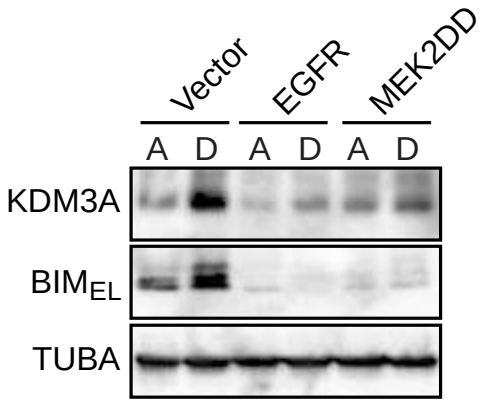

Figure 3.9. Ectopic expression of EGFR or an activated form of MEK blocks the induction of KDM3A upon detachment from the ECM. Immunoblot monitoring levels of KDM3A and BIM_{EL} in MCF10A cells expressing either vector, EGFR or MEK2DD and cultured as attached (A) or detached (D) cells grown in suspension for 24 h.

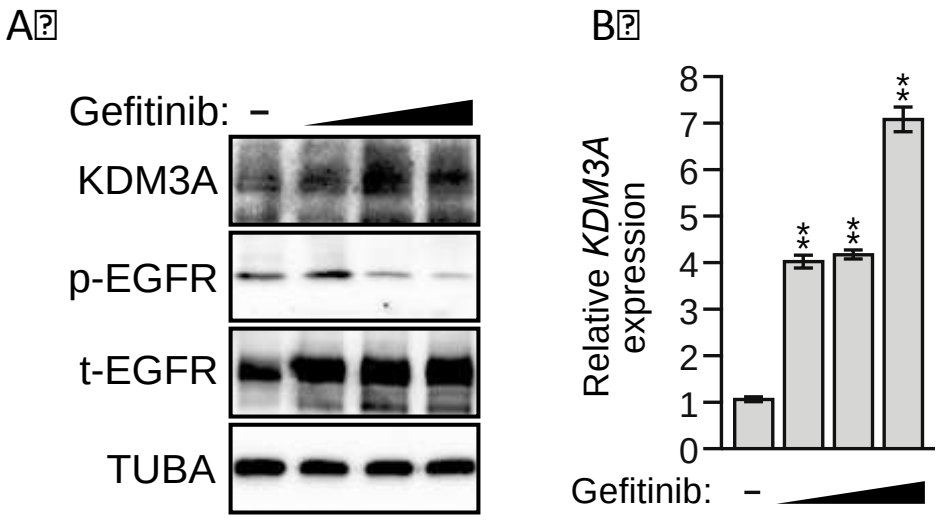

Figure 3.10. Inhibition of EGFR in attached MCF10A cells causes induction of KDM3A. (**A**) Immunoblot monitoring levels of KDM3A, phosphorylated EGFR (p-EGFR) or total EGFR (t-EGFR) in MCF10A cells treated for 48 hours with 0, 1, 5 or 10 µM Gefitinib. (**B**) qRT-PCR analysis monitoring *KDM3A* expression in MCF10A cells treated for 48 hours with 0, 1, 5 or 10 µM Gefitinib.

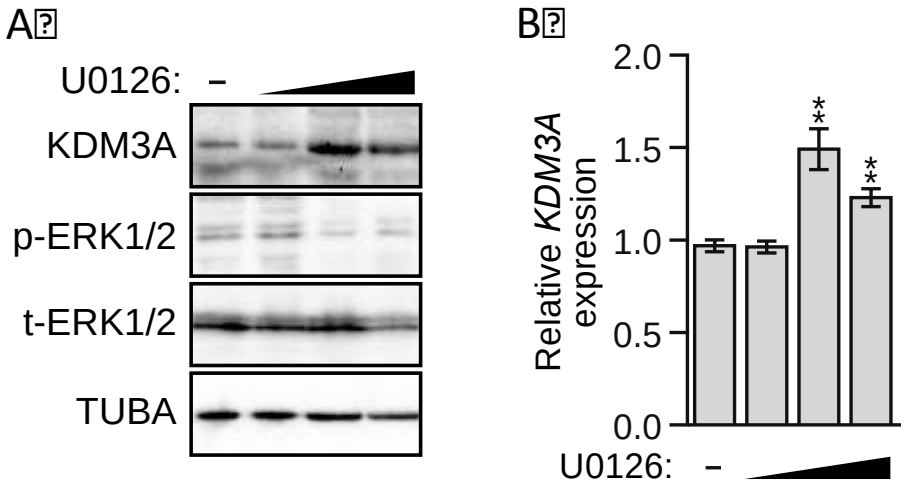

Figure 3.11. Inhibition of ERK in attached MCF10A cells causes induction of KDM3A. (**A**) Immunoblot monitoring levels of KDM3A, phosphorylated ERK (p-ERK) or total ERK (t-ERK) in MCF10A cells treated for 48 hours with 0, 1, 5 or 10 μM U0126. (**B**) qRT-PCR analysis monitoring *KDM3A* expression in MCF10A cells treated for 48 hours with 0, 1, 5 or 10 μM U0126.

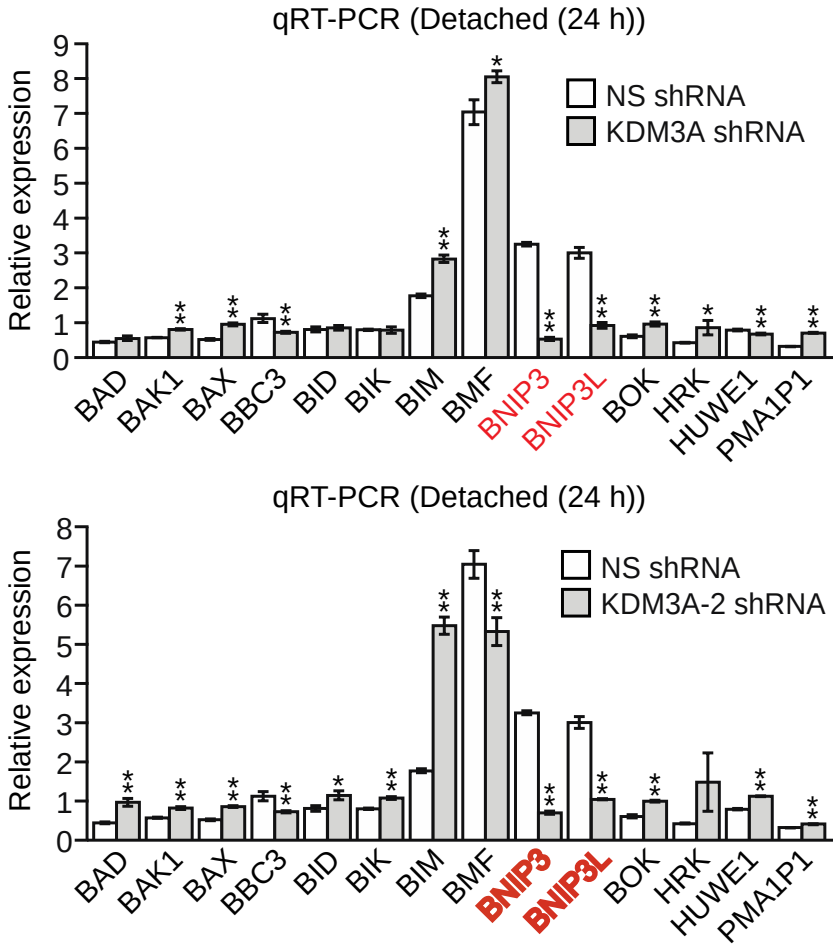

Figure 3.12. Knockdown of KDM3A abrogates the induction of BNIP3 and BNIP3L upon detachment of MCF10A cells from the ECM. (**A**) qRT-PCR analysis monitoring expression of pro-apoptotic BCL2 genes in detached MCF10A cells grown in suspension for 24 h and expressing a NS or *KDM3A* shRNA. The expression of each gene is shown relative to that obtained in attached cells expressing a NS shRNA, which was set to 1. *P* value comparisons for each gene are made to the NS shRNA control. Genes whose expression is decreased >2-fold upon *KDM3A* knockdown are indicated in red. (**B**) qRT-PCR analysis monitoring expression of BCL2 pro-apoptotic genes in detached MCF10A cells expressing a NS or a second, unrelated *KDM3A* shRNA to that used in Figure 3A. The expression of each gene is shown relative to that obtained in attached cells, which was set to 1. Error bars indicate SD. **P*<0.05; ***P*<0.01.

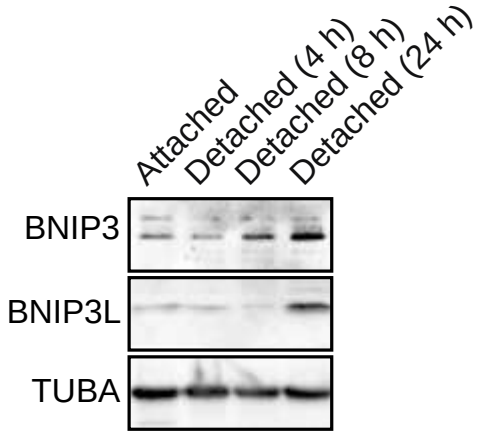

Figure 3.13. BNIP3 and BNIP3L are induced upon detachment from the ECM. Immunoblot analysis monitoring levels of BNIP3 and BNIP3L in attached MCF10A cells, and detached cells following growth in suspension for 4, 8 or 24 h.

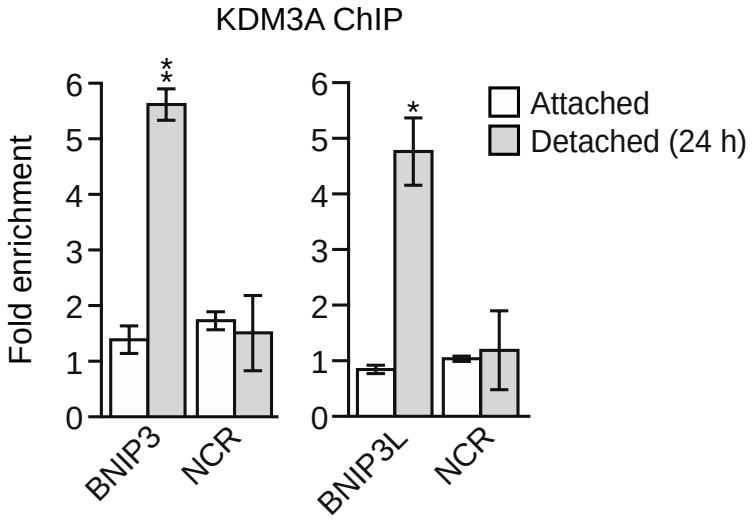

Figure 3.14. KDM3A is enriched on the promoters of BNIP3 and BNIP3L upon detachment from the ECM. ChIP monitoring binding of KDM3A on the promoters of *BNIP3* and *BNIP3L* or a negative control region (NCR) in attached MCF10A cells or detached cells grown in suspension for 24 h. *P* value comparisons for each region are made to the attached control. Error bars indicate SD. **P*<0.05; ***P*<0.01

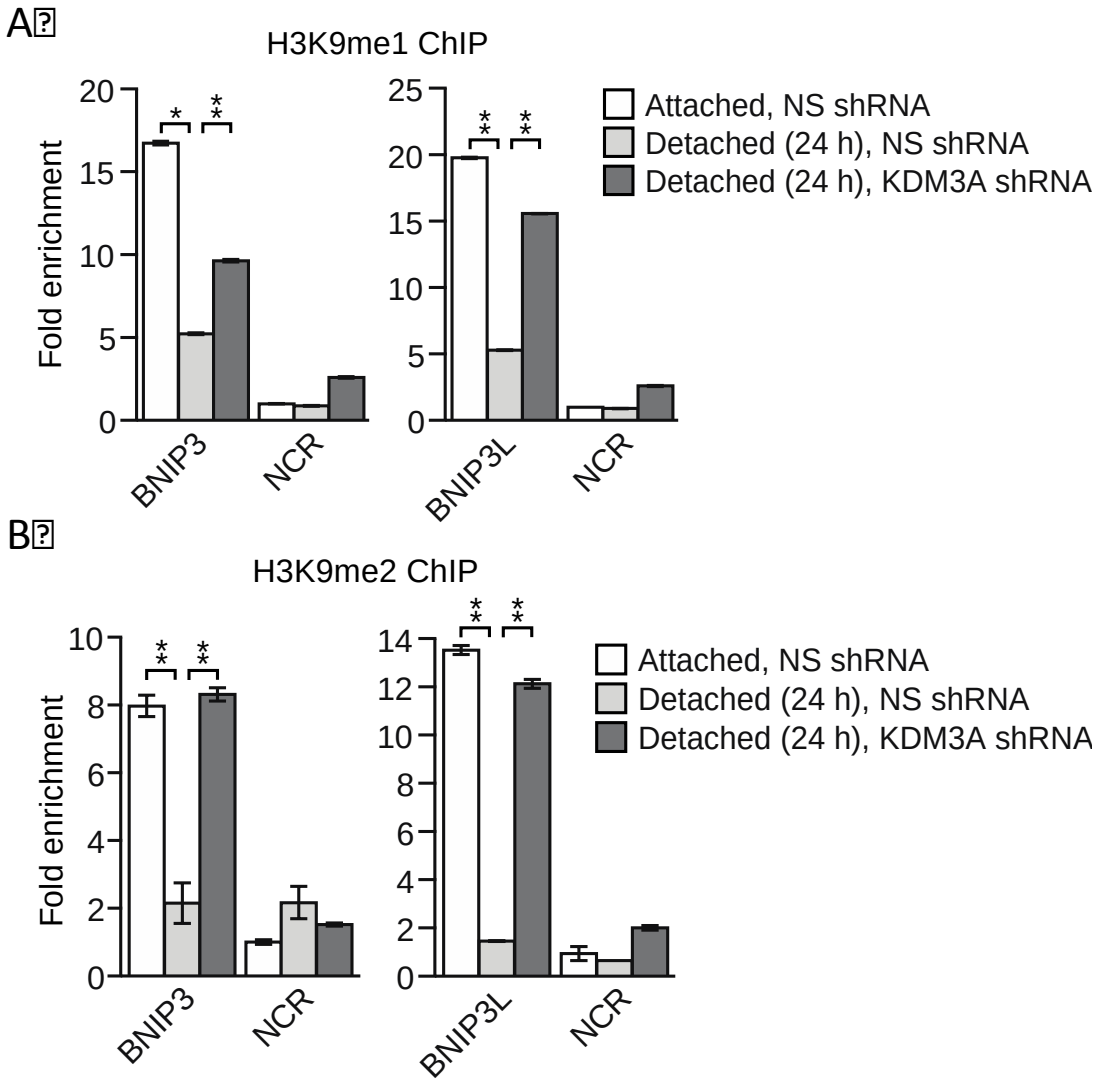

Figure 3.15. The levels of H3K9me1 and H3K9me2 on the *BNIP3* and *BNIP3L* promoters are diminished following detachment, which is counteracted by knockdown of *KDM3A*. (A) ChIP monitoring the levels of H3K9me1 on the promoters of *BNIP3* and *BNIP3L* or a negative control region (NCR) in attached MCF10A cells or detached cells expressing a NS or *KDM3A* shRNA and grown in suspension for 24 h. (B)ChIP monitoring the levels of H3K9me2 on the promoters of *BNIP3* and *BNIP3L* or a negative control region in attached MCF10A cells or detached cells expressing a NS or *KDM3A* shRNA and grown in suspension for 24 h. *P* value comparisons for each region are made to the detached, NS shRNA control. Error bars indicate SD. **P*<0.05; ***P*<0.01.

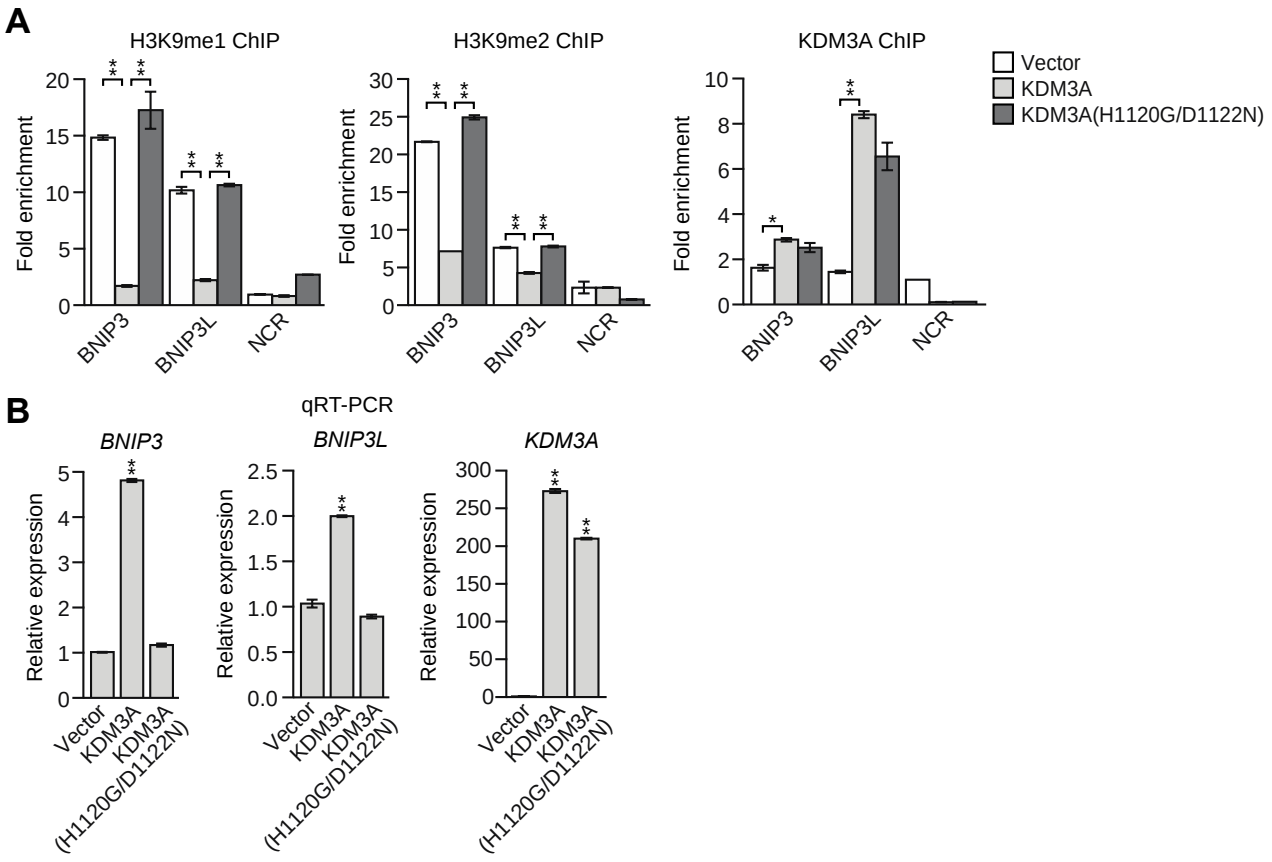

Figure 3.16. Overexpression of KDM3A, but not KDM3A(H1120G/D1122N), in attached MCF10A cells results in decreased levels of H3K9me1 and H3K9me2 on the *BNIP3* and *BNIP3L* promoters and increased expression of *BNIP3* and *BNIP3L*. (**A**) ChIP monitoring the levels of H3K9me1, H3K9me2 and KDM3A on the promoters of *BNIP3* and *BNIP3L* or a negative control region (NCR) in attached MCF10A cells expressing empty vector, wild-type KDM3A or KDM3A(H1120G/D1122N). The increased occupancy of KDM3A(H1120G/D1122N) on the *BNIP3* and *BNIP3L* promoters is not unexpected because the mutations are in the catalytic domain and should not affect DNA binding. (**B**) qRT-PCR analysis monitoring expression of *BNIP3*, *BNIP3L* or *KDM3A* in attached MCF10A cells expressing empty vector, wild-type KDM3A or KDM3A(H1120G/D1122N). Error bars indicate SD. **P*<0.05; ***P*<0.01.

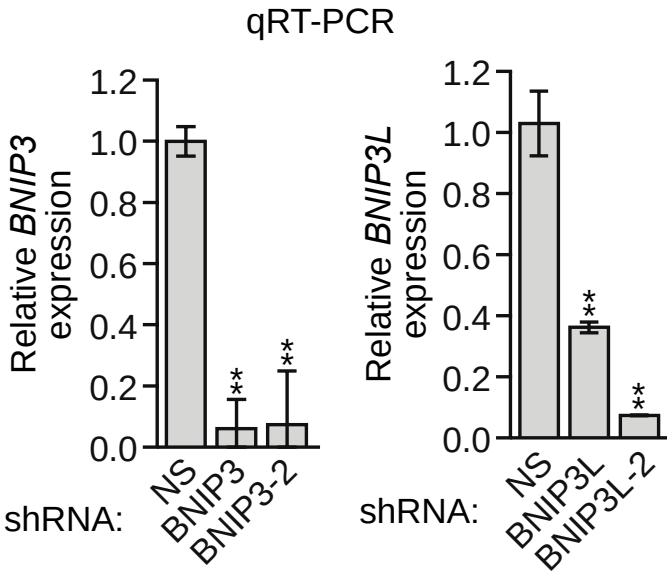

Figure 3.17. Analysis of *BNIP3* and *BNIP3L* shRNA knockdown efficiencies. qRT-PCR analysis monitoring knockdown efficiency of two unrelated *BNIP3* and *BNIP3L* shRNAs in MCF10A cells. Error bars indicate SD. ***P*<0.01.

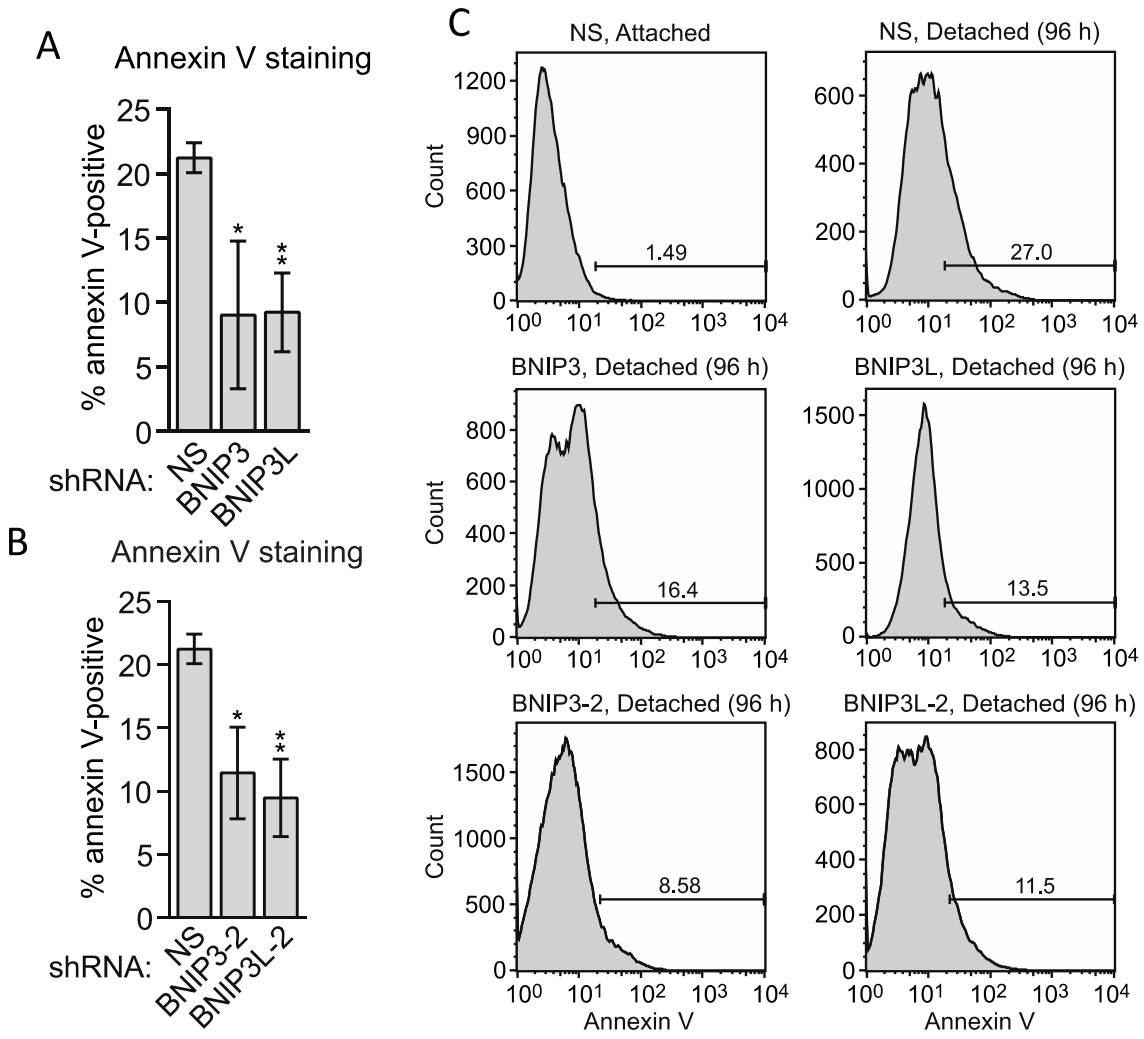

Figure 3.18. Knockdown of BNIP3 and BNIP3L causes resistance to anoikis upon detachment from the ECM. (**A**) Cell death, monitored by annexin V staining, in MCF10A cells expressing a NS, *BNIP3* or *BNIP3L* shRNA. (**B**) Cell death, monitored by annexin V staining, in MCF10A cells expressing a non-silencing (NS) shRNA or *BNIP* or BNIP3L *shRNA* unrelated to that used in A. Error bars indicate SD. **P*<0.05; ***P*<0.01. (**C**) Representative FACS plots corresponding to A and B

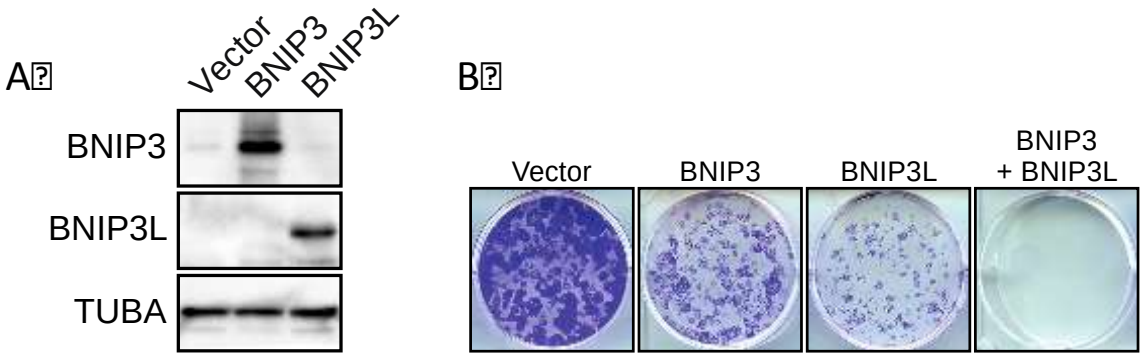

Figure 3.19. Ectopic expression of BNIP3 and BNIP3L causes cell death in attached MCF10A cells. (**A**) Immunoblot analysis monitoring levels of BNIP3 or BNIP3L in MCF10A cells expressing vector, BNIP3 or BNIP3L. The results confirm increased expression of the proteins. α-tubulin (TUBA) was monitored as a loading control. (**B**) Crystal violet staining of MCF10A cells expressing vector, BNIP3, BNIP3L or both BNIP3 and BNIP3L

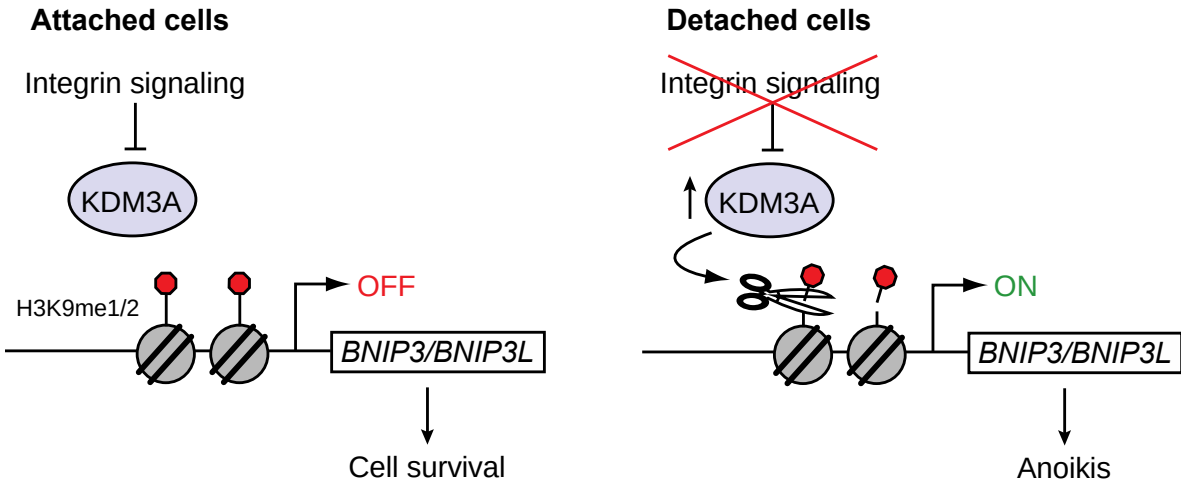

Figure 3.20. KDM3A induces anoikis by transcriptionally activating *BNIP3* and *BNIP3L*. Model of KDM3A activity in response to detachment from the ECM in MCF10A cells. When MCF10A cells are detached from the ECM the loss of integrin signaling leads to the induction of KDM3A, which then demethylates H3K9me1 and H3K9me2 on the promoters of *BNIP3* and *BNIP3L* leading to transcriptional activation and subsequent cell death.

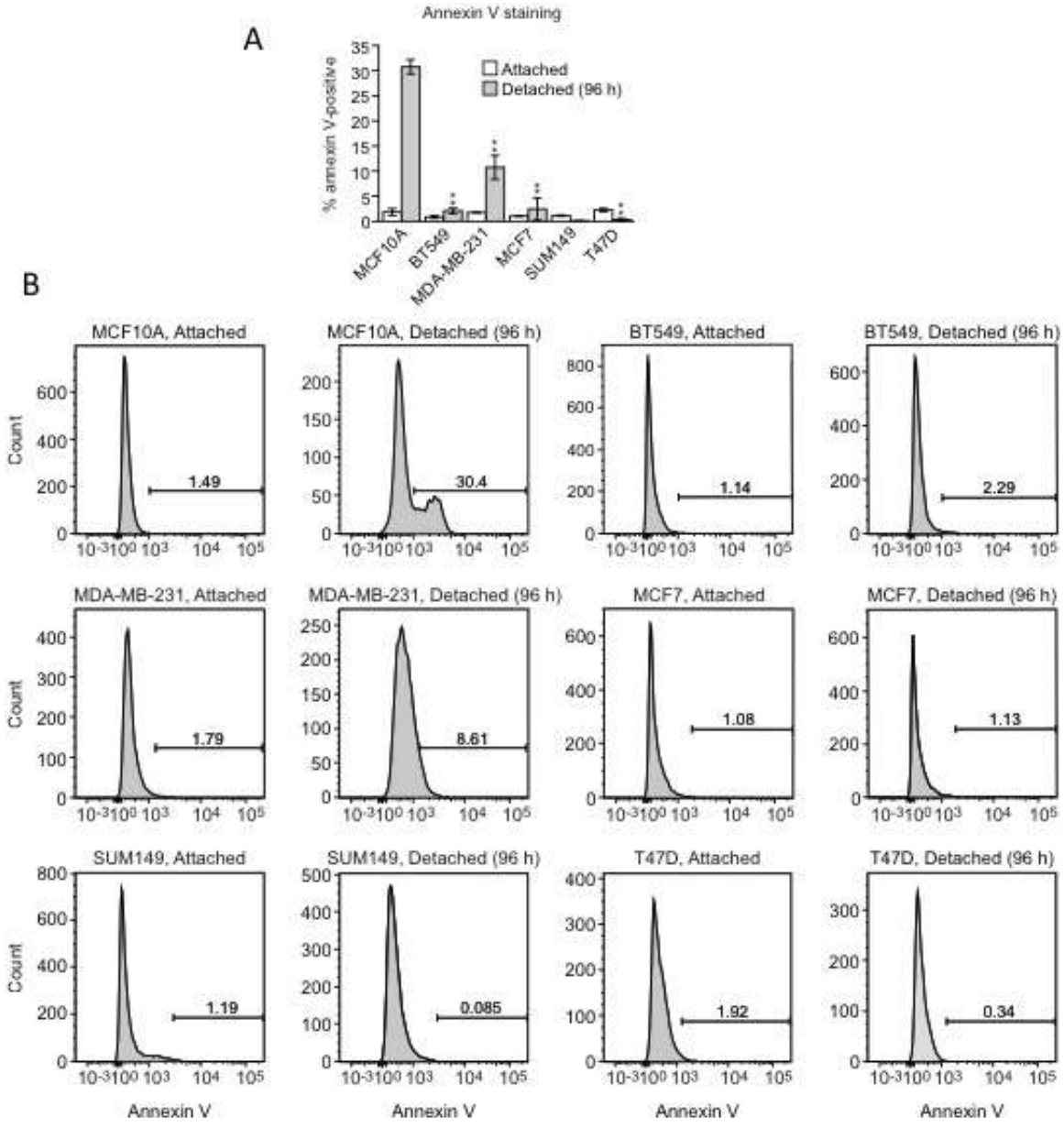

Figure 3.21. Breast cancer cell lines are resistant to anoikis. (**A**) Cell death, monitored by annexin V staining, in MCF10A cells and a panel of human breast cancer cell lines cultured as attached cells or detached following growth in suspension for 96 h. Error bars indicate SD. *P* value comparisons for each breast cancer cell line are made to the detached MCF10A sample. **P*<0.05; ***P*<0.01. (**B**) Representative FACS plots corresponding to A.

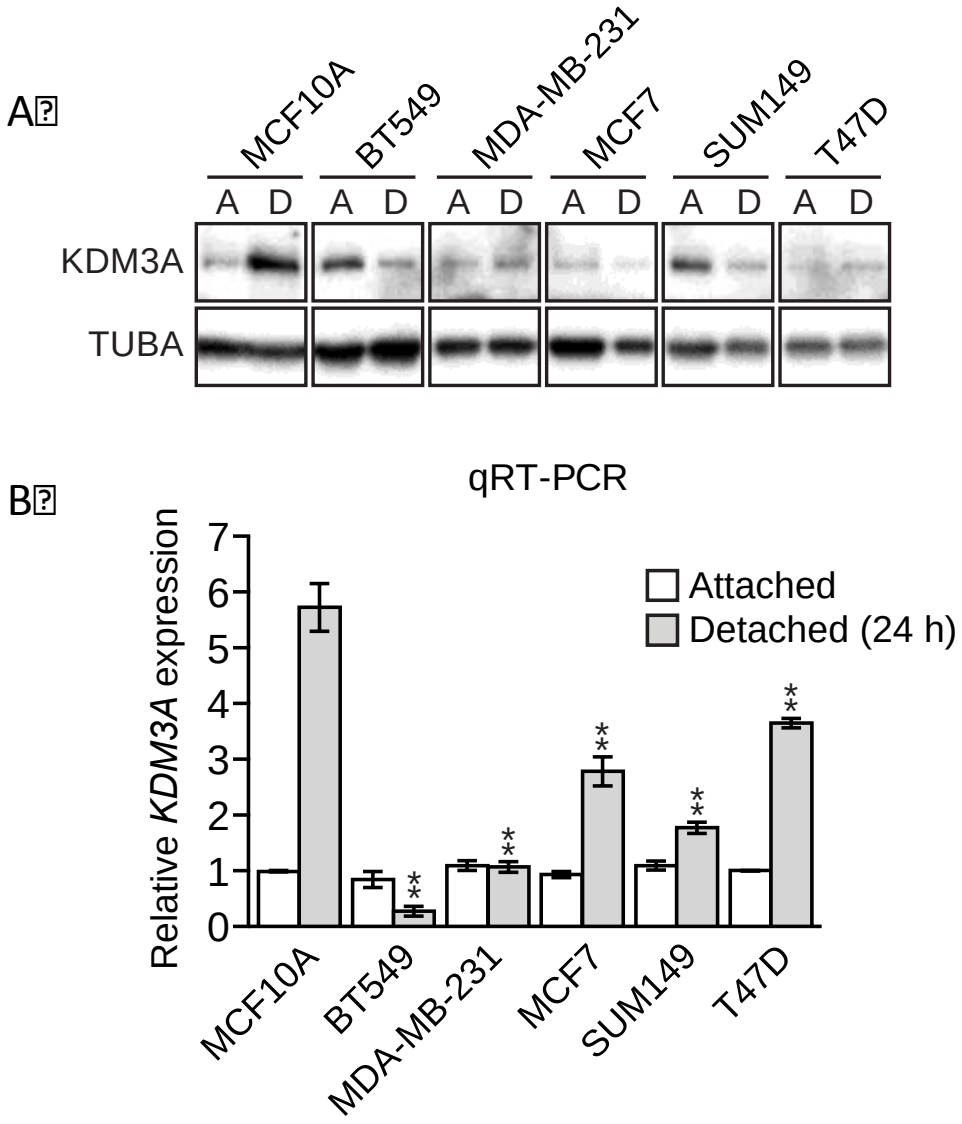

Figure 3.22. KDM3A is not induced in anoikis resistant breast cancer cell lines upon detachment from the ECM. (**A**) Immunoblot analysis monitoring KDM3A levels in MCF10A cells and a panel of human breast cancer cell lines cultured as attached (A) cells or detached (D) following growth in suspension for 24 h. All images for the KDM3A antibody were cropped from the same blot, and thus were processed and exposed in the same manner, as were images for the TUBA loading control. (**B**) qRT-PCR analysis monitoring *KDM3A* expression in MCF10A cells and a panel of human breast cancer cell lines cultured as attached cells or detached following growth in suspension for 24 h. Error bars indicate SD. *P* value comparisons for each breast cancer cell line are made to the detached MCF10A sample. **P*<0.05; ***P*<0.01.

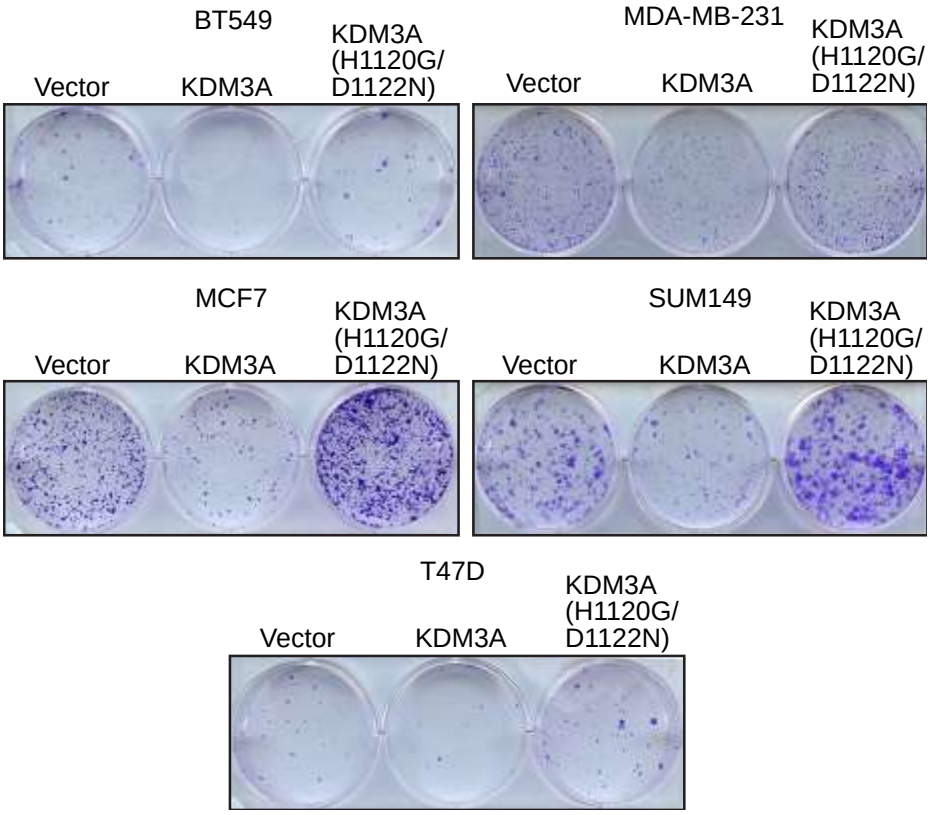

Figure 3.23. Ectopic expression of WT KDM3A, but not catalytically inactive KDM3A, causes cell death in a panel of breast cancer cell lines. Crystal violet staining of human breast cancer cells expressing vector, KDM3A or KDM3A(H1120G/D1122N).

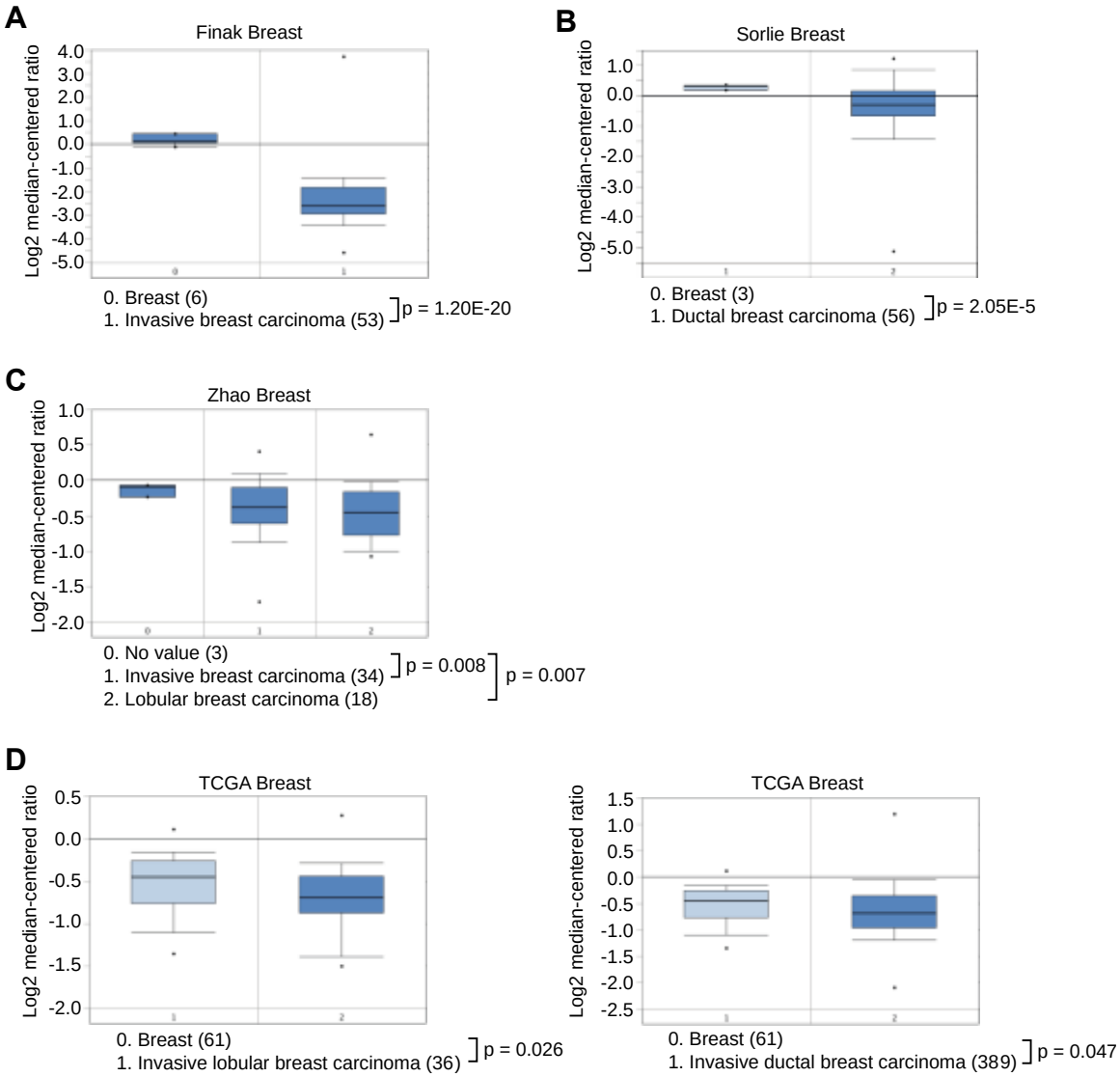

Figure 3.24. Oncomine analysis of *KDM3A* expression in breast cancer. The Oncomine Cancer Profiling database was queried to access Finak (A), Sorlie (B), Zhao (C) and The Cancer Genome Atlas (TCGA) (D) breast cancer data sets. The results reveal that *KDM3A* is significantly under-expressed in breast carcinoma relative to normal tissue.

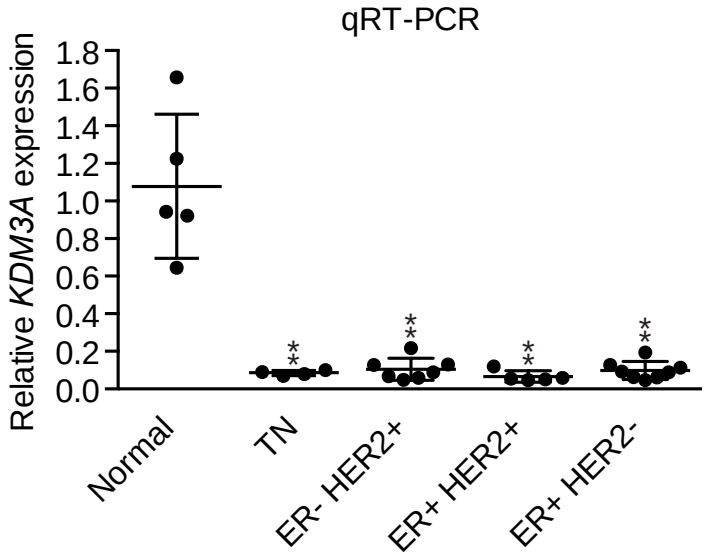

Figure 3.25. Human breast cancers have a low expression of *KDM3A* compared to normal breast tissue. qRT-PCR analysis monitoring *KDM3A* expression in normal breast epithelial cells and human breast tumors. TN, triple negative [estrogen receptor-negative (ER-), human epidermal growth factor receptor 2-negative (HER2-) and progesterone receptor-negative (PR-)]. Error bars indicate SD. The differences in expression between subtypes were not statistically significant. **P*<0.05; ***P*<0.01.

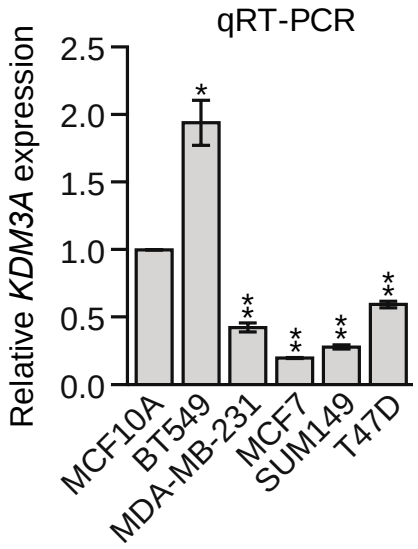

Figure 3.26. A panel of breast cancer cells have a low level of basal KDM3A expression in attached cells. qRT-PCR analysis of *KDM3A* expression in MCF10A cells and a panel of human breast cancer cell lines cultured as attached cells. The results were normalized to that obtained in MCF10A cells, which was set to 1. The results show that basal *KDM3A* expression levels were diminished in four of five human breast cancer cell lines analyzed. Error bars indicate SD. **P*<0.05; ***P*<0.01.

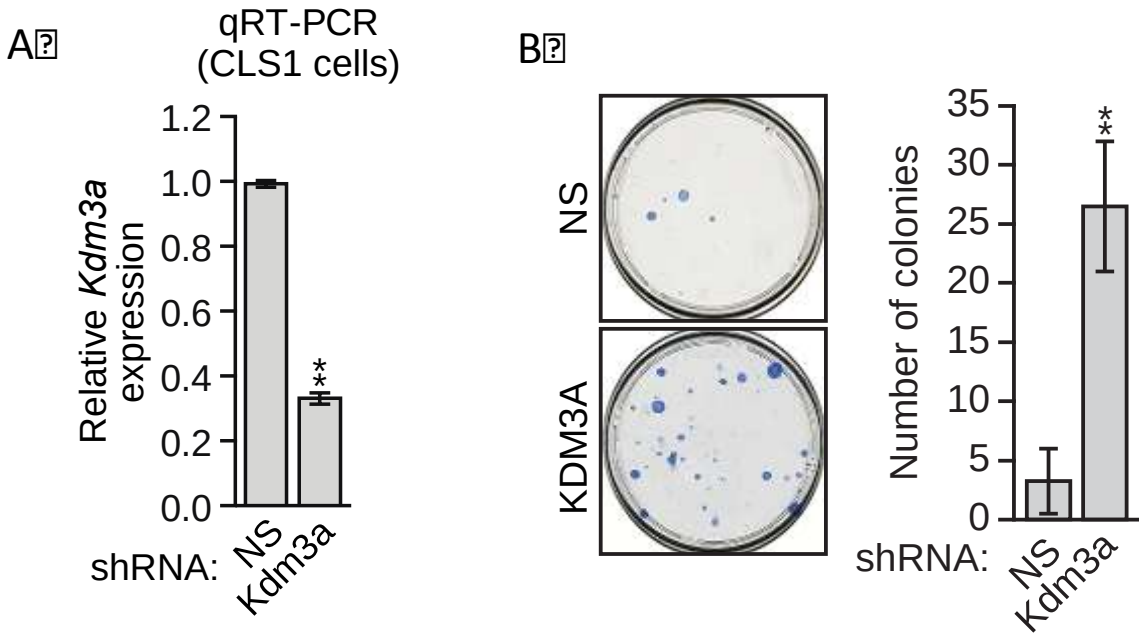

Figure 3.27. Knockdown of Kdm3a in CLS1 cells causes resistance to anoikis *in vivo*. (A) qRT-PCR analysis monitoring knockdown efficiency of *Kdm3a* in CLS1 cells. Error bars indicate SD. (B) Mouse pulmonary survival assay. (Left) Representative plates showing colony formation of CLS1 cells expressing a NS or *Kdm3a* shRNA that had been isolated from mouse lungs following tail vein injection. (Right) Quantification of colony formation (n=4 mice per shRNA). Error bars indicate SD. **P*<0.05; ***P*<0.01.

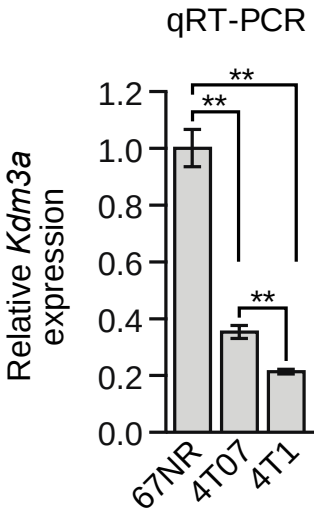

Figure 3.28. *Kdm3a* expression progressively decreases across a mouse breast cancer carcinoma progression series. qRT-PCR analysis of *Kdm3a* expression in 67NR, 4T07, and 4T1 cells. Error bars indicate SD. ***P*<0.01.

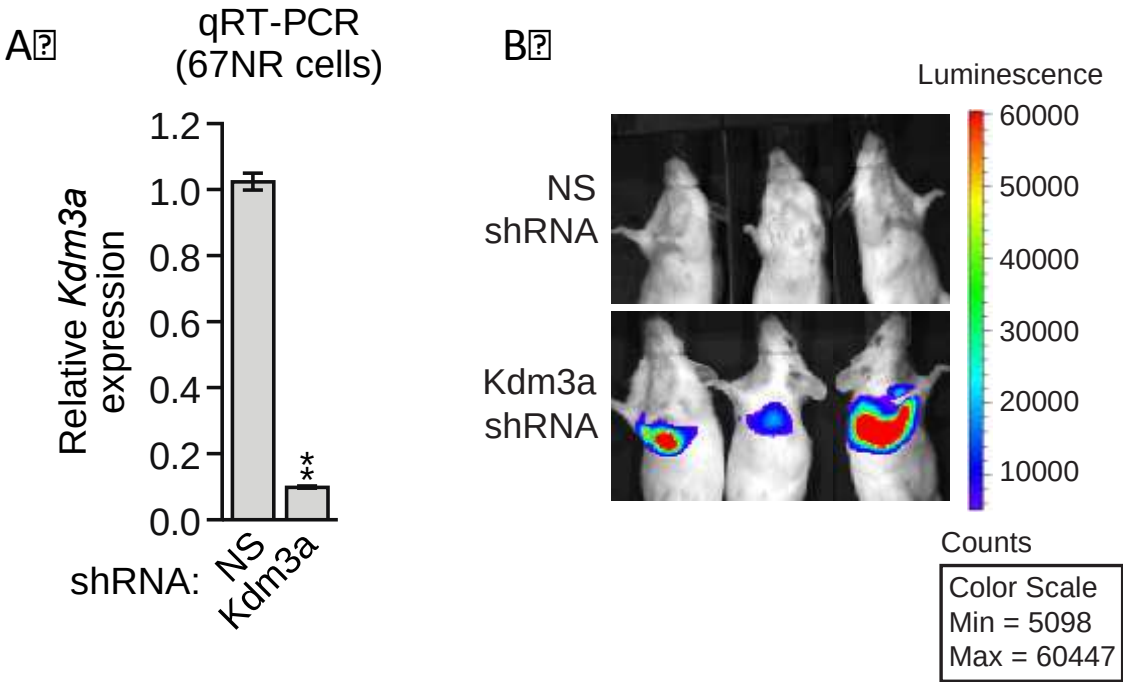

Figure 3.29. Knockdown of *Kdm3a* in 67NR cells causes tumor growth in the lungs. (**A**) Analysis of *Kdm3a* shRNA knockdown efficiency in mouse 67NR cells. qRT-PCR analysis monitoring knockdown efficiency of *Kdm3a* in 67NR cells. Error bars indicate SD. ***P*<0.01. (**B**) Live animal imaging monitoring lung tumor metastasis in mice following injection of 67NR cells expressing a NS or *Kdm3a* shRNA (n=3 mice per group).

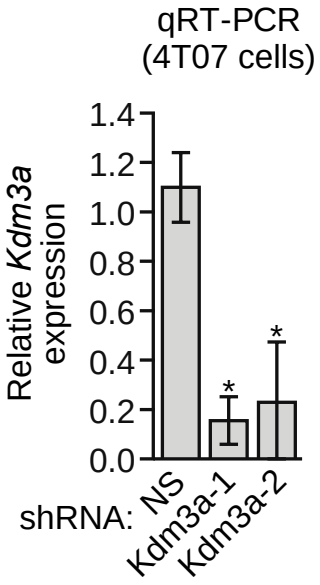

Figure 3.30. Analysis of *Kdm3a* shRNA knockdown efficiency in mouse 4T07 cells. qRT-PCR analysis monitoring knockdown efficiency of two unrelated *Kdm3a* shRNAs in 4T07 cells. Error bars indicate SEM. **P*<0.05.

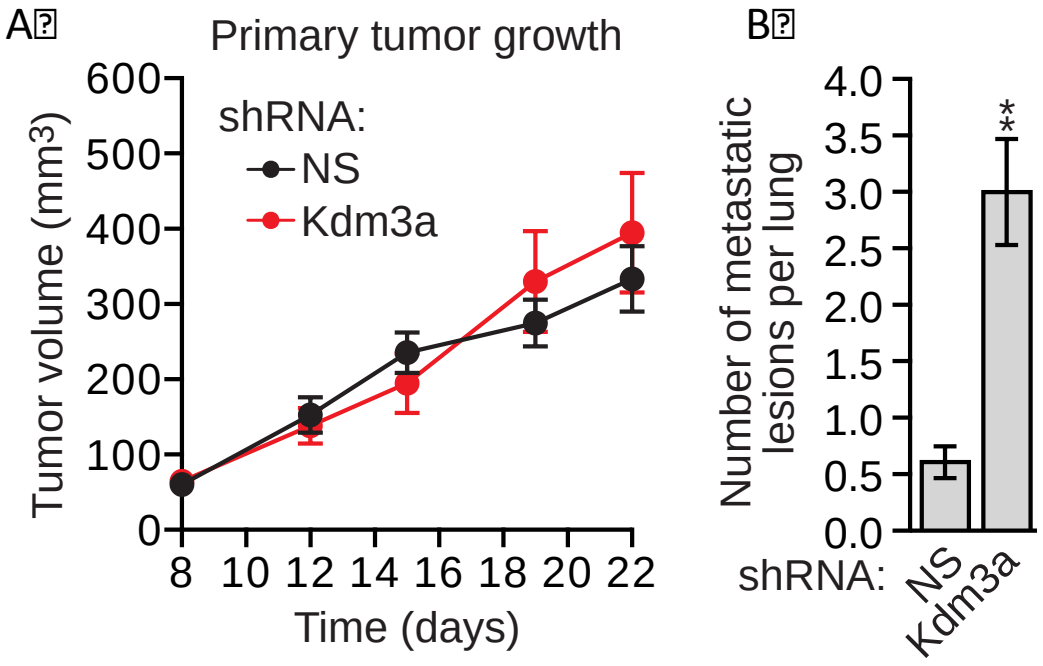

Figure 3.31. Knockdown of *Kdm3a* in 4T07 cells leads to increased metastatic burden in the lungs. (**A**) Primary tumor growth in mice injected with 4T07 cells expressing a NS (n=7) or *Kdm3a* (n=8) shRNA. Error bars indicate SEM. The differences in primary tumor growth between groups were not statistically significant. (**B**) Metastatic burden. Number of metastatic lesions per lung in mice injected with 4T07 cells expressing a NS (n=7) or *Kdm3a* (n=8) shRNA. Error bars indicate SEM. ***P*<0.01.

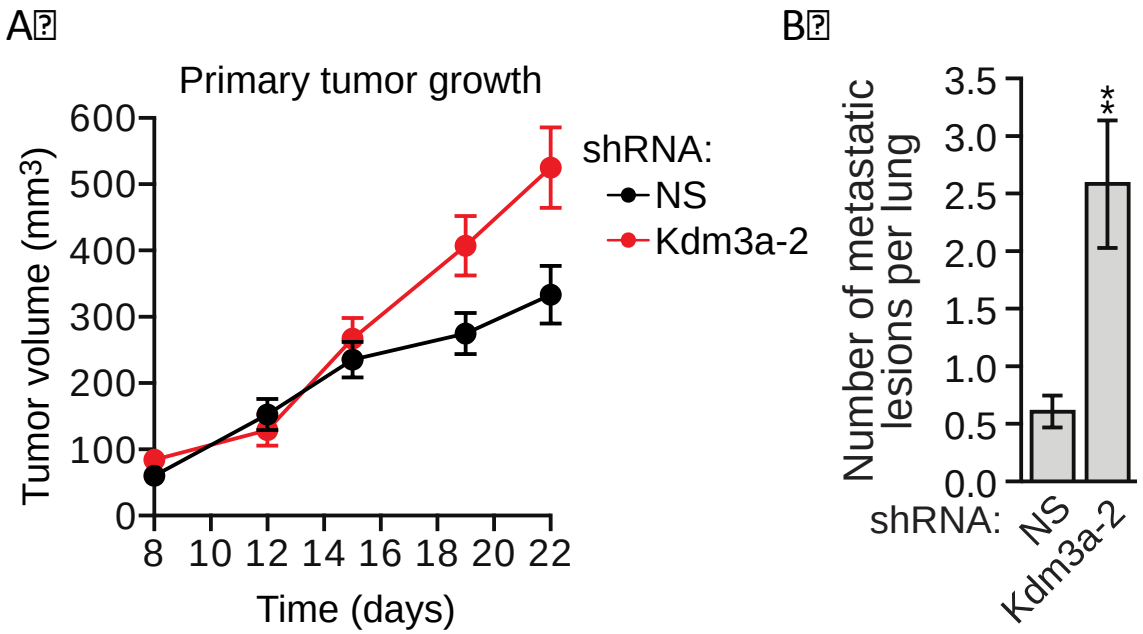

Figure 3.32. Confirmation of the results of Figure 3-31 with a second unrelated *Kdm3a* shRNA. (A) Primary tumor growth in mice injected with 4T07 cells expressing a NS (n=7) or *Kdm3a* (n=9) shRNA unrelated to that used in Figure 3-31. Error bars indicate SEM. (B) Number of metastatic lesions per lung in mice injected with 4T07 cells expressing a NS (n=7) or *Kdm3a* (n=9) shRNA unrelated to that used in Figure 4I. Error bars indicate SEM. ***P*<0.01. The differences in primary tumor growth between groups were not statistically significant.

Conclusions

Based on the results presented above, we propose a model of anoikis induction that is illustrated in Figure 3.20 and discussed below. Following detachment of non-transformed cells, integrin signaling is decreased leading to decreased FAK, EGFR and RAF/MEK/ERK signaling and subsequent transcriptional induction of *KDM3A*. The increased levels of KDM3A result in its recruitment to the pro-apoptotic genes *BNIP3* and *BNIP3L,* where it promotes demethylation of inhibitory H3K9me1/2 marks and transcriptional activation of the two genes, resulting in anoikis induction. Consistent with this model, previous studies have shown that hypoxia results in transcriptional activation of *KDM3A*, *BNIP3* and *BNIP3L* (Beyer et al., 2008; Sowter et al., 2001).

We have found that in anoikis-resistant human breast cancer cell lines and tumors, *KDM3A* expression is defective, highlighting the importance of this pathway in promoting anoikis. And we found that the knockdown of *Kdm3a* caused a non-metastatic mouse mammary carcinoma cell line to metastatize to the lung. In agreement with this result it has been previously shown that the knockdown of *BNIP3* causes enhanced metastasis to the lung in the same mouse cell line (Manka et al., 2005). Collectively, our results reveal a novel

transcriptional regulatory program that mediates anoikis in non-transformed cells and is disabled during cancer development.

As described above, previous studies have shown that BIM and BMF are also effectors of anoikis (Reginato et al., 2003; Schmelzle et al., 2007). However, we have found that unlike BNIP3 and BNIP3L, BIM and BMF are not regulated by KDM3A. Thus, our results reveal that anoikis is promoted by multiple non-redundant pathways, which may help prevent the development of anoikis resistance.

The role of KDM3A in cancer has not been thoroughly studied and has so far been controversial. There has been evidence to suggest that KDM3A has both an anti-oncogenic effect on cancer, as we presented here, (Du et al., 2011) and a pro-oncogenic effect (Krieg et al., 2010). In fact, in the time since we submitted our manuscript another group has published a study that shows KDM3A plays a pro-oncogenic role in breast cancer and that the knockdown of KDM3A sensitized breast cancer stem cells to chemotherapeutic drugs (Ramadoss et al., 2016). Although this other study on KDM3A did not specifically study anoikis, it is contradictory to our results in breast cancer. However, the opposing study does not use the same cell lines or mouse model of breast cancer as we do, leaving open the possibility that the role of KDM3A is context dependent and can even differ within the same cancer type. Further research is

needed to fully elucidate the context dependent mechanism by which KDM3A functions in breast cancer and in other types of cancer.

One aspect that has so far not been studied is the transcriptional control of KDM3A. We find that KDM3A is transcriptionally activated upon the loss of integrin signaling and the subsequent loss of FAK, EGFR and RAF/MEK/ERK signaling. However, we have not identified the specific transcription factors or complexes that control the expression of KDM3A, which could be factors in identifying how the role of KDM3A differs between cancers. It is also possible that KDM3A activates the transcription of genes other than BNIP3 and BNIP3L following detachment, as we did not perform genome wide ChIP-sequencing experiments to identify all possible KDM3A sites.

In conclusion, our results provide identification of a novel pathway that promotes anoikis and furthers the knowledge of the function of KDM3A. We offer insight into a potential mechanism of anoikis resistance in breast cancer and show that this mechanism of anoikis resisance can lead to increased metastasis. Taken together, our results have had a significant impact on the field of anoikis research.

CHAPTER IV: miR-203 regulates anoikis through targeting a network of pro-survival genes

Preface

This research chapter derives from a project that I designed and initiated in 2012 and has continued until the preparation of this dissertation. Michael Green and I had discussed the potential role of miRNAs during anoikis and after realizing that miRNA expression profiling during anoikis had not yet been performed, I set out to do just that. Desiree Brady, a graduate student in Phillip Zamore's lab assisted me with the initial small RNA sequencing, which I performed in the Zamore lab with the help of Desiree. Phillip Zamore and his lab provided me with expertise, reagents, and protocols to assist in the successful completion of the small RNA sequencing. The small RNA sequencing data was generated by the UMMS Deep Sequencing Core Facility and analyzed by Lihua (Julie) Zhu and Jianhong Ou. The TCGA data was analyzed by Jun Yu.

The total RNA sequencing and AGO2-Immunoprecipitation RNA sequencing was conceived of and designed by me and performed by Alexander Boardman, a UMMS medical student who did a research project in the Green lab. All of the RNA sequencing data was also generated by the UMMS Deep

Sequencing Core Facility and analyzed by Lihua (Julie) Zhu and Jianhong Ou. Amy Virbasius and the UMMS shRNA Core Facility provided targeted shRNAs.

Tessa Simone assisted with the Annexin-V FACS experiments. Michael Green and myself conceived of and designed all other experiments and I performed all of the other experiments. I analyzed all the data and composed all of the figures with editorial assistance from Sara Deibler. Lynn Chamberlain provided experimental assistance with most of the qRT-PCR experiments.

Abstract

Anoikis, apoptosis after detachment of cells from the ECM, is a complex and diverse biological process that is not yet fully understood. While genome wide studies have been performed to identify gene expression changes that play a role in anoikis, similar genome wide microRNA (miRNA) studies have not yet been done. Here, I completed miRNA expression profiling during the early stages of anoikis in breast epithelial cells and have identified miR-203 as a critical pro-anoikis miRNA. After detachment, miR-203 is significantly upregulated and ectopic expression of miR-203 in attached cells causes widespread cell death. Likewise, inhibition of miR-203 causes a resistance to anoikis. Coordinated RNA sequencing and AGO2-immunoprecipitation RNA sequencing revealed miR-203 directly targets a network of pro-survival genes after detachment to promote anoikis. Finally, I show that the elevation of four anoikis-related pro-survival miR-203 target genes are elevated in breast cancers that have low miR-203.

Introduction

Anoikis, cell death after detachment of epithelial cells from the extra cellular matrix (ECM) happens due to the loss of integrin signaling. Resistance to anoikis is a critical step in metastasis (reviewed in (Simpson et al., 2008)) however, the mechanism by which metastatic cells become resistant to anoikis is not well understood. Here, we performed genome wide small RNA sequencing analysis in anoikis-sensitive breast epithelial cells to determine changes in miRNA expression upon detachment from the ECM. We identified miR-203 as an anoikis effector miRNA and show that miR-203 is highly induced upon detachment and that inhibition of miR-203 results in a resistance to anoikis. Furthermore, we find that ectopic expression of miR-203 is sufficient to induce apoptosis in attached cells. Finally, we identified direct miR-203 target mRNAs through a dual functional- and expression-based RNA-sequencing approach. We show that a subset of miR-203 target genes contributes to cell survival and upon detachment, miR-203 targets this subset of mRNAs subsequently leading to detachment-induced apoptosis.

The detachment-induced loss of integrin signaling triggers downstream intercellular signaling events leading to cell death. Many signaling pathways are known to be involved in anoikis, including FAK and RAF/MEK/ERK signaling. When cells are attached to the ECM, integrin signaling activates FAK which recruits and activates SRC. The activation of SRC then leads to

autophosphorylation and further activation of FAK, which activates PI3K and RAF/MEK/ERK signaling. In addition to FAK, SRC activation also leads to phosphorylation and activation of EGFR, in a ligand-independent manner, which also activates RAF/MEK/ERK signaling. All of these signaling events in attached cells contribute to proliferation, growth, and survival of cells and when this signaling is lost upon detachment from the ECM it results in anoikis.

Many studies to date have identified genes involved in anoikis whose expression is altered upon detachment (Pedanou et al., 2016; Reginato et al., 2003; Schmelzle et al., 2007) leading to the hypothesis that anoikis is the consequence of global changes in gene expression upon detachment. While there have been studies that explore global mRNA expression changes upon detachment (Schmelzle et al., 2007), another mode of gene expression control that has yet to be well studied upon detachment is changes in microRNA (miRNA) expression. miRNAs control mRNA and protein expression by binding to the 3’UTRs of specific target genes which inhibits translation and degrades the mRNA. To date, few miRNAs have been shown to play a role in anoikis however, the global change in miRNA expression upon detachment has not been studied.

While miRNAs have not been well studied in anoikis, they have been widely studied in breast cancer. Profiling studies have revealed multiple miRNAs that are either up- or down-regulated at different stages of breast cancer

progression (Luo et al., 2013; Wang and Wang, 2012). This led us to hypothesize that there are global changes in miRNA expression that are critical for anoikis and the alteration of these miRNAs in cancer could lead to anoikis resistance. Since the only studies to date that link miRNAs to anoikis investigate single (or a few) miRNAs, it is likely that we do not yet have a clear picture of the role of miRNAs during the process of anoikis.

Here, we investigate changes in miRNA levels upon detachment of breast epithelial cells by small RNA sequencing. We show miR-203 is significantly induced upon detachment of cells and this induction is critical for anoikis. Additionally, we utilized a dual RNA-sequencing approach to identify direct miR-203 target genes. We further show that a subset of these target genes contributes to cell survival and miR-203 targeted repression of these genes after detachment from the ECM contributes to anoikis. Finally, we found that four direct miR-203 anoikis-related target genes are significantly elevated in triple negative breast cancer, a subset of breast cancer where miR-203 has been shown to be highly downregulated compared to other types of breast cancer. Together, these results implicate miR-203 as an anoikis effector miRNA and suggest a link between decreased miR-203 expression and anoikis resistance in triple negative breast cancer.

Results

Small RNA profiling identifies miR-203 as an anoikis effector in breast epithelial cells

To investigate the role of miRNAs in anoikis we sought to measure changes in miRNA expression upon detachment of cells using small RNA sequencing (small RNA-seq). The small RNA-seq was performed in MCF10A cells, an immortalized but non-transformed breast epithelial cell line that is sensitive to anoikis in cell culture (Debnath et al., 2002; Reginato et al., 2003). Briefly, small RNA (18-24 nucleotides) was isolated from total RNA from attached MCF10A cells and detached MCF10A cells, cultured in suspension for 24 hours (on polyHEMA coated plates). After mapping the deep sequencing reads to the human miRNA genome, the analysis showed the miRNA content of each small RNA-seq sample was over 75% (Table 4.1). The deep sequencing analysis identified 9 upregulated miRNAs and 8 downregulated miRNAs that were greater than 100 counts per million in the sequencing reads and had P-values of less than 0.01 following detachment from the ECM (Table 4.2 and Figure 4.1). We were interested in the miRNAs that were upregulated post-detachment because the induction suggested that those miRNAs could be critical anoikis effector miRNAs.

To validate the upregulated miRNAs we first identified which miRNAs were either implicated as tumor suppressive miRNAs or were implicated as pro-apoptosis miRNAs. We then measured the level of individual miRNAs in MCF10A cells after detachment by directed miRNA-qRT-PCR analysis. We found that 3 of these miRNAs, miR-197 (Yang et al., 2015), miR-324 (XU et al., 2014), and miR-203 (Wang et al., 2013) were significantly induced in MCF10A cells following detachment for 24 and 48 hours (Figure 4.2).

Both the small RNA-seq data and the miRNA-qRT-PCR revealed miR-203 to be the most highly upregulated miRNA upon detachment, which we further confirmed by northern blot (Figure 4.3). Additionally, miR-203 has been shown to inhibit cancer cell invasion and proliferation (Benaich et al., 2014) and inhibits stem cell self-renewal (Yi et al., 2008). These data suggest that miR-203 is critical for anoikis and the loss of miR-203 potentially contributes to anoikis resistance in invasive cancers, therefore we focused our experiments on the role of miR-203 in anoikis. In order to identify the mechanism by which miR-203 is induced, we tested transcriptional activation of the precursor-miR-203 (pre-miR-203). Increased transcription of the primary miR-203 (pri-miR-203) transcript would result in an increased expression of pre-miR-203 however, the results of Figure 4.4 show that only the mature miR-203 is significantly induced upon detachment whereas the expression of pre-miR-203 is not significantly changed. These results suggest that the induction of miR-203 is due to the increased

processing of mature miR-203 instead of increased transcription of the primary miR-203 transcript.

miR-203 is critical for anoikis and is induced by the loss of integrin signaling

To determine if the induction of miR-203 promotes cell death after detachment from the ECM we ectopically expressed miR-203 in attached cells by transducing MCF10A cells with a retrovirus containing pre-miR-203 (Figure 4.5), which leads to high levels of mature miR-203 as a result of endogenous processing machinery (Isobe et al., 2014) or an empty vector control. The cells were treated with puromycin for 4 days after which survival was monitored by crystal violet staining and cell death was monitored by annexin-V.. The cells that contain the ectopically expressed pre-miR-203 show a significant decrease in survival (Figure 4.6) and a significant increase in cell death (Figure 4.7) as compared to an empty vector control in attached MCF10A cells. This data demonstrates that the increased level of miR-203 causes cell death in MCF10A cells.

In order to prove that miR-203 is critical for detachment-induced apoptosis we performed inhibition experiments in MCF10A cells. Briefly, we transduced MCF10A cells with a lentiviral miR-203 inhibitor or a lentiviral scrambled control and cultured the cells in attached conditions or detached conditions for 96 hours

and analyzed cell death by annexin-V staining. We observed significantly decreased cell death in MCF10A cells expressing the miR-203 inhibitor upon detachment from the ECM as compared to the scrambled control expressing detached MCF10A cells (Figure 4.8). We confirmed the activity of the miR-203 inhibitor in 293T cells with a GFP miR-203 sensor. The miR-203 sensor is manufactured to contain 2 miR-203 seed sequence sites in the 3'UTR of GFP so that increased GFP expression would indicate lower miR-203 activity and vice versa (Figure 4.9). This data shows that not only is miR-203 sufficient to cause cell death in MCF10A cells but it is necessary for normal levels of anoikis in MCF10A cells upon detachment from the ECM.

Anoikis occurs after cells detach from the ECM primarily because of the loss of integrin signaling (Frisch and Ruoslahti, 1997). We sought to confirm that induction of miR-203 after detachment is also primarily due to the loss of integrin signaling in order to solidify miR-203 as an anoikis effector. We restored integrin signaling in detached cells by adding growth factor reduced matrigel to the media and monitored the expression of miR-203 by miRNA-qRT-PCR. The results of Figure 4.10 show that the addition of growth factor reduced Matrigel basement membrane-like matrix, which restores integrin signaling, to the media significantly blocks the induction of miR-203 in detached cells. Therefore, miR-203 is induced following detachment from the ECM due to the loss of integrin signaling.

Identification of miR-203 target genes in breast epithelial cells through RNA-seq and AGO2-IP-RNA-seq

We next sought to determine the direct target genes that are critical for the function of miR-203 during anoikis by utilizing a dual unbiased, deep sequencing approach (Furuta et al., 2013). First, we performed RNA co-immunoprecipitation with an anti-Ago2 antibody in MCF10A cells expressing pre-miR-203 or an empty vector control followed by RNA-sequencing of the mRNAs from the Ago2-IP (Ago2-IP-Seq). A previous study has shown that the ectopically expressed miRNA overloads the RISC machinery in comparison to the endogenous miRNAs and the majority of mRNAs that are enriched in the Ago2-IP are direct targets of the miRNA of interest; however false positives are still a problem (Furuta et al., 2013). To rule out false positives from the AGO2-IP-Seq, we measured the global gene expression changes caused by the induction of miR-203 by performing genome wide expression profiling RNA-sequencing in MCF10A cells that were transduced with either pre-miR-203 or an empty vector control. We then compared the negatively correlated genes in both sets of experiments (with p-values of less than 0.05) that were downregulated in the total-RNA-seq data but enriched in the AGO2-IP-RNA-seq data (Figure 4.11). We then compared the negatively correlated data with the list of predicted miR-203 target genes from TargetScan (Appendix I). The combination of these data

analyses produced a list of 41 direct miR-203 target genes in MCF10A cells (Figure 4.12).

Recent evidence suggests that the dominant mechanism by which miRNAs repress their target genes is through mRNA degradation (Guo et al., 2010) therefore, we validated miR-203 candidate target genes by monitoring mRNA expression using qRT-PCR analysis after ectopic expression of miR-203. We transduced MCF10A cells with pre-miR-203 or an empty vector control and monitored the expression of each target gene by qRT-PCR. The results of Figure 4.13 show that 30 miR-203 target genes were significantly downregulated after ectopic expression of miR-203. Thus, these 30 genes are likely direct targets of miR-203 in MCF10A cells.

We then hypothesized that upon detachment, the induction of miR-203 causes repression of at least a subset of miR-203 candidate target genes. To test this hypothesis, we measured the expression levels of the 41 miR-203 candidate target gene mRNAs in detached MCF10A cells, cultured in suspension for 24 hours, by qRT-PCR analysis. The expression of 24 candidate target genes was significantly downregulated in detached cells as compared to attached MCF10A cells (Figure 4.14). These results suggest that the induction of miR-203 after detachment of MCF10A cells leads to the downregulation of direct target mRNAs.

miR-203 targets a network of pro-survival genes to induce cell death upon detachment

In the subset of the 24 miR-203 target genes that are downregulated upon detachment in MCF10A cells, 18 of those target genes correlate with the validated miR-203 target genes (Figures 4.13, 4.14 and Table 4.3). After pathway and biological process analysis, these 18 anoikis-related miR-203 target genes do not seem to belong to the same pathway or contribute to the same biological process, therefore we hypothesized that these genes might contribute to cell survival and the repression of these genes upon miR-203 induction promotes anoikis. To test this hypothesis we transduced MCF10A cells with shRNAs against each of the 18 miR-203 anoikis-related target genes and monitored cell survival by crystal violet staining. Ten days after the shRNA transduction we stained the surviving cells with crystal violet to visualize the surviving colonies of each knockdown cell line. The results of Figure 4.15 show that the knockdown of 10 miR-203 target genes leads to some level of decreased survival or decreased proliferation in attached MCF10A cells as compared to a non-silencing (NS) control shRNA. We further confirmed these results by using a second unrelated shRNA against all 10 genes (Figure 4.16). These results suggest that miR-203 promotes anoikis by targeting and repressing a network of pro-survival genes in MCF10A cells upon detachment from the ECM.

miR-203 down regulation in invasive breast cancer cells contributes to anoikis resistance

Finally, miR-203 has previously been implicated as a tumor suppressive miRNA (Bueno et al., 2008) and as a suppressor of migration and invasion (Wang et al., 2012). Additionally, miR-203 has been shown to be highly downgregulated in triple negative breast cancer cells lines as compared to normal breast epithelial cells and less-invasive breast cancer cells lines by miRNA-microarray analysis (Luo et al., 2013). Certain subtypes of triple negative (not expressing the HER2, PR, or ER receptors, also named “basal-like”) breast cancers have been shown to be highly invasive and result in a poor prognosis (Cheang et al., 2008). These findings suggest the intriguing possibility that miR-203 is critical for anoikis and that the loss of miR-203 and subsequent increase in anoikis resistance can contribute to invasiveness a subset of triple negative breast cancer cell lines.

We sought to determine the role of downregulation of miR-203 in invasive triple negative breast cancer cells. First, consistent with previous studies (Luo et al., 2013) we observed that miR-203 is highly downregulated in two triple negative breast cancer cell lines, MDA-MB-231 and HS578T, as compared to MCF10A cells and less-invasive types of breast cancer cell lines, MCF7, BT474, and T47D cells (Figure 4.18). We have previously shown that all of these breast cancer cell lines are resistant to anoikis in cell culture (Pedanou et al., 2016).

Therefore, we proposed that miR-203 would not be induced upon detachment in these breast cancer cell lines, which could contribute to anoikis resistance. To test this hypothesis, we measured the expression of miR-203 by miRNA-qRT-PCR in attached and detached MDA-MB-231 cells using MCF10A as a control. As expected, miR-203 was not induced upon detachment in MDA-MB-231 cells but was significantly induced upon detachment in MCF10A suggesting that miR-203 is not functional in MDA-MB-231 cells (Figure 4.19). Next, we tested whether ectopic expression of miR-203 would be sufficient to decreased cell survival in MDA-MB-231 cells. We transduced MDA-MB-231 cells with pre-miR-203 or an empty vector control and monitored cell survival by crystal violet staining. Ten days after transduction we stained the cells with crystal violet to visualize the surviving colonies and found that the ectopic expression of miR-203 results in increased decreased survival or decreased proliferation in MDA-MB-231 cells.

Finally, we sought to determine if the loss of miR-203 in triple negative breast cancer cells causes the elevation of the pro-survival anoikis-related miR-203 target genes. We utilized The Cancer Genome Atlas (TCGA) database for breast cancer samples (Cancer Genome Atlas, 2012) and analyzed the expression of all 10 pro-survival anoikis-related miR-203 target genes (Figure 4.15) in triple negative breast cancer tumors in comparison to the other 3 subtypes of breast cancer (Her2, Luminal A, and Luminal B). Our analysis shows that 4 of these genes (*WDR69*, *PRKAB1*, *HBEGF*, and *PRPS2*) are significantly

elevated in triple negative breast cancer (Figure 4.21). We next tested if the repression of these 4 elevated genes would lead to decreased survival in MDA-MB-231 cells by transducing the cells with shRNAs against *WDR69*, *PRKAB1*, *HBEGF*, and *PRPS2*. Ten days after transduction we stained the cells with crystal violet to monitor the surviving cells. We show that the knockdown of all 4 genes results in the decrease survival or decreased proliferation in MDA-MB-231 cells (Figure 4.22). These results demonstrate that the elevation of *WDR69*, *PRKAB1*, *HBEGF*, and *PRPS2* likely contributes to cell survival in triple negative breast cancer. Our results, together with previous studies that show the ectopic expression of miR-203 in MDA-MB-231 cells causes decreased invasion (Wang et al., 2012) suggests that the loss of miR-203 in triple negative breast cancer cells leads to anoikis resistance and contributes to the invasiveness of those cells.

Figures

Sample	Read Count	% miRNA
ATT_1	14,488,438	85.40%
ATT_2	10,059,871	85.90%
ATT_3	12,154,307	85.60%
DET24H_1	18,775,691	85.50%
DET24H_2	13,829,444	78.90%

Table 4.1. Each sample for small RNA sequencing had a miRNA content of greater than 75%. After mapping to the human genome, the sequencing read count and percent miRNA for each attached (ATT) and detached (DET24H) small RNA sample from MCF10A cells is shown.

miRNA	Log2 Fold Change	P-Value
hsa-miR-186-5p	-4.618775671	8.10E-24
hsa-miR-25-3p	-3.028709298	2.33E-09
hsa-miR-221-3p	-2.975523674	1.34E-09
hsa-miR-222-3p	-2.905830044	6.66E-09
hsa-miR-769-5p	-2.117528652	0.000166001
hsa-miR-99b-3p	-1.792771293	0.002713491
hsa-miR-33a-5p	-1.752293009	0.00070066
hsa-miR-671-5p	-1.563884613	0.005425343
hsa-miR-301a-3p	1.705978293	0.006965854
hsa-miR-15a-5p	1.765685166	0.00754879
hsa-miR-4301	1.824008742	0.004810525
hsa-miR-197-3p	1.903970642	0.008652361
hsa-miR-324-5p	1.941355323	0.007021097
hsa-miR-15b-5p	1.96426179	0.00202066
hsa-miR-1246	2.229184889	0.000488131
hsa-miR-17-5p	2.856327723	3.27E-05
hsa-miR-203a	3.313176801	1.62E-06

Table 4.2. **Changes in miRNA expression after detachment.** The miRNAs that change in expression 24 hours post detachment in MCF10A cells are listed. The Log2 fold change is compared to attached MCF10A cells. All miRNAs included had a count per million that was greater than 100.

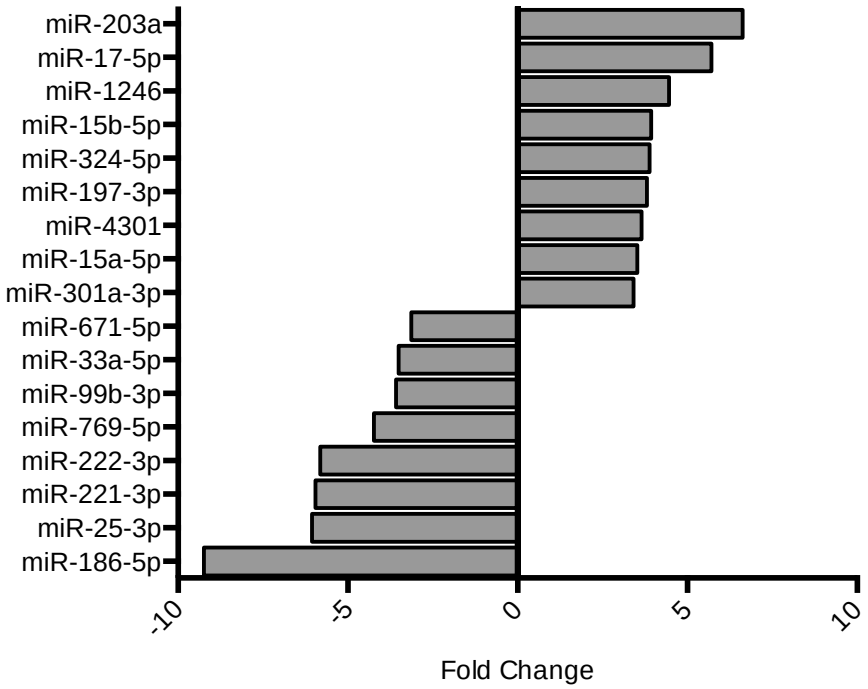

Figure 4.1. Several miRNAs show a significant change in expression upon detachment in MCF10A cells. Small RNA sequencing reveals that 9 miRNAs are significantly ($P<0.01$) upregulated and 8 miRNAs are significantly ($P<0.01$) downregulated 24 hours after detachment in MCF10A cells.

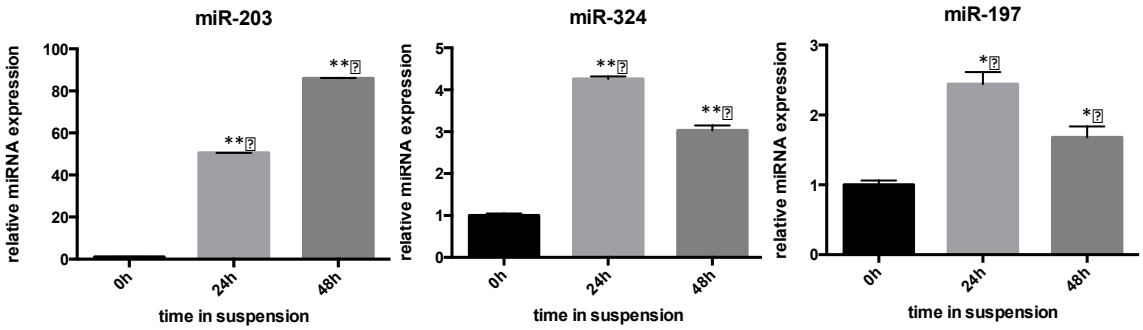

Figure 4.2. Three miRNAs are significantly upregulated upon detachment in MCF10A cells. miRNA-qRT-PCR analysis of miR-203, miR-197, and miR-324 at 24 and 48 hours post detachment in MCF10A cells. Statistics are compared to the values in attached cells, which were set to 1. U6 RNA was used as an internal control. Error bars indicate SD. *P<0.05; **P<0.01.

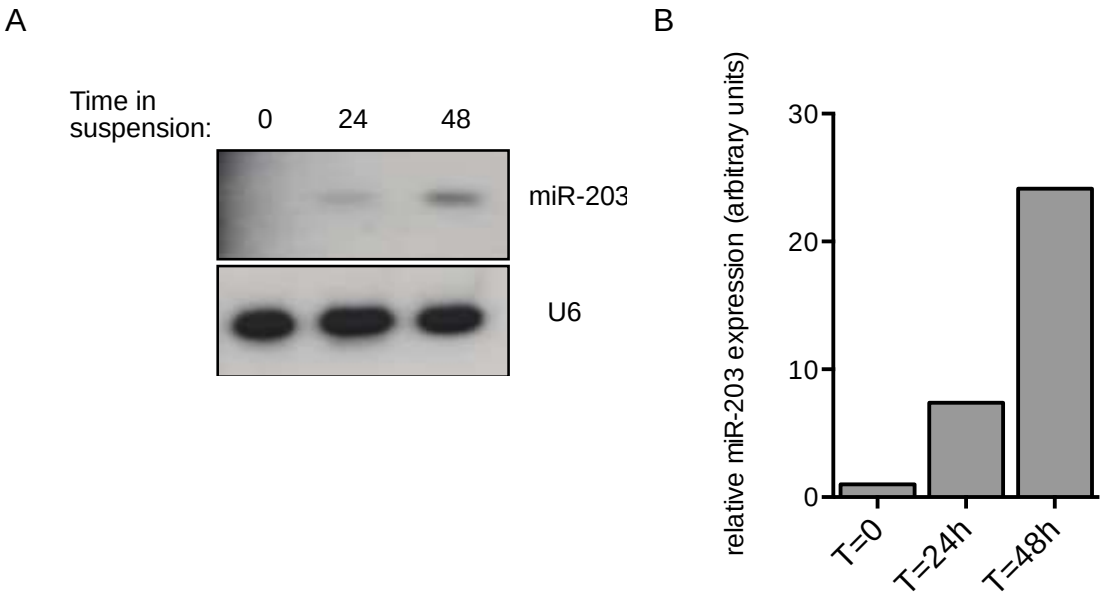

Figure 4.3. **Confirmation of miR-203 upregulation upon detachment in MCF10A cells**. (**A**) Northern blot analysis of miR-203 expression 24 and 48 hours post detachment of MCF10A cells. (**B**) Quantification of the northern blot in A, using U6 as a loading control.

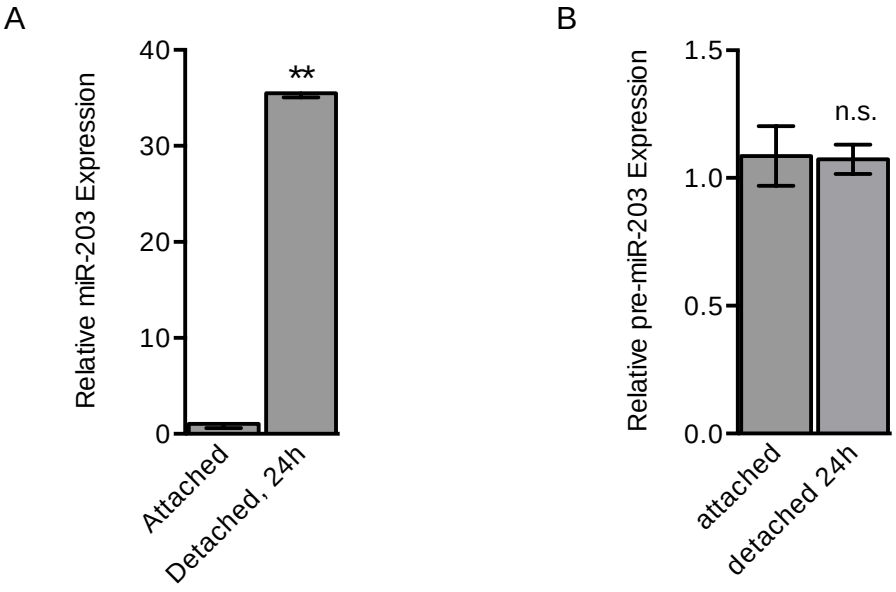

Figure 4.4. The induction of miR-203 is due to increased processing of the mature miRNA. (**A**) miRNA-qRT-PCR analysis of miR-203 in attached and detached MCF10A cells. U6 was used as an internal control. (**B**) qRT-PCR analysis of pre-miR-203 in the same attached and detached MCF10A samples used in A. RPL41 was used as an internal control. Error bars indicate SD. ***P*<0.01. n.s.= not significant.

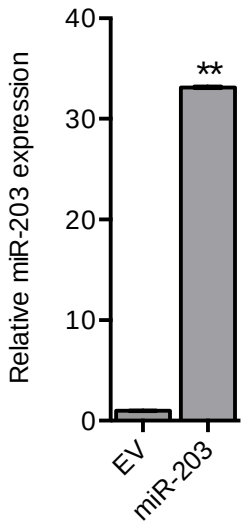

Figure 4.5. Ectopic expression of miR-203 in MCF10A cells. miRNA-qRT-PCR analysis shows successful ectopic expression of miR-203 in MCF10A cells as compared to an empty vector control (EV). Error bars indicate SD. ***P*<0.01.

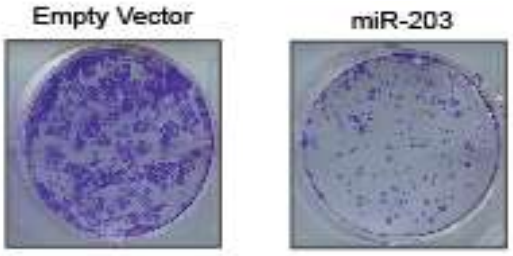

Figure 4.6. Ectopic expression of miR-203 results in decreased cell survival or decreased proliferation in MCF10A cells. Crystal violet staining of MCF10A cells expressing vector or pre-miR-203.

A

B

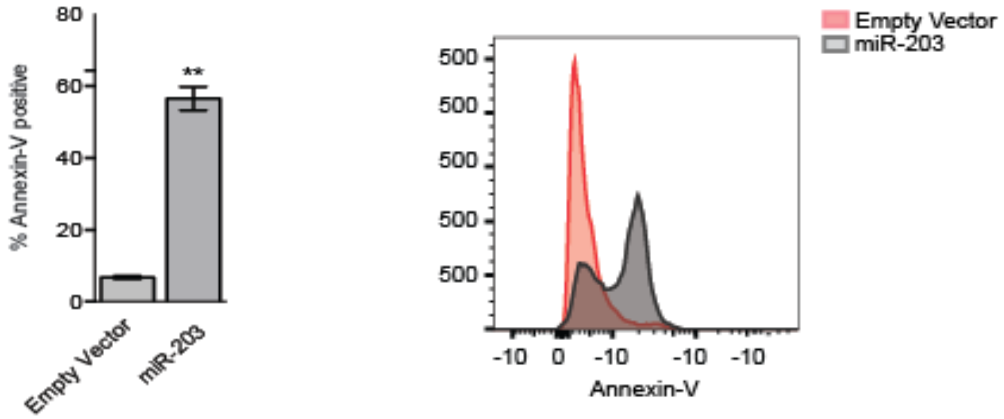

Figure 4.7. Ectopic expression of miR-203 results in cell death in MCF10A cells. (**A**) Cell death, monitored by annexin-V staining, in MCF10A cells expressing an empty vector control or pre-miR-203. Error bars indicate SD. ***P*<0.01. (**B**) Representative FACS plots corresponding to A.

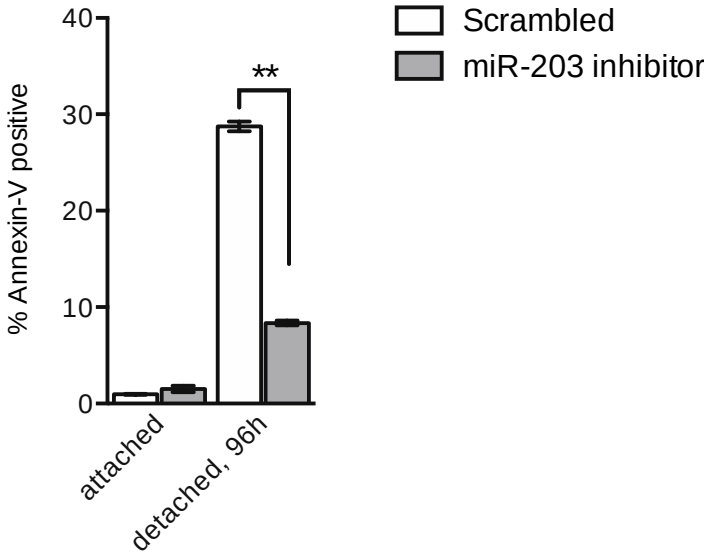

Figure 4.8. Inhibition of miR-203 causes resistance to anoikis in MCF10A cells. Cell death, monitored by annexin-V staining, in attached or detached (cultured in suspension for 96 h) MCF10A cells stably expressing a miR-203 inhibitor or a scrambled control. Error bars indicate SD. ***P*<0.01.

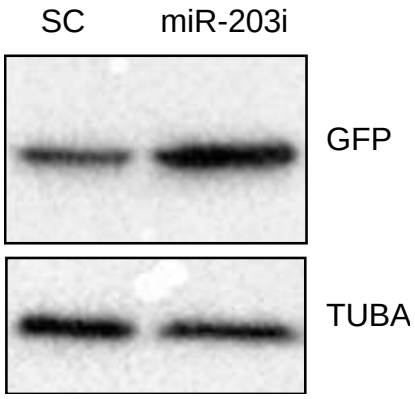

Figure 4.9. Confirmation of miR-203 inhibitor activity in 293T cells. Immunoblot analysis monitoring GFP expression after transfection of a GFP miR-203 sensor in 293T cells stably expressing either the miR-203 inhibitor (miR-203i) or a scrambled control (SC). α–tubulin was monitored as a loading control.

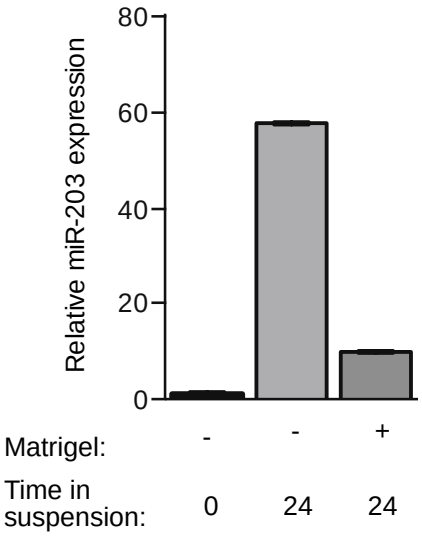

Figure 4.10. The induction of miR-203 after detachment from the ECM is due to the loss of integrin signaling. miRNA-qRT-PCR analysis of miR-203 in attached MCF10A cells or detached MCF10A cells cultured in suspension for 24 h and treated in the presence or absence of Matrigel. U6 was used as an internal control. Error bars indicate SD.

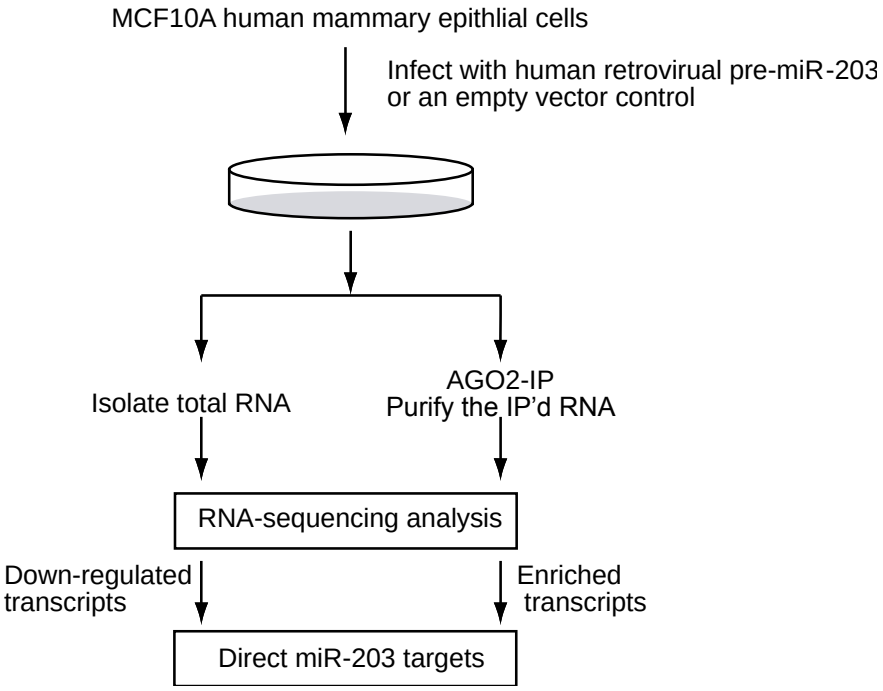

Figure 4.11. Schematic of the design of the dual RNA sequencing approach to identify direct targets of miR-203.

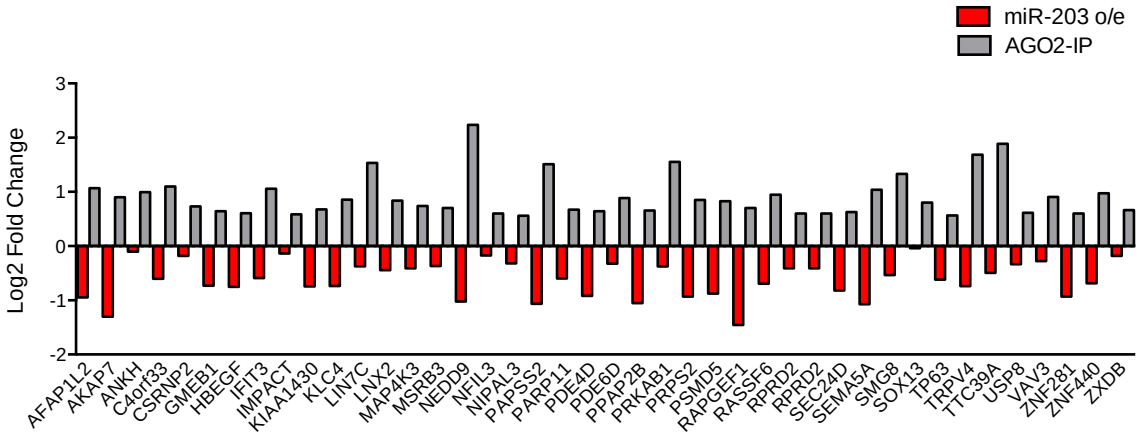

Figure 4.12. **Forty-two candidate miR-203 target genes were identified by the dual RNA sequencing approach.** Log2 fold change of genes that were significantly (P<0.05) enriched in the AGO2-IP sequencing and significantly (P<0.05) downregulated in the miR-203 ectopic expression RNA sequencing, all of which are also identified as potential miR-203 target genes in the Targetscan database.

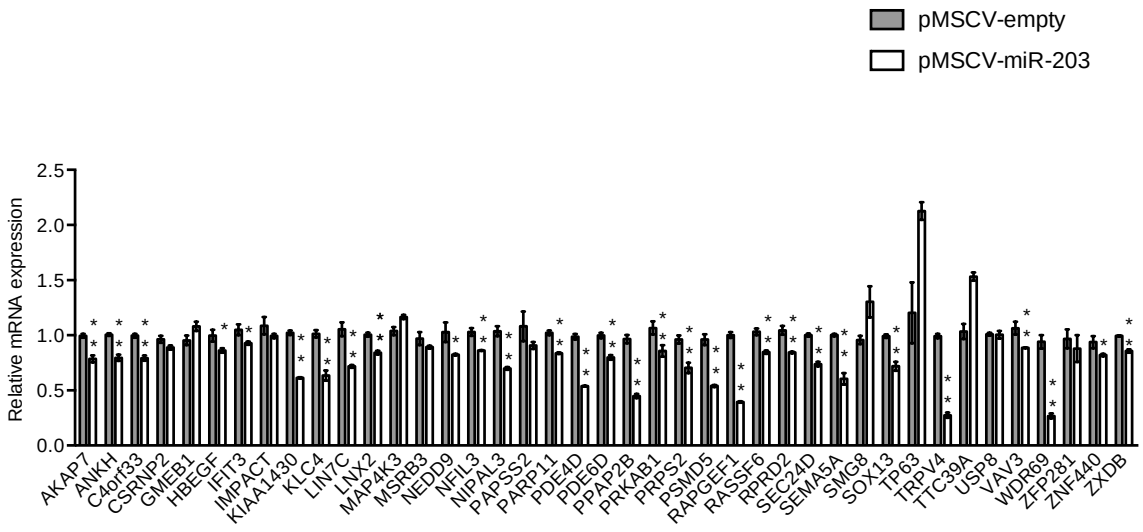

Figure 4.13. Validation of thirty direct miR-203 target genes. qRT-PCR analysis of miR-203 target genes in MCF10A cells ectopically expressing miR-203 or an empty vector control. The expression of each gene is shown relative to that obtained in attached cells which was set to 1. RPL41 was used as an internal control. Error bars indicate SD. **P*<0.05; ***P*<0.01.

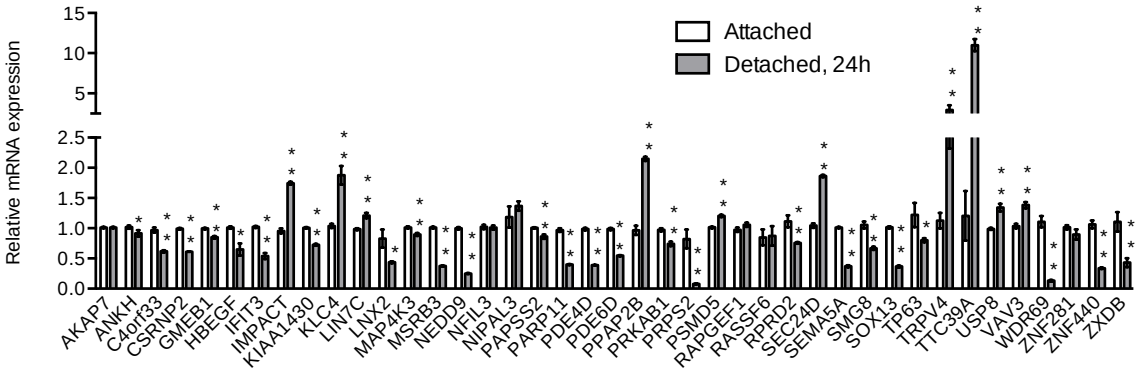

Figure 4.14. Twenty-five miR-203 target genes are significantly downregulated upon MCF10A cell detachment from the ECM. qRT-PCR analysis of the expression levels of miR-203 target genes in MCF10A cells cultured in suspension for 24 h. The expression of each gene is shown relative to that obtained in attached cells which was set to 1. RPL41 was used as an internal control. Error bars indicate SD. **P*<0.05; ***P*<0.01.

Biological Process	Gene Symbol	Gene name
Signal Transduction	*WDR69*	dynein assembly factor with WD repeats 1
	PDE6D	phosphodiesterase 6D
	PRKAB1	protein kinase AMP-activated non-catalytic subunit beta 1
Positive regulation of cell migration or proliferation	*HBEGF*	heparin binding EGF like growth facto
	IFIT3	Interferon induced protein with tetratricopeptide repeats 3
	SEMA5A	semaphorin 5A
Transcription regulation	*RPRD2*	regulation of nuclear pre-mRNA domain containing 2
	SOX13	SRY-box 13
	ZNF440	zinc finger protein 440
	ZXDB	zinc finger, X-linked, duplicated B
Nucleotide biosynthesis	*PRPS2*	phosphoribosyl pyrophosphate synthetase 2
Transporter	*ANKH*	ANKH inorganic pyrophosphate transport regulator
Cell adhesion	*NEDD9*	neural precursor cell expressed, developmentally down-regulated 9
Cell differentiation	*PARP11*	poly(ADP-ribose) polymerase family member 11
Unkown	*KIAA1430*	KIAA1430
	LNX2	ligand of numb-protein X 2
	C4orf33	chromosome 4 open reading frame 33
	PDE4D	phosphodiesterase 4D

Table 4.3. The list of miR-203 direct target genes that are degraded by miR-203 after detachment from the ECM in MCF10A cells. The target genes are sorted by biological process.

Figure 4.15. **The knockdown of ten miR-203 target genes results in decreased cell survival or decreased proliferation in MCF10A cells.** Crystal violet staining of MCF10A cells expressing shRNAs against ten direct miR-203 target genes or a NS control shRNA.

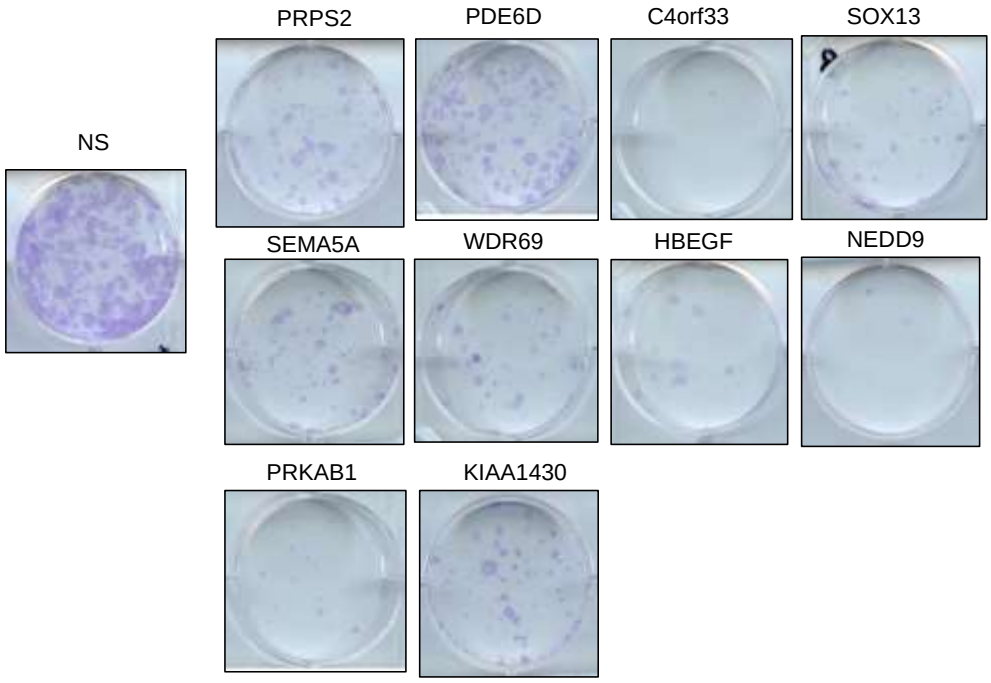

Figure 4.16. **Confirmation of the results of Figure 4.15 with a second unrelated shRNA.** Crystal violet staining of MCF10A cells expressing shRNAs against ten direct miR-203 target genes or a NS control shRNA.

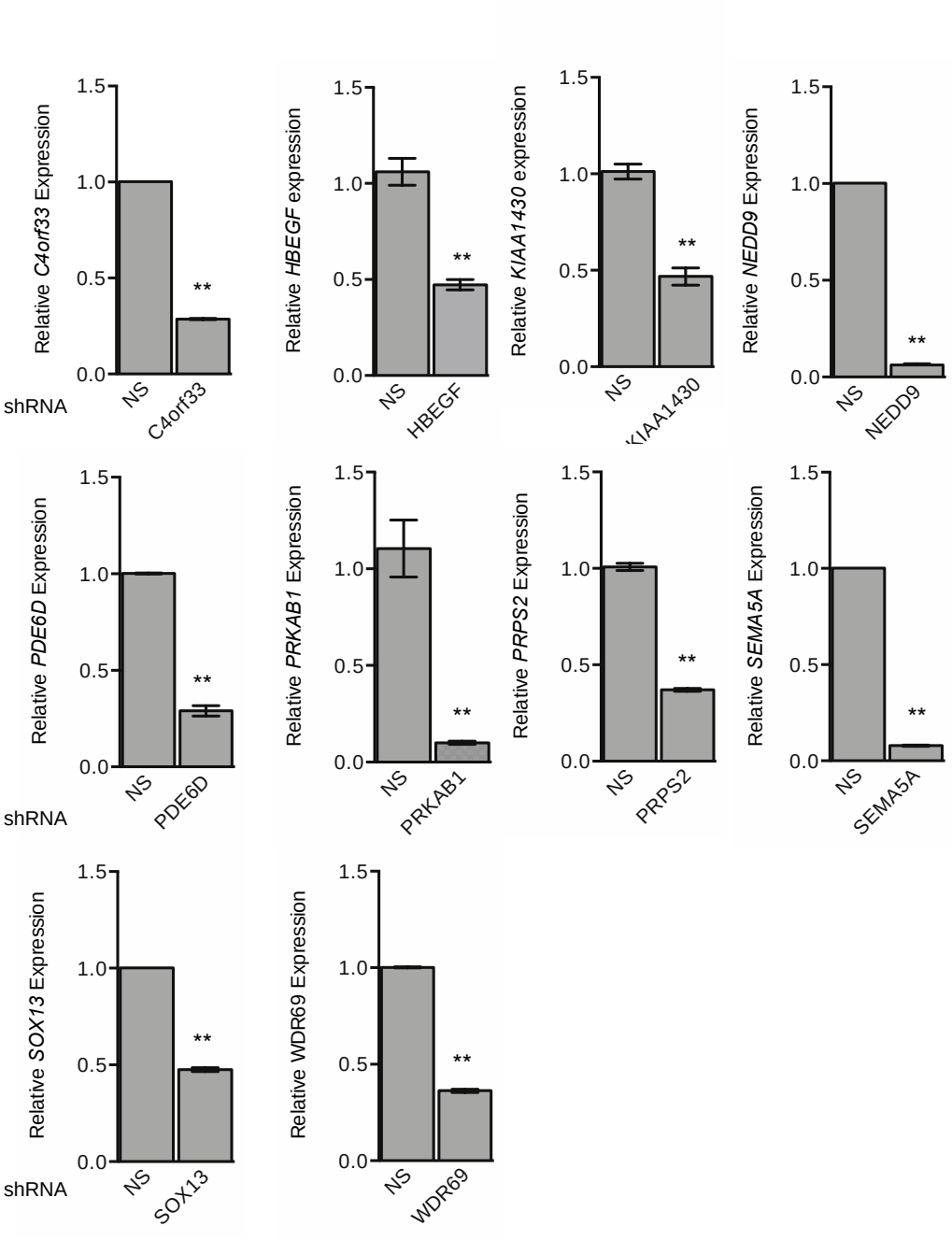

Figure 4.17. Analysis miR-203 target shRNA knockdown efficiencies. qRT-PCR analysis monitoring knockdown efficiencies of shRNAs directed against ten miR-203 target genes in MCF10A cells. Error bars indicate SD. ***P*<0.01.

Gene	shRNA sequence
C4ORF33	GAAGCTCTTTACCCTGTACCT
HBEGF	CTTCTCATGTTTAGGTACCAT
KIAA1430	CCTCCCAAAGTGTTGGGATTA
NEDD9	GCAGCTCAAGACCATAGTCAT
PDE6D	GCACATCCAGAGTGAGACTTT
PRKAB1	GCCTGGCTATGGAACTAAATA
PRPS2	GTCACAAACACAATTCCGCAA
SEMA5A	CCACAGATTACGGAACCATTA
SOX13	CCTAAGACTATGTTGGTACTT
WDR69	GCAGCAAGGATAATACCTGTA

Table 4.4. List of shRNA sequences against ten miR-203 target genes.

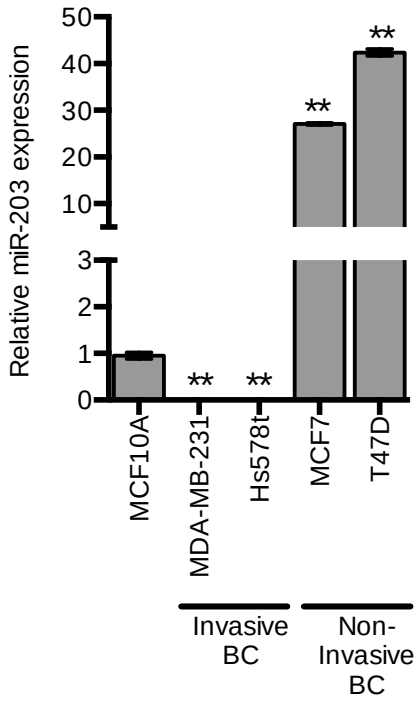

Figure 4.18. miR-203 is highly downregulated in invasive breast cancer cell lines. miRNA-qRT-PCR analysis of miR-203 in 2 triple negative and invasive breast cancer cell lines (MDA-MB-231 and Hs578t) compared to MCF10A cells and 2 luminal type, non-invasive breast cancer cell lines (MCF7 and T47D). U6 was used as an internal control. Error bars indicate SD. ***P*<0.01

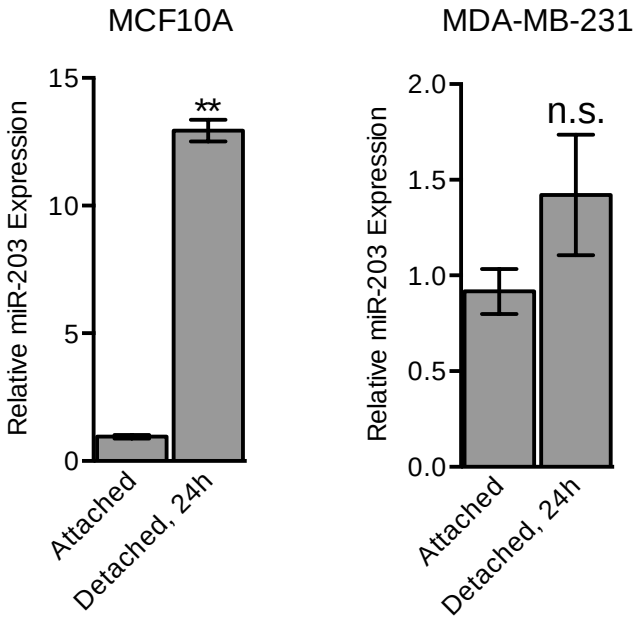

Figure 4.19. miR-203 is not induced upon detachment in a triple negative breast cancer cell line. miRNA-qRT-PCR analysis of miR-203 in attached and detached MCF10A cells (left) and MDA-MB-231 cells (right). Each detached sample was compared to the attached sample of the same cell line, which was set to 1. U6 was used as an internal control. Error bars indicate SD. ***P*<0.01

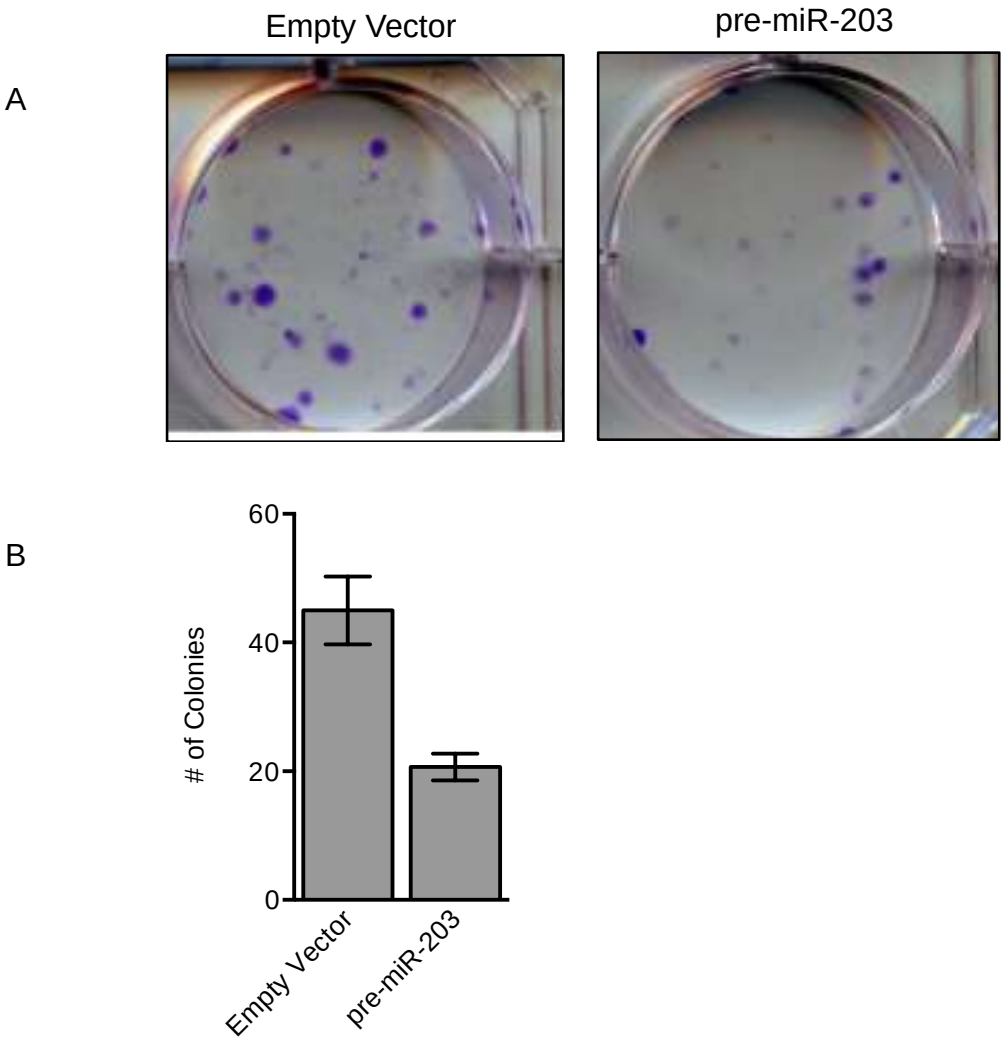

Figure 4.20. Ectopic expression of miR-203 causes decreased cell survival or decreased proliferation in a triple negative breast cancer cell line. (A) Crystal violet staining of MDA-MB-231 expressing an empty vector control or pre-miR-203. (B) Quantification of the crystal violet staining from A.

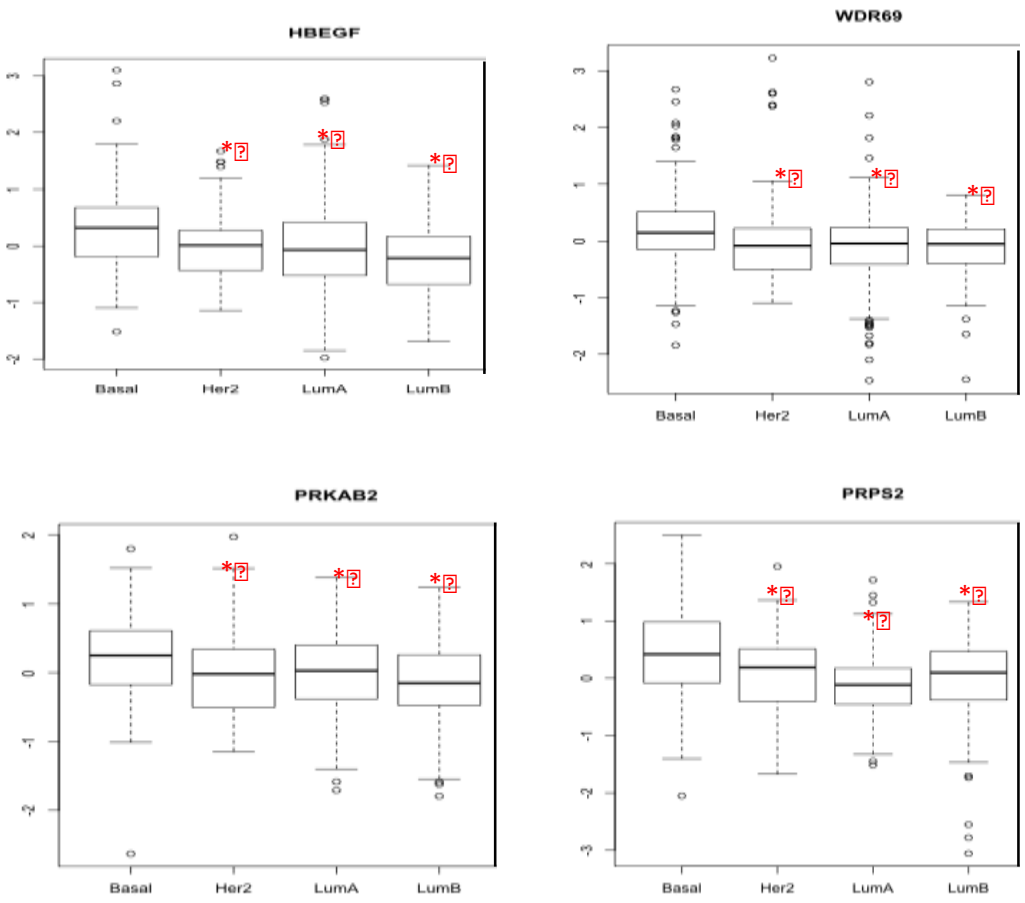

Figure 4.21. Four miR-203 target genes are elevated in triple negative breast cancer samples from the TCGA dataset. RNA-sequencing analysis of the TCGA dataset comparing the expression of miR-203 target genes in the four subtypes of breast cancer (Basal, Her2, Luminal A, and Luminal B). *P<0.05

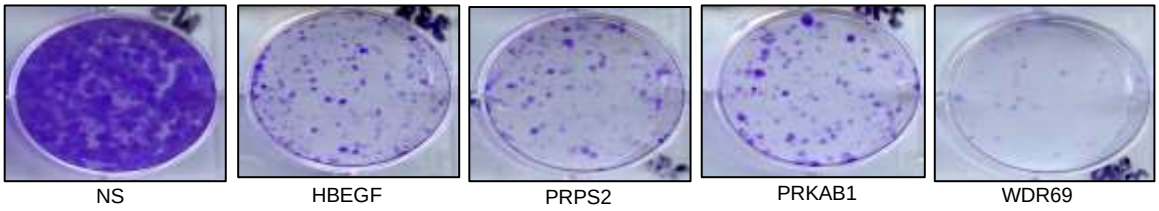

Figure 4.22. Knockdown of the four miR-203 target genes that are elevated in triple negative breast cancer results in decreased cell survival or decreased proliferation in a triple negative breast cancer cell line. Crystal violet staining of MDA-MB-231 cells expressing shRNAs directed against the four miR-203 target genes or a NS control.

Conclusions

In this study, we have identified miR-203 as an anoikis effector miRNA. We initially discovered that miR-203 is induced upon detachment of breast epithelial cells through unbiased small RNA sequencing. We then found that miR-203 is both necessary and sufficient for detachment-induced cell death. Furthermore, we have identified several direct targets of miR-203 that act as pro-survival genes in attached cells. We propose a model where, upon detachment, miR-203 is induced and subsequently binds to the 3'UTRs of direct target genes resulting in mRNA degradation of those pro-survival target genes finally resulting in anoikis (Figure 4.23).

These results both provide further insight into the mechanisms of detachment-induced cell death and further define the role of miR-203 as a growth and invasion suppressor miRNA. With this study we provide an intriguing link between miR-203 expression and function and anoikis resistance. As miR-203 was previously identified to be a tumor-, migration-, and invasion-suppresor miRNA but has not been studied in the context of anoikis (Chen et al., 2015; Viticchie et al., 2011).

We have shown that the induction of miR-203 upon detachment is due to the loss of integrin signaling. Furthermore, we have demonstrated that this

induction is due to the increased processing of the mature miR-203 rather than increased transcriptional activation of the precursor miR-203. This is an intriguing result because the most common cause of elevated expression of specific miRNAs is due to the increased transcription of the precursor miRNA (Bail et al., 2010; Calin et al., 2002). This is potentially one of the most interesting avenues of future research stemming from our investigation. Further research into the mechanism of increased processing of miR-203 upon the loss of integrin signaling would provide further understanding of the mechanism of miR-203 during anoikis and potentially further our understanding of the loss of miR-203 in invasive breast cancer.

We have identified a network of pro-survival direct miR-203 target genes that are downregulated following the induction of miR-203, most likely by mRNA degradation. While these target genes are not known to be part of the same biological pathways (as shown in Table 4-4), we have identified that 10 of the target genes (*SEC24D*, *PRPS2*, *HBEGF*, *WDR69*, *KIAA1430*, *PRKAB1*, *C4orf33*, *PDE6D*, *NEDD9*, and *SOX13*) are pro-survival genes in MCF10A cells. Four of those pro-survival target genes (*HBEGF*, *PRKAB1, PRPS2*, and *WDR69*) are elevated in and potentially contribute to anoikis resistance in invasive breast cancer. Continued studies should concentrate on further defining the mechanism of how these genes contribute to cell survival.

To date there has been no genome wide study of miRNAs involved in anoikis. There are only a few dozen directed studies of the role of specific miRNAs in anoikis, which leaves the field wide open for advances in miRNA research (Howe et al., 2012; Yu et al., 2013; Zhang et al., 2013). On the other hand, miRNAs have been very well studied in cancer, especially breast cancer (Hesse et al., 2013; Luo et al., 2013). This creates the possibility of correlating specific miRNA expression changes in anoikis with the corresponding expression level in the cancer of interest. We have done this with miR-203 by finding that miR-203 is induced upon detachment and subsequently found that miR-203 is highly downregulated invasive breast cancer cell lines. Since miR-203 was already implicated as a tumor- and invasion-suppressor, our data further defines the role of miR-203 and provides a link between miR-203 and anoikis resistance in cancer.

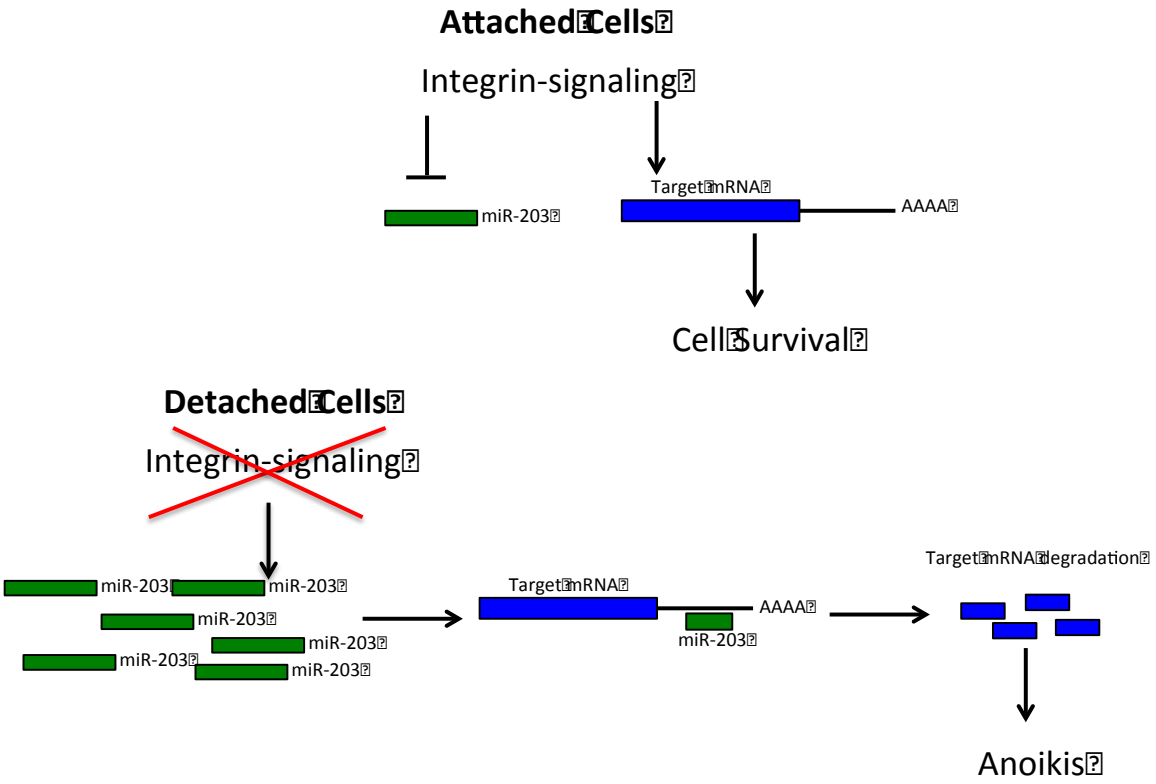

Figure 4.23. Model of miR-203 during detachment. In attached cells miR-203 is expressed at low levels, which leaves its pro-survival target genes expressed at normal levels leading to cell survival. Following detachment and the loss of integrin signaling, miR-203 is induced. The increased levels of miR-203 then bind to the 3'UTR of target genes and cause mRNA degradation of those target genes.

CHAPTER V: DISCUSSION AND CONCLUDING REMARKS

Collectively, the results I present here in my dissertation reveal two novel anoikis pathways that provide further insight into the process of detachment-induced apoptosis. My studies have revealed that (I) the histone demethylase, KDM3A is induced upon detachment from the ECM, which leads to cell death through the pro-apoptotic BNIP3 and BNIP3L BH3-only proteins and (II) miR-203 is also induced following detachment from the ECM subsequently targeting and degrading a panel of pro-survival genes. Both of these pathways are dysfunctional in at least some types of breast cancer, which contributes to anoikis resistance in breast cancer cells.

In my first investigation I used an unbiased genome wide shRNA screen to identify the H3K9me1/2 demethylase KDM3A as an anoikis effector. I show that the knockdown of *KDM3A* leads to anoikis resistance in a breast epithelial cell line. Furthermore, I found that *KDM3A* is transcriptionally induced upon detachment from the ECM due to the loss of integrin signaling and subsequent loss of FAK, EGFR and RAF/MEK/ERK signaling. I showed that KDM3A then demethylates H3K9me1/2 on the promoters of the pro-apoptotic proteins BNIP3 and BNIP3L to promote anoikis. Finally, I revealed that *KDM3A* expression is low in human breast cancer samples and that the knockdown of *Kdm3a* causes a non-metastatic mouse breast carcinoma cell line to metastasize to the lungs.

Together, these results reveal a novel role for KDM3A in anoikis and provide insight into a potential mechanism of anoikis resistance.

My results, combined with other published investigations discussed in Chapter I, suggest that there are multiple non-redundant pathways that promote anoikis, including the pathway that promotes Bim mediated cell death and the pathway identified in my study where KDM3A promotes BNIP3 and BNIP3L mediated cell death. Inhibition of each individual pathway results in approximately a 2-fold reduction in anoikis (Pedanou et al., 2016; Reginato et al., 2003) suggesting that multiple factors are responsible for detachment induced cell death. To directly test this hypothesis, further experiments such as using shRNAs to knockdown both Bim and BNIP3 to determine if the double knockdown would result in a synergistic resistance to anoikis in detached MCF10A cells. These results could help to confirm that these pathways work separately from each other to result in anoikis.

Although BNIP3 and BNIP3L, like Bim, are pro-apoptotic proteins they function differently than Bim, which could account for the results that BNIP3 and BNIP3L promote anoikis in a pathway that is separate from Bim. Bim is a classic BH3-only pro-apoptotic protein that functions primarily through BAX or BAK induced apoptosis (Willis et al., 2007). Alternatively, BNIP3 and BNIP3L are also BH3-only pro-apoptotic proteins that function through BAX or BAK induced

apoptosis but also function through Beclin-1 induced authophagy and possibly necrosis (Dhingra et al., 2014; Sowter et al., 2001). While Bim, BNIP3 and BNIP3L all function as general pro-apoptotic proteins, the specific mechanism of Bim differs from that of BNIP3 and BNIP3L leading to the possibility that these pro-apoptotic factors promote anoikis through separate mechanisms.

In addition to the conclusions of my first investigation, I have also developed a novel assay to study anoikis *in vivo*. Classically, anoikis has been difficult to study *in vivo.* In cell culture experiments the cells can be forcibly detached from the ECM and grown in suspension whereas the same cannot be done in a mouse. This leaves many studies to only test tumor growth and metastasis *in vivo* to make inferences about anoikis instead of directly studying anoikis. The *in vivo* anoikis assay I present in my investigation takes advantage of the fact that normal epithelial cells require their native ECM signals to survive and when those cells encounter a foreign ECM the normal survival signaling would not be initiated leading to anoikis. I used a mouse breast epithelial cell line and injected this cell line into the lungs of syngeneic mice (via tail vein injection) with the premise that the cells should not survive in the foreign environment of the lung. As we expected, the vast majority of the control cells did not survive whereas a significantly higher number of the *Kdm3a* knockdown cells did survive. As this was consistent with my *in vitro* cell culture results, it shows that this assay

is sufficient to test anoikis *in vivo* and will now allow cell culture results to be confirmed in a mouse model.

The basis of anoikis is that when cells detach from the ECM, integrin signaling is lost leading to cell death as discussed in depth in Chapter I, this was also the principle that both of my investigations were based on. However, I must add that while this is true in normal and non-malignant epithelial cells, such as MCF10A and MDCK cells (Frisch et al., 1996; Reginato et al., 2003), in most transformed cell lines integrin signaling is not lost upon detachment because some components of the pathway are constitutively activated (Shaw et al., 1997). This helps to explain why most cancer cell lines are not sensitive to anoikis in cell culture assays, as I showed for breast cancer cell lines in Figure 3.21.

As stated in the Discussion of Chapter III, there have been differing conclusions about the function of KDM3A in cancer. I hypothesize that there are factors upstream of KDM3A, such as transcription factors or miRNAs that control the transcriptional activation of *KDM3A* and these factors may differ between tissue types and may even differ between subtypes of the same cancer type. We know that the inactivation of the FAK, EGFR, and RAF/MEK/ERK pathways leads to induction of KDM3A but we have not defined the exact mechanism of this induction. I hypothesize that either integrin, FAK, EGFR, and RAF/MEK/ERK signaling activate a transcriptional or translational repressor of KDM3A under

normal attached conditions or that the loss of these signaling pathways activates a transcriptional activator of KDM3A under detached conditions. There are examples in the literature of transcription and translation factors that are controlled by these signaling pathways (Decarlo et al., 2015; Gilley et al., 2003). A scientist following up on my KDM3A data could perform directed experiments with these known factors by using shRNA or CRISPR knockout to determine if the depletion of any of these transcription or translation factors affects the expression of KDM3A. Another method of testing this hypothesis would be to analyze the promoter of KDM3A for transcription factor binding sites and analyzing the interaction of those transcription factors in attached versus detached conditions. This hypothesis warrants further research to identify such factors and gain further insight into the role of KDM3A in cancer. Once these upstream factors are identified, their potential role in cancer might be able to explain the differences in KDM3A being both pro- and anti-oncogenic.

In addition to transcription and translation factors that potentially control the expression of *KDM3A*, there is also the possibility that a miRNA could regulate *KDM3A* expression. Analyzing the 3’ UTR of KDM3A for miRNA seed sequences should reveal potential miRNA candidates. It would be especially interesting if one of the miRNAs identified as being significantly downregulated in Chapter IV of this dissertation were to control KDM3A expression so that in attached conditions the miRNA represses expression of KDM3A and upon

detachment and the loss of integrin signaling that miRNA is downregulated leading to increased expression of KDM3A. After identification of a miRNA that controls KDM3A expression, it would be interesting to test if levels of that miRNA are controlled by FAK, EGFR, and/or RAK/MEK/ERK signaling which has been demonstrated in the past and would correlate well with all of my KDM3A data (Mito et al., 2013).

While my results oppose most of the results in the other recently published study on KDM3A in breast cancer (Ramadoss et al., 2016), there is one unpublished observation that I made while performing my KDM3A knockdown experiments that could be consistent with the other published study. When I deplete KDM3A using shRNA in MCF10A cells I have observed that the cells seem to senesce, the cells proliferate slower than the non-silencing controls and the cells seem to flatten out on the plates. I have not measured this in any way so it is an unconfirmed opinion but it does warrant further investigation, as this would be consistent with the recent study from the Wang group. I hypothesize that the depletion of KDM3A causes MCF10A cells to senesce, which provides protection from anoikis upon detachment. The phenomenon of senescence being anti-apoptotic has been demonstrated in previous studies (Seluanov et al., 2001) and warrants further investigation in the case of KDM3A during anoikis. To test this hypothesis initially, one could assess the level of senescence following KDM3A knockdown through SA-beta-galactosidase staining (Dimri et al., 1995).

In my KDM3A investigation, in collaboration with Dr. Peter Siegel's lab at McGill University, we found that the knockdown of Kdm3a increased metastasis to the lungs, whereas the Wang group found that knockdown of KDM3A decreased metastasis to the lungs. These results stick out as the most glaring opposition between our investigations. While we used different model systems, ours was the 4T1 series of cell lines using syngeneic mice and the Wang group used a human breast cancer cell line with nude mice, both models were breast cancer so I would not anticipate such opposing results. While there is the unfortunate possibility that one of these studies could be due to some unknown experimental artifact, it should also be noted that the Wang group never performed a full metastatic assay where the cells are injected into the mammary fat pad and allowed to metastasize from there as we performed for my investigation. This could lead to some of the differences in results between the two studies.

My data also seems to conflict with the previously published observation that hypoxia protects against anoikis in mammary epithelial cells (Whelan and Reginato, 2014). The conflict is that HIF1alpha transcriptionally activates KDM3A under hypoxic conditions (Beyer et al., 2008) and we observe that the induction of KDM3A is critical for normal levels of anoikis. There is another piece to this puzzle however, that the induction of BNIP3 by HIF1alpha leads to autophagic

cell death under hypoxic conditions (Azad et al., 2008). Both published results give conflicting views on the influence of hypoxia on cell death.

Other aspects of the role of KDM3A that should be further studied are the global downstream transcriptional targets that are activated by KDM3A after detachment from the ECM. A genome wide ChIP-sequencing experiment in detached cells with both the KDM3A antibody and H3K9me1/2 antibodies would be a functional way of discovering all of the downstream targets of KDM3A. This avenue of study would offer even further insight into the function of KDM3A and would further define this novel anoikis pathway.

Further animal studies could also be performed in order to delineate the role of KDM3A in breast cancer progression and anoikis resistance and could maybe resolve the discrepancies between my data and the Wang group's KDM3A data. One could make a transgenic mouse with a conditional knock-in of KDM3A using a mammary specific promoter, such as WAP (Andres et al., 1988) in a mouse model of metastatic breast cancer (Fantozzi and Christofori, 2006). After the primary tumor has developed in the animals, we could add Cre, which would lead to expression of Kdm3a to determine if the ectopic expression of KDM3A would lead to decreased metastasis in this model. This experiment would constitute a "rescue" experiment that is missing from my study, as I used

RNAi experiments for the majority of the mechanistic studies in my investigation and used RNAi for all of the *in vivo* experiments.

One of the classic controls for RNAi experiments is the rescue experiment, where the gene of interest is manipulated to be resistant to the shRNA or siRNA being used, and then the gene is ectopically expressed in the knockdown cell line (Jackson et al., 2003a). This is done to “rescue” the phenotype that is observed with the knockdown of the gene of interest and confirms that the RNAi results are most likely specific to the gene of interest. This control experiment is missing in both my KDM3A investigation and miR-203 investigation. Adding rescue experiments to all of the RNAi results in each study would strengthen the overall results and conclusions of each, especially in the *in vivo* studies of the KDM3A investigation.

In Chapter III of this dissertation, many of the experiments I performed to support the hypothesis that KDM3A is novel anoikis effector genes involve depletion of KDM3A and other factors using shRNAs. While these experiments are standard in the field, they are not perfect because of the potential off target effects of shRNAs (Franceschini et al., 2014; Jackson et al., 2003b). In most experiments in both Chapter III and Chapter IV I tried to minimize the effect of off-target effects by using two shRNAs. Inconsistent results using two separate shRNAs for the same gene suggests that one of those shRNAs could be

targeting another gene that then affects the results of the assay. Our lab is especially careful with using two or more shRNAs when validating candidates from genome wide shRNA screens, where we rule out candidates if they only validate by one shRNA.

There are two *in vivo* experiments in Chapter III in which I only used one shRNA (Figures 3-27 and 3-29). The results and conclusions from these experiments would have been stronger had I used two shRNAs to rule out off target effects. In the future, it should be a requirement for publication to use at least two shRNAs in each experiment. There is also one experiment in Chapter IV where I only used one shRNA (Figure 4.22) from which the conclusions would be strengthened by using at least one more shRNA against each of the four genes I tested. I would suggest that this should be done before the results of Chapter IV are published.

Another limitation to my data is the lack of an integrin blocking experiment in the matrigel rescue experiments in Figure 3.7 and 4.10. For both experiments I used a growth factor reduced version of matrigel to limit the effect of growth factors in my results because I wanted to analyze the effect of integrin signaling alone and not growth factor signaling. However, there are likely residual growth factors in the matrigel (as it is labeled “reduced growth factors”, not “without growth factors”) so I should have included a control to demonstrate that the

results I observed were an effect of integrin signaling and not influenced by growth factor signaling. The addition of an integrin beta-1 blocking antibody to

In my second investigation I used another unbiased genome wide approach, small RNA sequencing, to identify miR-203 as an anoikis effector miRNA in breast epithelial cells. My results show that miR-203 is significantly induced upon detachment from the ECM and the induction of miR-203 leads to degradation of a network of pro-survival target genes leading to anoikis. Furthermore, the loss of miR-203 expression in triple negative breast cancer and corresponding elevation of a subset of the pro-survival target genes likely contributes to the invasiveness of the triple negative subtype of breast cancer. Collectively, these results present a additional evidence toward the tumor and invasiveness-suppresive role of miR-203 and reveal a novel miRNA pathway involved in anoikis.

Further studies should focus on the increased processing of miR-203 upon detachment from the ECM. The majority of miRNA expression changes stem from the transcriptional control of the pri-miRNA however, I found that following detachment the levels of the precursor of miR-203 (pre-miR-203) remains constant whereas only the mature form is induced leading to the hypothesis that the loss of integrin signaling leads to the increased DICER processing of miR-203. Factors that regulate DICER processing and specifically

factors that control specific miRNA processing differences have been studied only in recent years. This leaves the opportunity of identifying a novel miRNA processing control mechanism, specifically for miR-203 processing after detachment.

A limitation to the data in Chapter IV is that I only used crystal violet staining of colony forming assays to test our hypotheses about the effects of the knockdown of miR-203 target genes on cell survival (Figures 4.15, 4.16, 4.20, and 4.22). While this assay does provide information about the effect of these knockdowns on cell survival, I am not able to specifically assess the effects. Colony forming assays can demonstrate differences in, but not distinguish between, cell survival, cell death, changes in proliferation, and cell senescence, all of which would alter the number of colonies in these assays. In order to definitively say that the knockdown of these pro-survival genes results in cell death, future experiments should monitor annexin-V levels by FACS analysis. Additionally, the crystal violet assays I have included are not quantitative as I performed them with the plan to only present the photo of the crystal violet stained cells. However, these assays can be done in a quantitative way by seeding very few cells and making sure that the assay is stained at a time point where the colonies in the control plates are easy to count. In the assays in my data the colonies in the control NS plates merged making it very difficult to count individual colonies.

Another aspect of miR-203 that deserves a great deal more research is the loss of miR-203 in triple negative breast cancers. This result was known from previous studies and I expanded on it by showing that 4 anoikis-related miR-203 target genes are elevated in triple negative breast cancer, providing a link between anoikis resistance and an invasive form of breast cancer. The pro-invasive and pro-oncogenic role of these target genes could each warrant additional study, which would give further insight into the miR-203 pathway in anoikis and invasive cancer. Secondly, miRNAs are being tested in pre-clinical studies and even some clinical trials as gene therapy (Reid et al., 2016). In vivo mouse model studies that use miR-203 expression to treat triple negative breast cancer would provide an answer as to whether miR-203 could be considered as a viable treatment for patients with triple negative breast cancer.

Arguably the aspect of my second investigation that requires the most follow-up study is defining the role of the panel of 10 anoikis-related pro-survival target genes in normal attached cells (Figure 4.15). While a few of these genes have been implicated as pro-survival genes in previous studies (*HBEGF* and *PRPS2*), most of the genes have not been. My results suggest that these 10 genes all play a role in cell survival and upon detachment these genes are repressed by miR-203, which contributes to anoikis. Investigating the specific pro-survival role of these 10 genes could each be its own investigation.

Research into the mechanism of anoikis resistance is important to fully understand metastasis, as there are two steps in the metastatic cascade where anoikis resistance in necessary. Metastatic cells resist anoikis first when tumor cells detach from the primary tumor and from their primary ECM and again when the tumor cell enters a secondary microenvironment and encounters an ECM with different composition and therefore different signaling molecules. I have identified two novel pathways through which we have gained insight into anoikis resistance in breast cancer.

In addition to KDM3A and miR-203, both of the genome wide screens I completed have lists of multiple potential anoikis effectors genes and miRNAS (Tables 3.1 and 4.2). Genome wide screens create huge datasets that leave you with a massive amount of leads to follow up on, these lists can act as a blueprint for further studies on anoikis and anoikis resistance in breast epithelial cells and could most likely continue to be studied for years to come. One thing that my studies have taught me is that the initial genome wide screen is the “easy” part of the experimental plan whereas deciding how to follow up on massive data sets can prove to be difficult. In both of my investigations I decided to follow and delineate the mechanism of one factor identified in each screen. On the other hand, other studies from the Green lab have taken a more network centered follow-up approach (Bhatnagar et al., 2014; Lin et al., 2014; Ma et al., 2014).

Either way, each genome wide study leaves a large amount of data that could potentially initiate a multitude of future investigations in the lab.

Additionally, a systems biology approach that could incorporate the datasets from both of my investigations would likely give a clearer picture of the process of anoikis on a genome wide level. There do exist methods to integrate biological datasets that could be used to integrate the datasets I produced for my studies to define a biological network that is critical for anoikis in MCF10A cells (Gligorijević and Pržulj, 2015). Another data integration approach is to input all of the genes and miRNAs from datasets in my dissertation into a Gene Ontology (GO, (Consortium, 2000)) or Ingenuity analysis (Raponi et al., 2004) to determine and common pathways or biological processes.

Taken together, these two investigations have allowed me to gain an appreciation for the complexity of studying biological processes. In both of my research projects I studied the general process of anoikis and sought to identify novel anoikis pathways, in the first study I identified a novel anoikis effector gene, KDM3A, and in my second study I identified a novel anoikis effector miRNA, miR-203. I have also shown that both KDM3A and miR-203 likely contribute to anoikis resistance in at least some breast cancers. In looking at the lists of genes and miRNAs that were generated from both of my projects, I conclude with the finding that anoikis, along with all other biological processes, is an extremely complex

process that cannot be defined from the mechanism of just one factor or pathway, however I propose that my investigations have moved the field one step forward towards the understanding of this complex process.

APPENDIX I

List of predicted miR-203 target genes from Targetscan (www.targetscan.org)

Target gene	Representative transcript	Gene name
3-Sep	NM_019106	septin 3
AAK1	NM_014911	AP2 associated kinase 1
ABCE1	NM_001040876	ATP-binding cassette, sub-family E (OABP), member 1
ABL1	NM_005157	c-abl oncogene 1, non-receptor tyrosine kinase
ABLIM3	NM_014945	actin binding LIM protein family, member 3
ACADSB	NM_001609	acyl-CoA dehydrogenase, short/branched chain
ACO2	NM_001098	aconitase 2, mitochondrial
ACSL1	NM_001995	acyl-CoA synthetase long-chain family member 1
ACSL3	NM_004457	acyl-CoA synthetase long-chain family member 3
ACSL6	NM_001009185	acyl-CoA synthetase long-chain family member 6
ACTR10	NM_018477	actin-related protein 10 homolog (S. cerevisiae)
ACVR2A	NM_001616	activin A receptor, type IIA
ACVR2B	NM_001106	activin A receptor, type IIB
ADAMTS15	NM_139055	ADAM metallopeptidase with thrombospondin type 1 motif, 15
ADAMTS17	NM_139057	ADAM metallopeptidase with thrombospondin type 1 motif, 17
ADAMTS5	NM_007038	ADAM metallopeptidase with thrombospondin type 1 motif, 5
ADAMTS6	NM_197941	ADAM metallopeptidase with thrombospondin type 1 motif, 6
ADAMTS8	NM_007037	ADAM metallopeptidase with thrombospondin type 1 motif, 8
ADARB2	NM_018702	adenosine deaminase, RNA-specific, B2
ADCY9	NM_001116	adenylate cyclase 9
ADK	NM_001123	adenosine kinase
ADPGK	NM_031284	ADP-dependent glucokinase
ADRBK2	NM_005160	adrenergic, beta, receptor kinase 2
AFAP1L2	NM_001001936	actin filament associated protein 1-like 2
AFF2	NM_001169122	AF4/FMR2 family, member 2
AFF4	NM_014423	AF4/FMR2 family, member 4
AGPAT6	NM_178819	1-acylglycerol-3-phosphate O-acyltransferase 6
AGPS	NM_003659	alkylglycerone phosphate synthase
AHR	NM_001621	aryl hydrocarbon receptor
AK4	NM_001005353	adenylate kinase 4
AKAP13	NM_006738	A kinase (PRKA) anchor protein 13
AKAP6	NM_004274	A kinase (PRKA) anchor protein 6

AKIRIN1	NM_001136275	akirin 1
AKIRIN2	NM_018064	akirin 2
AKT2	NM_001626	v-akt murine thymoma viral oncogene homolog 2
ALG10B	NM_001013620	asparagine-linked glycosylation 10, alpha-1,2-glucosyltransferase
AMFR	NM_001144	autocrine motility factor receptor
AMOT	NM_001113490	angiomotin
AMOTL1	NM_130847	angiomotin like 1
AMPD3	NM_000480	adenosine monophosphate deaminase 3
ANGPTL1	NM_004673	angiopoietin-like 1
ANKH	NM_054027	ankylosis, progressive homolog (mouse)
ANKRD13B	NM_152345	ankyrin repeat domain 13B
ANKRD13C	NM_030816	ankyrin repeat domain 13C
ANKRD17	NM_032217	ankyrin repeat domain 17
ANKRD44	NM_001195144	ankyrin repeat domain 44
ANKRD52	NM_173595	ankyrin repeat domain 52
ANKRD7	NM_019644	ankyrin repeat domain 7
ANO8	NM_020959	anoctamin 8
ANP32A	NM_006305	acidic (leucine-rich) nuclear phosphoprotein 32 family, member A
ANP32E	NM_001136478	acidic (leucine-rich) nuclear phosphoprotein 32 family, member E
ANTXR2	NM_058172	anthrax toxin receptor 2
ANXA4	NM_001153	annexin A4
AP1S2	NM_003916	adaptor-related protein complex 1, sigma 2 subunit
AP2B1	NM_001030006	adaptor-related protein complex 2, beta 1 subunit
APBB2	NM_001166050	amyloid beta (A4) precursor protein-binding, family B, member 2
APC	NM_000038	adenomatous polyposis coli
APLP1	NM_001024807	amyloid beta (A4) precursor-like protein 1
APOOL	NM_198450	apolipoprotein O-like
APPL1	NM_012096	adaptor protein, phosphotyrosine interaction, PH domain leucine zipper 1
ARHGAP1	NM_004308	Rho GTPase activating protein 1
ARHGAP32	NM_001142685	Rho GTPase activating protein 32
ARHGAP42	NM_152432	Rho GTPase activating protein 42
ARHGEF3	NM_001128615	Rho guanine nucleotide exchange factor (GEF) 3
ARID1B	NM_017519	AT rich interactive domain 1B (SWI1-like)
ARID2	NM_152641	AT rich interactive domain 2 (ARID, RFX-like)
ARID3B	NM_006465	AT rich interactive domain 3B (BRIGHT-like)
ARNTL	NM_001030272	aryl hydrocarbon receptor nuclear translocator-like
ARSB	NM_000046	arylsulfatase B
ASB4	NM_016116	ankyrin repeat and SOCS box containing 4

ASPH	NM_001164750	aspartate beta-hydroxylase
ASXL1	NM_015338	additional sex combs like 1 (Drosophila)
ATG14	NM_014924	ATG14 autophagy related 14 homolog (S. cerevisiae)
ATM	NM_000051	ataxia telangiectasia mutated
ATP10D	NM_020453	ATPase, class V, type 10D
ATP11B	NM_014616	ATPase, class VI, type 11B
ATP1B4	NM_001142447	ATPase, Na+/K+ transporting, beta 4 polypeptide
ATP2B1	NM_001001323	ATPase, Ca++ transporting, plasma membrane 1
ATP2C1	NM_001199179	ATPase, Ca++ transporting, type 2C, member 1
ATP5G3	NM_001190329	ATP synthase, H+ transporting, mitochondrial Fo complex, subunit C3
B3GALNT2	NM_152490	beta-1,3-N-acetylgalactosaminyltransferase 2
B3GNT5	NM_032047	UDP-GlcNAc:betaGal beta-1,3-N-acetylglucosaminyltransferase 5
BAGE2	NM_182482	B melanoma antigen family, member 2
BAGE3	NM_182481	B melanoma antigen family, member 3
BAHD1	NM_014952	bromo adjacent homology domain containing 1
BANF1	NM_001143985	barrier to autointegration factor 1
BCL11B	NM_022898	B-cell CLL/lymphoma 11B (zinc finger protein)
BCL2L2	NM_001199839	BCL2-like 2
BCL7A	NM_001024808	B-cell CLL/lymphoma 7A
BEND4	NM_001159547	BEN domain containing 4
BIRC5	NM_001012270	baculoviral IAP repeat containing 5
BMI1	NM_005180	BMI1 polycomb ring finger oncogene
BPTF	NM_004459	bromodomain PHD finger transcription factor
BSN	NM_003458	bassoon (presynaptic cytomatrix protein)
BTBD7	NM_001002860	BTB (POZ) domain containing 7
C10orf46	NM_153810	chromosome 10 open reading frame 46
C11orf68	NM_001135635	chromosome 11 open reading frame 68
C11orf91	NM_001166692	chromosome 11 open reading frame 91
C12orf4	NM_020374	chromosome 12 open reading frame 4
C12orf75	NM_001145199	chromosome 12 open reading frame 75
C13orf23	NM_025138	chromosome 13 open reading frame 23
C14orf129	NM_016472	chromosome 14 open reading frame 129
C14orf147	NM_138288	chromosome 14 open reading frame 147
C14orf28	NM_001017923	chromosome 14 open reading frame 28
C16orf45	NM_001142469	chromosome 16 open reading frame 45
C18orf1	NM_001003674	chromosome 18 open reading frame 1
C18orf34	NM_001105528	chromosome 18 open reading frame 34
C1orf122	NM_001142726	chromosome 1 open reading frame 122

C1orf144	NM_001114600	chromosome 1 open reading frame 144
C1orf172	NM_152365	chromosome 1 open reading frame 172
C1orf173	NM_001002912	chromosome 1 open reading frame 173
C1orf210	NM_001164829	chromosome 1 open reading frame 210
C20orf11	NM_017896	chromosome 20 open reading frame 11
C20orf24	NM_001199534	chromosome 20 open reading frame 24
C2orf80	NM_001099334	chromosome 2 open reading frame 80
C3orf15	NM_033364	chromosome 3 open reading frame 15
C3orf17	NM_015412	chromosome 3 open reading frame 17
C3orf63	NM_001112736	chromosome 3 open reading frame 63
C4orf33	NM_001099783	chromosome 4 open reading frame 33
C5orf41	NM_153607	chromosome 5 open reading frame 41
C6orf35	NM_018452	chromosome 6 open reading frame 35
C7orf42	NM_017994	chromosome 7 open reading frame 42
C8orf4	NM_020130	chromosome 8 open reading frame 4
C8orf44-SGK3	NM_001204173	C8orf44-SGK3 readthrough
CAB39	NM_001130849	calcium binding protein 39
CABP7	NM_182527	calcium binding protein 7
CACNA1E	NM_000721	calcium channel, voltage-dependent, R type, alpha 1E subunit
CACNG7	NM_031896	calcium channel, voltage-dependent, gamma subunit 7
CALML4	NM_001031733	calmodulin-like 4
CAMTA1	NM_001195563	calmodulin binding transcription activator 1
CAPN14	NM_001145122	calpain 14
CAPRIN1	NM_005898	cell cycle associated protein 1
CAPS	NM_004058	calcyphosine
CASC4	NM_138423	cancer susceptibility candidate 4
CASK	NM_001126054	calcium/calmodulin-dependent serine protein kinase (MAGUK family)
CAV1	NM_001172895	caveolin 1, caveolae protein, 22kDa
CBL	NM_005188	Cas-Br-M (murine) ecotropic retroviral transforming sequence
CBX5	NM_001127321	chromobox homolog 5
CCDC141	NM_173648	coiled-coil domain containing 141
CCDC148	NM_138803	coiled-coil domain containing 148
CCDC50	NM_174908	coiled-coil domain containing 50
CCNG1	NM_004060	cyclin G1
CCNG2	NM_004354	cyclin G2
CCNY	NM_145012	cyclin Y
CDH10	NM_006727	cadherin 10, type 2 (T2-cadherin)
CDH6	NM_004932	cadherin 6, type 2, K-cadherin (fetal kidney)

CDHR3	NM_152750	cadherin-related family member 3
CDK13	NM_003718	cyclin-dependent kinase 13
CDKL2	NM_003948	cyclin-dependent kinase-like 2 (CDC2-related kinase)
CDV3	NM_001134422	CDV3 homolog (mouse)
CEP68	NM_015147	centrosomal protein 68kDa
CHD2	NM_001271	chromodomain helicase DNA binding protein 2
CHD9	NM_025134	chromodomain helicase DNA binding protein 9
CHORDC1	NM_001144073	cysteine and histidine-rich domain (CHORD) containing 1
CHST7	NM_019886	carbohydrate (N-acetylglucosamine 6-O) sulfotransferase 7
CIT	NM_001206999	citron (rho-interacting, serine/threonine kinase 21)
CITED2	NM_001168388	Cbp/p300-interacting transactivator 2
CKAP2	NM_001098525	cytoskeleton associated protein 2
CLASP2	NM_001207044	cytoplasmic linker associated protein 2
CLDN1	NM_021101	claudin 1
CLEC12B	NM_001129998	C-type lectin domain family 12, member B
CLLU1	NM_001025233	chronic lymphocytic leukemia up-regulated 1
CLOCK	NM_004898	clock homolog (mouse)
CLSTN3	NM_014718	calsyntenin 3
CLTC	NM_004859	clathrin, heavy chain (Hc)
CNNM3	NM_017623	cyclin M3
CNTFR	NM_001207011	ciliary neurotrophic factor receptor
COL17A1	NM_000494	collagen, type XVII, alpha 1
COL4A4	NM_000092	collagen, type IV, alpha 4
COMMD3-BMI1	NM_001204062	COMMD3-BMI1 readthrough
COPS7B	NM_022730	COP9 constitutive photomorphogenic homolog subunit 7B (Arabidopsis)
CORO1C	NM_014325	coronin, actin binding protein, 1C
COX10	NM_001303	COX10 homolog, cytochrome c oxidase assembly protein
COX15	NM_004376	COX15 homolog, cytochrome c oxidase assembly protein (yeast)
CPEB4	NM_030627	cytoplasmic polyadenylation element binding protein 4
CPNE8	NM_153634	copine VIII
CREB1	NM_004379	cAMP responsive element binding protein 1
CREB3	NM_006368	cAMP responsive element binding protein 3
CREBZF	NM_001039618	CREB/ATF bZIP transcription factor
CRK	NM_005206	v-crk sarcoma virus CT10 oncogene homolog (avian)
CSN2	NM_001891	casein beta
CSRNP2	NM_030809	cysteine-serine-rich nuclear protein 2
CTDSPL2	NM_016396	CTD small phosphatase like 2
CTSS	NM_001199739	cathepsin S

CUL1	NM_003592	cullin 1
CUL2	NM_001198777	cullin 2
CXorf1	NM_004709	chromosome X open reading frame 1
CXorf21	NM_025159	chromosome X open reading frame 21
CXorf23	NM_198279	chromosome X open reading frame 23
CXorf38	NM_144970	chromosome X open reading frame 38
CYP8B1	NM_004391	cytochrome P450, family 8, subfamily B, polypeptide 1
D4S234E	NM_001040101	DNA segment on chromosome 4 (unique) 234 expressed sequence
DAB2	NM_001343	disabled homolog 2, mitogen-responsive phosphoprotein (Drosophila)
DAZAP2	NM_001136264	DAZ associated protein 2
DCC	NM_005215	deleted in colorectal carcinoma
DCP1A	NM_018403	DCP1 decapping enzyme homolog A (S. cerevisiae)
DCP2	NM_001242377	DCP2 decapping enzyme homolog (S. cerevisiae)
DCUN1D3	NM_173475	DCN1, defective in cullin neddylation 1, domain containing 3
DCUN1D4	NM_001040402	DCN1, defective in cullin neddylation 1, domain containing 4
DCUN1D5	NM_032299	DCN1, defective in cullin neddylation 1, domain containing 5
DCX	NM_000555	doublecortin
DDX6	NM_004397	DEAD (Asp-Glu-Ala-Asp) box polypeptide 6
DGCR2	NM_001173533	DiGeorge syndrome critical region gene 2
DGKB	NM_004080	diacylglycerol kinase, beta 90kDa
DGKE	NM_003647	diacylglycerol kinase, epsilon 64kDa
DGKZ	NM_001105540	diacylglycerol kinase, zeta
DICER1	NM_001195573	dicer 1, ribonuclease type III
DIO2	NM_000793	deiodinase, iodothyronine, type II
DIXDC1	NM_001037954	DIX domain containing 1
DLG5	NM_004747	discs, large homolog 5 (Drosophila)
DLX5	NM_005221	distal-less homeobox 5
DMRT2	NM_001130865	doublesex and mab-3 related transcription factor 2
DNAJC14	NM_032364	DnaJ (Hsp40) homolog, subfamily C, member 14
DNAJC21	NM_001012339	DnaJ (Hsp40) homolog, subfamily C, member 21
DNAJC24	NM_181706	DnaJ (Hsp40) homolog, subfamily C, member 24
DNAJC27	NM_001198559	DnaJ (Hsp40) homolog, subfamily C, member 27
DNAL1	NM_001201366	dynein, axonemal, light chain 1
DNM1L	NM_005690	dynamin 1-like
DNMT3B	NM_001207055	DNA (cytosine-5-)-methyltransferase 3 beta
DOCK10	NM_014689	dedicator of cytokinesis 10
DPH3	NM_001047434	DPH3, KTI11 homolog (S. cerevisiae)
DPY19L4	NM_181787	dpy-19-like 4 (C. elegans)

DR1	NM_001938	down-regulator of transcription 1, TBP-binding (negative cofactor 2)
DUSP5	NM_004419	dual specificity phosphatase 5
DUT	NM_001025248	deoxyuridine triphosphatase
DYRK1A	NM_001396	dual-specificity tyrosine-(Y)-phosphorylation regulated kinase 1A
E2F3	NM_001949	E2F transcription factor 3
EBF1	NM_024007	early B-cell factor 1
EBF3	NM_001005463	early B-cell factor 3
ECHDC2	NM_001198961	enoyl CoA hydratase domain containing 2
EDA	NM_001005609	ectodysplasin A
EDNRA	NM_001166055	endothelin receptor type A
EGR3	NM_001199880	early growth response 3
EHF	NM_001206615	ets homologous factor
EID2	NM_153232	EP300 interacting inhibitor of differentiation 2
EIF4E	NM_001130678	eukaryotic translation initiation factor 4E
EIF5A2	NM_020390	eukaryotic translation initiation factor 5A2
ELK4	NM_001973	ELK4, ETS-domain protein (SRF accessory protein 1)
ELL2	NM_012081	elongation factor, RNA polymerase II, 2
ELMOD1	NM_001130037	ELMO/CED-12 domain containing 1
ELMOD2	NM_153702	ELMO/CED-12 domain containing 2
ELOVL6	NM_001130721	ELOVL fatty acid elongase 6
EN2	NM_001427	engrailed homeobox 2
ENAH	NM_001008493	enabled homolog (Drosophila)
EPC2	NM_015630	enhancer of polycomb homolog 2 (Drosophila)
EPHA3	NM_005233	EPH receptor A3
ERLIN2	NM_001003790	ER lipid raft associated 2
ESR1	NM_000125	estrogen receptor 1
ETS2	NM_005239	v-ets erythroblastosis virus E26 oncogene homolog 2 (avian)
ETV1	NM_001163147	ets variant 1
EVI2B	NM_006495	ecotropic viral integration site 2B
EYA4	NM_004100	eyes absent homolog 4 (Drosophila)
FAM104A	NM_001098832	family with sequence similarity 104, member A
FAM114A1	NM_138389	family with sequence similarity 114, member A1
FAM116A	NM_152678	family with sequence similarity 116, member A
FAM117B	NM_173511	family with sequence similarity 117, member B
FAM120C	NM_017848	family with sequence similarity 120C
FAM126A	NM_032581	family with sequence similarity 126, member A
FAM126B	NM_173822	family with sequence similarity 126, member B
FAM135B	NM_015912	family with sequence similarity 135, member B
FAM13A	NM_001015045	family with sequence similarity 13, member A

FAM155A	NM_001080396	family with sequence similarity 155, member A
FAM170B	NM_001164484	family with sequence similarity 170, member B
FAM198B	NM_001031700	family with sequence similarity 198, member B
FAM55C	NM_001134456	family with sequence similarity 55, member C
FAM84A	NM_145175	family with sequence similarity 84, member A
FAM8A1	NM_016255	family with sequence similarity 8, member A1
FASTKD2	NM_001136193	FAST kinase domains 2
FAT3	NM_001008781	FAT tumor suppressor homolog 3 (Drosophila)
FBXL19	NM_001099784	F-box and leucine-rich repeat protein 19
FBXL20	NM_001184906	F-box and leucine-rich repeat protein 20
FBXO11	NM_001190274	F-box protein 11
FBXO28	NM_001136115	F-box protein 28
FBXO44	NM_001014765	F-box protein 44
FBXO45	NM_001105573	F-box protein 45
FGD4	NM_139241	FYVE, RhoGEF and PH domain containing 4
FGF2	NM_002006	fibroblast growth factor 2 (basic)
FGF5	NM_004464	fibroblast growth factor 5
FGL2	NM_006682	fibrinogen-like 2
FJX1	NM_014344	four jointed box 1 (Drosophila)
FKBP5	NM_001145775	FK506 binding protein 5
FKBP7	NM_001135212	FK506 binding protein 7
FLRT2	NM_013231	fibronectin leucine rich transmembrane protein 2
FMOD	NM_002023	fibromodulin
FOSL2	NM_005253	FOS-like antigen 2
FOXJ3	NM_001198850	forkhead box J3
FOXK1	NM_001037165	forkhead box K1
FOXK2	NM_004514	forkhead box K2
FOXP1	NM_032682	forkhead box P1
FOXP2	NM_001172766	forkhead box P2
FUBP3	NM_003934	far upstream element (FUSE) binding protein 3
G6PC2	NM_001081686	glucose-6-phosphatase, catalytic, 2
GABARAPL 1	NM_031412	GABA(A) receptor-associated protein like 1
GABBR2	NM_005458	gamma-aminobutyric acid (GABA) B receptor, 2
GABRA1	NM_000806	gamma-aminobutyric acid (GABA) A receptor, alpha 1
GABRA5	NM_000810	gamma-aminobutyric acid (GABA) A receptor, alpha 5
GABRB2	NM_000813	gamma-aminobutyric acid (GABA) A receptor, beta 2
GALNT10	NM_198321	UDP-N-acetyl-alpha-D-galactosamine:polypeptide N-acetylgalactosaminyltransferase 10
GALNT7	NM_017423	UDP-N-acetyl-alpha-D-galactosamine:polypeptide N-acetylgalactosaminyltransferase 7

GATC	NM_176818	glutamyl-tRNA(Gln) amidotransferase, subunit C homolog (bacterial)
GDA	NM_001242506	guanine deaminase
GDAP1	NM_001040875	ganglioside-induced differentiation-associated protein 1
GEMIN8	NM_001042479	gem (nuclear organelle) associated protein 8
GINS4	NM_032336	GINS complex subunit 4 (Sld5 homolog)
GJB6	NM_001110219	gap junction protein, beta 6, 30kDa
GLCCI1	NM_138426	glucocorticoid induced transcript 1
GLI3	NM_000168	GLI family zinc finger 3
GLS	NM_014905	glutaminase
GLTP	NM_016433	glycolipid transfer protein
GMFB	NM_004124	glia maturation factor, beta
GNG2	NM_053064	guanine nucleotide binding protein (G protein), gamma 2
GNG4	NM_001098721	guanine nucleotide binding protein (G protein), gamma 4
GOSR1	NM_001007024	golgi SNAP receptor complex member 1
GP5	NM_004488	glycoprotein V (platelet)
GPATCH1	NM_018025	G patch domain containing 1
GPBP1L1	NM_021639	GC-rich promoter binding protein 1-like 1
GPHN	NM_001024218	gephyrin
GPKOW	NM_015698	G patch domain and KOW motifs
GPR155	NM_001033045	G protein-coupled receptor 155
GPR180	NM_180989	G protein-coupled receptor 180
GPR26	NM_153442	G protein-coupled receptor 26
GPR85	NM_001146265	G protein-coupled receptor 85
GRHL3	NM_001195010	grainyhead-like 3 (Drosophila)
GRPR	NM_005314	gastrin-releasing peptide receptor
GRSF1	NM_001098477	G-rich RNA sequence binding factor 1
GTF3C3	NM_012086	general transcription factor IIIC, polypeptide 3, 102kDa
GXYLT1	NM_001099650	glucoside xylosyltransferase 1
GYS1	NM_001161587	glycogen synthase 1 (muscle)
HADHB	NM_000183	hydroxyacyl-CoA dehydrogenase/3-ketoacyl-CoA thiolase beta subunit
HBEGF	NM_001945	heparin-binding EGF-like growth factor
HBP1	NM_012257	HMG-box transcription factor 1
HCAR2	NM_177551	hydroxycarboxylic acid receptor 2
HCAR3	NM_006018	hydroxycarboxylic acid receptor 3
HCCS	NM_001122608	holocytochrome c synthase
HDX	NM_001177478	highly divergent homeobox
HERC2	NM_004667	hect domain and RLD 2
HERPUD2	NM_022373	HERPUD family member 2

HLA-DOA	NM_002119	major histocompatibility complex, class II, DO alpha
HMGN2	NM_005517	high mobility group nucleosomal binding domain 2
HNRNPA2 B1	NM_002137	heterogeneous nuclear ribonucleoprotein A2/B1
HNRNPL	NM_001005335	heterogeneous nuclear ribonucleoprotein L
HNRNPR	NM_001102397	heterogeneous nuclear ribonucleoprotein R
HNRNPUL2	NM_001079559	heterogeneous nuclear ribonucleoprotein U-like 2
HOMER1	NM_004272	homer homolog 1 (Drosophila)
HOOK3	NM_032410	hook homolog 3 (Drosophila)
HPS3	NM_032383	Hermansky-Pudlak syndrome 3
HRASLS5	NM_001146728	HRAS-like suppressor family, member 5
HS6ST3	NM_153456	heparan sulfate 6-O-sulfotransferase 3
HSPB8	NM_014365	heat shock 22kDa protein 8
HSPC159	NM_014181	galectin-related protein
HTR2A	NM_000621	5-hydroxytryptamine (serotonin) receptor 2A
HTR2C	NM_000868	5-hydroxytryptamine (serotonin) receptor 2C
ID4	NM_001546	inhibitor of DNA binding 4, dominant negative helix-loop-helix protein
IFNA2	NM_000605	interferon, alpha 2
IGF2R	NM_000876	insulin-like growth factor 2 receptor
IGFBP5	NM_000599	insulin-like growth factor binding protein 5
IL15	NM_000585	interleukin 15
IL24	NM_001185156	interleukin 24
ILDR2	NM_199351	immunoglobulin-like domain containing receptor 2
IMPA1	NM_001144878	inositol(myo)-1(or 4)-monophosphatase 1
IMPACT	NM_018439	Impact homolog (mouse)
INA	NM_032727	internexin neuronal intermediate filament protein, alpha
INO80D	NM_017759	INO80 complex subunit D
INSIG1	NM_005542	insulin induced gene 1
INTS6	NM_001039938	integrator complex subunit 6
IPO7	NM_006391	importin 7
IRS2	NM_003749	insulin receptor substrate 2
ITGA2	NM_002203	integrin, alpha 2 (CD49B, alpha 2 subunit of VLA-2 receptor)
ITGAV	NM_001144999	integrin, alpha V
ITPR2	NM_002223	inositol 1,4,5-trisphosphate receptor, type 2
IVNS1ABP	NM_006469	influenza virus NS1A binding protein
JMY	NM_152405	junction mediating and regulatory protein, p53 cofactor
JOSD1	NM_014876	Josephin domain containing 1
KAT6A	NM_001099412	K(lysine) acetyltransferase 6A
KAZN	NM_001017999	kazrin, periplakin interacting protein

KCMF1	NM_020122	potassium channel modulatory factor 1
KCNC1	NM_004976	potassium voltage-gated channel, Shaw-related subfamily, member 1
KCNE2	NM_172201	potassium voltage-gated channel, Isk-related family, member 2
KCNJ15	NM_002243	potassium inwardly-rectifying channel, subfamily J, member 15
KCNK10	NM_021161	potassium channel, subfamily K, member 10
KCNN3	NM_001204087	potassium calcium-activated channel, subfamily N, member 3
KCNQ5	NM_001160130	potassium voltage-gated channel, KQT-like subfamily, member 5
KCTD16	NM_020768	potassium channel tetramerisation domain containing 16
KCTD9	NM_017634	potassium channel tetramerisation domain containing 9
KHDRBS1	NM_006559	KH domain containing, RNA binding, signal transduction associated 1
KIAA0240	NM_015349	KIAA0240
KIAA0247	NM_014734	KIAA0247
KIAA0664	NM_015229	KIAA0664
KIAA0930	NM_001009880	KIAA0930
KIAA1009	NM_014895	KIAA1009
KIAA1147	NM_001080392	KIAA1147
KIAA1211	NM_020722	KIAA1211
KIAA1244	NM_020340	KIAA1244
KIAA1429	NM_015496	KIAA1429
KIAA1804	NM_032435	mixed lineage kinase 4
KIAA1919	NM_153369	KIAA1919
KIF2A	NM_001098511	kinesin heavy chain member 2A
KIRREL2	NM_032123	kin of IRRE like 2 (Drosophila)
KLHL15	NM_030624	kelch-like 15 (Drosophila)
KPNB1	NM_002265	karyopherin (importin) beta 1
KRT1	NM_006121	keratin 1
KRT35	NM_002280	keratin 35
KRT85	NM_002283	keratin 85
KYNU	NM_001032998	kynureninase
LAMC1	NM_002293	laminin, gamma 1 (formerly LAMB2)
LAMP2	NM_013995	lysosomal-associated membrane protein 2
LARP1B	NM_018078	La ribonucleoprotein domain family, member 1B
LASP1	NM_006148	LIM and SH3 protein 1
LCOR	NM_001170765	ligand dependent nuclear receptor corepressor
LCORL	NM_001166139	ligand dependent nuclear receptor corepressor-like
LIFR	NM_001127671	leukemia inhibitory factor receptor alpha
LIMCH1	NM_001112717	LIM and calponin homology domains 1
LIN28B	NM_001004317	lin-28 homolog B (C. elegans)

LIN7C	NM_018362	lin-7 homolog C (C. elegans)
LMO4	NM_006769	LIM domain only 4
LNX2	NM_153371	ligand of numb-protein X 2
LOC100507421	NM_001195278	transmembrane protein 178-like
LOX	NM_001178102	lysyl oxidase
LPHN1	NM_001008701	latrophilin 1
LPIN1	NM_145693	lipin 1
LPO	NM_001160102	lactoperoxidase
LPP	NM_001167671	LIM domain containing preferred translocation partner in lipoma
LRAT	NM_004744	lecithin retinol acyltransferase(phosphatidylcholine-retinol O-acyltransferase)
LRRTM2	NM_015564	leucine rich repeat transmembrane neuronal 2
LUZP2	NM_001009909	leucine zipper protein 2
MAFB	NM_005461	v-maf musculoaponeurotic fibrosarcoma oncogene homolog B
MAGI1	NM_004742	membrane associated guanylate kinase, 1
MAN1A2	NM_006699	mannosidase, alpha, class 1A, member 2
MAP3K1	NM_005921	mitogen-activated protein kinase kinase kinase 1
MAP3K13	NM_001242314	mitogen-activated protein kinase kinase kinase 13
MAP3K2	NM_006609	mitogen-activated protein kinase kinase kinase 2
MAPK10	NM_002753	mitogen-activated protein kinase 10
MAPK1IP1L	NM_144578	mitogen-activated protein kinase 1 interacting protein 1-like
MAPK9	NM_002752	mitogen-activated protein kinase 9
MAPRE1	NM_012325	microtubule-associated protein, RP/EB family, member 1
MAST4	NM_001164664	microtubule associated serine/threonine kinase family member 4
MATR3	NM_001194954	matrin 3
MBD6	NM_052897	methyl-CpG binding domain protein 6
MBNL1	NM_021038	muscleblind-like (Drosophila)
MBNL3	NM_001170701	muscleblind-like 3 (Drosophila)
MCCC2	NM_022132	methylcrotonoyl-CoA carboxylase 2 (beta)
MCTP2	NM_001159643	multiple C2 domains, transmembrane 2
MED14	NM_004229	mediator complex subunit 14
MEF2C	NM_001131005	myocyte enhancer factor 2C
MEGF11	NM_032445	multiple EGF-like-domains 11
METTL8	NM_024770	methyltransferase like 8
MEX3C	NM_016626	mex-3 homolog C (C. elegans)
MGAT3	NM_001098270	mannosyl (beta-1,4-)-glycoprotein beta-1,4-N-acetylglucosaminyltransferase
MIDN	NM_177401	midnolin
MINA	NM_001042533	MYC induced nuclear antigen

MKL2	NM_014048	MKL/myocardin-like 2
MKLN1	NM_001145354	muskelin 1, intracellular mediator containing kelch motifs
MLANA	NM_005511	melan-A
MLLT4	NM_001040000	myeloid/lymphoid or mixed-lineage leukemia); translocated to, 4
MMAB	NM_052845	methylmalonic aciduria (cobalamin deficiency) cblB type
MMP24	NM_006690	matrix metallopeptidase 24 (membrane-inserted)
MON2	NM_015026	MON2 homolog (S. cerevisiae)
MORF4L1	NM_006791	mortality factor 4 like 1
MORF4L2	NM_001142418	mortality factor 4 like 2
MPP3	NM_001932	membrane protein, palmitoylated 3 (MAGUK p55 subfamily member 3)
MRVI1	NM_001098579	murine retrovirus integration site 1 homolog
MSL1	NM_001012241	male-specific lethal 1 homolog (Drosophila)
MSR1	NM_002445	macrophage scavenger receptor 1
MYEF2	NM_016132	myelin expression factor 2
MYLK4	NM_001012418	myosin light chain kinase family, member 4
MYO5A	NM_000259	myosin VA (heavy chain 12, myoxin)
MYOZ2	NM_016599	myozenin 2
N4BP3	NM_015111	NEDD4 binding protein 3
NAA30	NM_001011713	N(alpha)-acetyltransferase 30, NatC catalytic subunit
NAA50	NM_025146	N(alpha)-acetyltransferase 50, NatE catalytic subunit
NAP1L4	NM_005969	nucleosome assembly protein 1-like 4
NBEA	NM_001204197	neurobeachin
NCALD	NM_001040624	neurocalcin delta
NCL	NM_005381	nucleolin
NDRG3	NM_022477	NDRG family member 3
NDST3	NM_004784	N-deacetylase/N-sulfotransferase (heparan glucosaminyl) 3
NEDD4L	NM_001144964	neural precursor cell expressed, developmentally down-regulated 4-like
NEDD9	NM_001142393	neural precursor cell expressed, developmentally down-regulated 9
NEGR1	NM_173808	neuronal growth regulator 1
NEMF	NM_004713	nuclear export mediator factor
NFIB	NM_001190737	nuclear factor I/B
NFIL3	NM_005384	nuclear factor, interleukin 3 regulated
NFYA	NM_002505	nuclear transcription factor Y, alpha
NIPSNAP3B	NM_018376	nipsnap homolog 3B (C. elegans)
NKD1	NM_033119	naked cuticle homolog 1 (Drosophila)
NLK	NM_016231	nemo-like kinase
NMNAT2	NM_015039	nicotinamide nucleotide adenylyltransferase 2

NOVA1	NM_002515	neuro-oncological ventral antigen 1
NPAS4	NM_178864	neuronal PAS domain protein 4
NPR3	NM_000908	natriuretic peptide receptor C/guanylate cyclase C
NPRL2	NM_006545	nitrogen permease regulator-like 2 (S. cerevisiae)
NR1D2	NM_001145425	nuclear receptor subfamily 1, group D, member 2
NR2C2	NM_003298	nuclear receptor subfamily 2, group C, member 2
NR5A2	NM_003822	nuclear receptor subfamily 5, group A, member 2
NRBP2	NM_178564	nuclear receptor binding protein 2
NRG1	NM_001159995	neuregulin 1
NRG2	NM_001184935	neuregulin 2
NSL1	NM_001042549	NSL1, MIND kinetochore complex component, homolog
NSUN7	NM_024677	NOP2/Sun domain family, member 7
NUAK1	NM_014840	NUAK family, SNF1-like kinase, 1
NUDT21	NM_007006	nudix (nucleoside diphosphate linked moiety X)-type motif 21
NUFIP2	NM_020772	nuclear fragile X mental retardation protein interacting protein 2
NUMBL	NM_004756	numb homolog (Drosophila)-like
NXPH3	NM_007225	neurexophilin 3
OBFC1	NM_024928	oligonucleotide/oligosaccharide-binding fold containing 1
OCLN	NM_001205254	occludin
OLFM1	NM_006334	olfactomedin 1
OLIG3	NM_175747	oligodendrocyte transcription factor 3
OPA1	NM_015560	optic atrophy 1 (autosomal dominant)
OR2L13	NM_175911	olfactory receptor, family 2, subfamily L, member 13
OR9Q1	NM_001005212	olfactory receptor, family 9, subfamily Q, member 1
ORC2	NM_006190	origin recognition complex, subunit 2
OSBPL1A	NM_001242508	oxysterol binding protein-like 1A
OSBPL8	NM_001003712	oxysterol binding protein-like 8
OVOL1	NM_004561	ovo-like 1(Drosophila)
PACS2	NM_001100913	phosphofurin acidic cluster sorting protein 2
PADI2	NM_007365	peptidyl arginine deiminase, type II
PAFAH1B2	NM_002572	platelet-activating factor acetylhydrolase 1b, catalytic subunit 2
PAIP2B	NM_020459	poly(A) binding protein interacting protein 2B
PALM2	NM_001037293	paralemmin 2
PAPD5	NM_001040284	PAP associated domain containing 5
PAPSS2	NM_001015880	3'-phosphoadenosine 5'-phosphosulfate synthase 2
PAQR3	NM_001040202	progestin and adipoQ receptor family member III
PARM1	NM_015393	prostate androgen-regulated mucin-like protein 1
PARP11	NM_020367	poly (ADP-ribose) polymerase family, member 11
PARP16	NM_017851	poly (ADP-ribose) polymerase family, member 16

PARP8	NM_001178055	poly (ADP-ribose) polymerase family, member 8
PBRM1	NM_018165	polybromo 1
PCBP2	NM_001098620	poly(rC) binding protein 2
PCDH10	NM_032961	protocadherin 10
PCDH19	NM_001105243	protocadherin 19
PCLO	NM_014510	piccolo (presynaptic cytomatrix protein)
PCSK1	NM_000439	proprotein convertase subtilisin/kexin type 1
PCSK2	NM_001201528	proprotein convertase subtilisin/kexin type 2
PDAP1	NM_014891	PDGFA associated protein 1
PDE3B	NM_000922	phosphodiesterase 3B, cGMP-inhibited
PDE4D	NM_001104631	phosphodiesterase 4D, cAMP-specific
PDE6D	NM_002601	phosphodiesterase 6D, cGMP-specific, rod, delta
PDE6H	NM_006205	phosphodiesterase 6H, cGMP-specific, cone, gamma
PDGFD	NM_025208	platelet derived growth factor D
PDGFRA	NM_006206	platelet-derived growth factor receptor, alpha polypeptide
PDHA1	NM_000284	pyruvate dehydrogenase (lipoamide) alpha 1
PDK3	NM_001142386	pyruvate dehydrogenase kinase, isozyme 3
PDPN	NM_001006624	podoplanin
PDSS2	NM_020381	prenyl (decaprenyl) diphosphate synthase, subunit 2
PEX3	NM_003630	peroxisomal biogenesis factor 3
PHACTR4	NM_001048183	phosphatase and actin regulator 4
PHC3	NM_024947	polyhomeotic homolog 3 (Drosophila)
PHF12	NM_001033561	PHD finger protein 12
PHF19	NM_015651	PHD finger protein 19
PHKA1	NM_001122670	phosphorylase kinase, alpha 1 (muscle)
PHLDA1	NM_007350	pleckstrin homology-like domain, family A, member 1
PHLDA3	NM_012396	pleckstrin homology-like domain, family A, member 3
PHLDB1	NM_001144758	pleckstrin homology-like domain, family B, member 1
PIK3CA	NM_006218	phosphoinositide-3-kinase, catalytic, alpha polypeptide
PIK3CD	NM_005026	phosphoinositide-3-kinase, catalytic, delta polypeptide
PIM3	NM_001001852	pim-3 oncogene
PITPNB	NM_012399	phosphatidylinositol transfer protein, beta
PKD2	NM_000297	polycystic kidney disease 2 (autosomal dominant)
PLAA	NM_001031689	phospholipase A2-activating protein
PLAGL2	NM_002657	pleiomorphic adenoma gene-like 2
PLD1	NM_001130081	phospholipase D1, phosphatidylcholine-specific
PLD2	NM_002663	phospholipase D2
PLEKHG3	NM_015549	pleckstrin homology domain containing, family G member 3
PNMA1	NM_006029	paraneoplastic antigen MA1

PPAP2B	NM_003713	phosphatidic acid phosphatase type 2B
PPM1A	NM_021003	protein phosphatase, Mg2+/Mn2+ dependent, 1A
PPM1D	NM_003620	protein phosphatase, Mg2+/Mn2+ dependent, 1D
PPM1E	NM_014906	protein phosphatase, Mg2+/Mn2+ dependent, 1E
PPP1CB	NM_002709	protein phosphatase 1, catalytic subunit, beta isozyme
PPP1R12A	NM_001143885	protein phosphatase 1, regulatory (inhibitor) subunit 12A
PPTC7	NM_139283	PTC7 protein phosphatase homolog (S. cerevisiae)
PRELP	NM_002725	proline/arginine-rich end leucine-rich repeat protein
PRICKLE2	NM_198859	prickle homolog 2 (Drosophila)
PRKAB1	NM_006253	protein kinase, AMP-activated, beta 1 non-catalytic subunit
PRKAB2	NM_005399	protein kinase, AMP-activated, beta 2 non-catalytic subunit
PRKAG2	NM_001040633	protein kinase, AMP-activated, gamma 2 non-catalytic subunit
PRKCA	NM_002737	protein kinase C, alpha
PRKCB	NM_002738	protein kinase C, beta
PRKCI	NM_002740	protein kinase C, iota
PRKX	NM_005044	protein kinase, X-linked
PRPF19	NM_014502	PRP19/PSO4 pre-mRNA processing factor 19 homolog
PRPS2	NM_001039091	phosphoribosyl pyrophosphate synthetase 2
PRUNE2	NM_015225	prune homolog 2 (Drosophila)
PSMA4	NM_001102667	proteasome (prosome, macropain) subunit, alpha type, 4
PTCH1	NM_000264	patched 1
PTGS1	NM_000962	prostaglandin-endoperoxide synthase 1
PTP4A1	NM_003463	protein tyrosine phosphatase type IVA, member 1
PTPN1	NM_002827	protein tyrosine phosphatase, non-receptor type 1
PTPN3	NM_001145368	protein tyrosine phosphatase, non-receptor type 3
PTPRB	NM_001109754	protein tyrosine phosphatase, receptor type, B
PURB	NM_033224	purine-rich element binding protein B
PXDN	NM_012293	peroxidasin homolog (Drosophila)
PXN	NM_001080855	paxillin
RAB10	NM_016131	RAB10, member RAS oncogene family
RAB15	NM_198686	RAB15, member RAS onocogene family
RAB22A	NM_020673	RAB22A, member RAS oncogene family
RAB27B	NM_004163	RAB27B, member RAS oncogene family
RAB31	NM_006868	RAB31, member RAS oncogene family
RAB3B	NM_002867	RAB3B, member RAS oncogene family
RALB	NM_002881	v-ral simian leukemia viral oncogene homolog B
RAP1A	NM_001010935	RAP1A, member of RAS oncogene family
RAP2A	NM_021033	RAP2A, member of RAS oncogene family
RAPGEF1	NM_005312	Rap guanine nucleotide exchange factor (GEF) 1

RAPH1	NM_213589	Ras association (RalGDS/AF-6) and pleckstrin homology domains 1
RASAL2	NM_004841	RAS protein activator like 2
RASGRF1	NM_001145648	Ras protein-specific guanine nucleotide-releasing factor 1
RAVER2	NM_018211	ribonucleoprotein, PTB-binding 2
RBBP5	NM_001193272	retinoblastoma binding protein 5
RBM20	NM_001134363	RNA binding motif protein 20
RBM25	NM_021239	RNA binding motif protein 25
RBM44	NM_001080504	RNA binding motif protein 44
RBM47	NM_001098634	RNA binding motif protein 47
RBMS1	NM_002897	RNA binding motif, single stranded interacting protein 1
RCN2	NM_002902	reticulocalbin 2, EF-hand calcium binding domain
RERG	NM_001190726	RAS-like, estrogen-regulated, growth inhibitor
RFX7	NM_022841	regulatory factor X, 7
RGS5	NM_001195303	regulator of G-protein signaling 5
RGS7	NM_002924	regulator of G-protein signaling 7
RHOQ	NM_012249	ras homolog gene family, member Q
RIOK3	NM_003831	RIO kinase 3 (yeast)
RLIM	NM_016120	ring finger protein, LIM domain interacting
RMND5A	NM_022780	required for meiotic nuclear division 5 homolog A (S. cerevisiae)
RNASE4	NM_002937	ribonuclease, RNase A family, 4
RNF144A	NM_014746	ring finger protein 144A
RNF38	NM_022781	ring finger protein 38
ROBO2	NM_001128929	roundabout, axon guidance receptor, homolog 2 (Drosophila)
RPGRIP1L	NM_001127897	RPGRIP1-like
RPL23A	NM_000984	ribosomal protein L23a
RPRD2	NM_015203	regulation of nuclear pre-mRNA domain containing 2
RS1	NM_000330	retinoschisin 1
RSBN1	NM_018364	round spermatid basic protein 1
RSPO1	NM_001038633	R-spondin 1
RTCD1	NM_001130841	RNA terminal phosphate cyclase domain 1
RTKN2	NM_145307	rhotekin 2
RUNX1T1	NM_001198625	runt-related transcription factor 1; translocated to, 1
RUNX2	NM_001015051	runt-related transcription factor 2
RWDD4	NM_152682	RWD domain containing 4
SAMD5	NM_001030060	sterile alpha motif domain containing 5
SAV1	NM_021818	salvador homolog 1 (Drosophila)
SBF2	NM_030962	SET binding factor 2
SCAF11	NM_004719	SR-related CTD-associated factor 11
SCARA5	NM_173833	scavenger receptor class A, member 5 (putative)

SCARB2	NM_001204255	scavenger receptor class B, member 2
SCCPDH	NM_016002	saccharopine dehydrogenase (putative)
SCEL	NM_001160706	sciellin
SCFD1	NM_016106	sec1 family domain containing 1
SCGB2A1	NM_002407	secretoglobin, family 2A, member 1
SCN1A	NM_001165963	sodium channel, voltage-gated, type I, alpha subunit
SCN9A	NM_002977	sodium channel, voltage-gated, type IX, alpha subunit
SDK1	NM_152744	sidekick homolog 1, cell adhesion molecule (chicken)
SEC62	NM_003262	SEC62 homolog (S. cerevisiae)
SEL1L	NM_005065	sel-1 suppressor of lin-12-like (C. elegans)
SELT	NM_016275	selenoprotein T
SEMA3A	NM_006080	sema domain, secreted, (semaphorin) 3A
SEMA5A	NM_003966	sema domain, (semaphorin) 5A
SEMA6A	NM_020796	sema domain, (semaphorin) 6A
SENP5	NM_152699	SUMO1/sentrin specific peptidase 5
SEPN1	NM_020451	selenoprotein N, 1
SESTD1	NM_178123	SEC14 and spectrin domains 1
SETBP1	NM_015559	SET binding protein 1
SETD7	NM_030648	SET domain containing (lysine methyltransferase) 7
SFI1	NM_001007467	Sfi1 homolog, spindle assembly associated (yeast)
SFRP1	NM_003012	secreted frizzled-related protein 1
SGK3	NM_001033578	serum/glucocorticoid regulated kinase family, member 3
SGK494	NM_001174103	uncharacterized serine/threonine-protein kinase SgK494
SGMS2	NM_001136257	sphingomyelin synthase 2
SGTB	NM_019072	small glutamine-rich tetratricopeptide repeat (TPR)-containing, beta
SH3BGR	NM_001001713	SH3 domain binding glutamic acid-rich protein
SH3BGRL2	NM_031469	SH3 domain binding glutamic acid-rich protein like 2
SHMT1	NM_004169	serine hydroxymethyltransferase 1 (soluble)
SIK1	NM_173354	salt-inducible kinase 1
SIK2	NM_015191	salt-inducible kinase 2
SIX3	NM_005413	SIX homeobox 3
SLC10A2	NM_000452	solute carrier family 10 member 2
SLC12A2	NM_001046	solute carrier family 12 member 2
SLC12A5	NM_001134771	solute carrier family 12 member 5
SLC16A2	NM_006517	solute carrier family 16, member 2
SLC22A23	NM_015482	solute carrier family 22, member 23
SLC24A1	NM_004727	solute carrier family 24, member 1
SLC24A2	NM_001193288	solute carrier family 24, member 2
SLC25A23	NM_024103	solute carrier family25, member 23

SLC25A36	NM_001104647	solute carrier family 25, member 36
SLC26A9	NM_052934	solute carrier family 26, member 9
SLC28A3	NM_001199633	solute carrier family 28 (sodium-coupled nucleoside transporter)
SLC2A13	NM_052885	solute carrier family 2 (facilitated glucose transporter), member 13
SLC2A3	NM_006931	solute carrier family 2 (facilitated glucose transporter), member 3
SLC30A6	NM_001193513	solute carrier family 30 (zinc transporter), member 6
SLC30A7	NM_001144884	solute carrier family 30 (zinc transporter), member 7
SLC39A1	NM_014437	solute carrier family 39 (zinc transporter), member 1
SLC39A9	NM_018375	solute carrier family 39 (zinc transporter), member 9
SLC4A4	NM_001098484	solute carrier family 4, sodium bicarbonate cotransporter, member 4
SLC5A12	NM_178498	solute carrier family 5 (sodium/glucose cotransporter), member 12
SLC7A14	NM_020949	solute carrier family 7 (orphan transporter), member 14
SLCO3A1	NM_013272	solute carrier organic anion transporter family, member 3A1
SLMAP	NM_007159	sarcolemma associated protein
SLMO2	NM_016045	slowmo homolog 2 (Drosophila)
SMAD3	NM_001145102	SMAD family member 3
SMAD9	NM_001127217	SMAD family member 9
SMU1	NM_018225	smu-1 suppressor of mec-8 and unc-52 homolog (C. elegans)
SMURF1	NM_001199847	SMAD specific E3 ubiquitin protein ligase 1
SNAI2	NM_003068	snail homolog 2 (Drosophila)
SNAP91	NM_001242792	synaptosomal-associated protein, 91kDa homolog (mouse)
SNN	NM_003498	stannin
SNRPD1	NM_006938	small nuclear ribonucleoprotein D1 polypeptide 16kDa
SNX13	NM_015132	sorting nexin 13
SNX24	NM_014035	sorting nexin 24
SOCS3	NM_003955	suppressor of cytokine signaling 3
SOCS6	NM_004232	suppressor of cytokine signaling 6
SOCS7	NM_014598	suppressor of cytokine signaling 7
SON	NM_138927	SON DNA binding protein
SOX13	NM_005686	SRY (sex determining region Y)-box 13
SP1	NM_003109	Sp1 transcription factor
SP4	NM_003112	Sp4 transcription factor
SPARC	NM_003118	secreted protein, acidic, cysteine-rich (osteonectin)
SPATA13	NM_001166271	spermatogenesis associated 13
SPATA5	NM_145207	spermatogenesis associated 5
SPEN	NM_015001	spen homolog, transcriptional regulator (Drosophila)
SPOPL	NM_001001664	speckle-type POZ protein-like
SPTBN1	NM_003128	spectrin, beta, non-erythrocytic 1

SPTY2D1	NM_194285	SPT2, Suppressor of Ty, domain containing 1 (S. cerevisiae)
SRA1	NM_001035235	steroid receptor RNA activator 1
SRC	NM_005417	v-src sarcoma (Schmidt-Ruppin A-2) viral oncogene homolog
SRD5A2	NM_000348	steroid-5-alpha-reductase, alpha polypeptide 2
SRSF1	NM_001078166	serine/arginine-rich splicing factor 1
SRSF10	NM_001191005	serine/arginine-rich splicing factor 10
SRSF12	NM_080743	serine/arginine-rich splicing factor 12
SRSF3	NM_003017	serine/arginine-rich splicing factor 3
SS18L1	NM_198935	synovial sarcoma translocation gene on chromosome 18-like 1
SSBP3	NM_001009955	single stranded DNA binding protein 3
ST8SIA4	NM_005668	ST8 alpha-N-acetyl-neuraminide alpha-2,8-sialyltransferase 4
STAC2	NM_198993	SH3 and cysteine rich domain 2
STAG3L4	NM_022906	stromal antigen 3-like 4
STEAP1	NM_012449	six transmembrane epithelial antigen of the prostate 1
STON1	NM_001198595	stonin 1
STRBP	NM_001171137	spermatid perinuclear RNA binding protein
STRN	NM_003162	striatin, calmodulin binding protein
STX16	NM_001001433	syntaxin 16
STXBP5L	NM_014980	syntaxin binding protein 5-like
SUDS3	NM_022491	suppressor of defective silencing 3 homolog (S. cerevisiae)
SV2B	NM_001167580	synaptic vesicle glycoprotein 2B
SYNC	NM_001161708	syncoilin, intermediate filament protein
SYNCRIP	NM_001159673	synaptotagmin binding, cytoplasmic RNA interacting protein
SYNJ1	NM_001160302	synaptojanin 1
TADA1	NM_053053	transcriptional adaptor 1
TADA2B	NM_152293	transcriptional adaptor 2B
TAF9B	NM_015975	TAF9B RNA polymerase II, TATA box binding protein (TBP)-associated factor
TARDBP	NM_007375	TAR DNA binding protein
TBC1D15	NM_001146213	TBC1 domain family, member 15
TBC1D9B	NM_015043	TBC1 domain family, member 9B (with GRAM domain)
TBK1	NM_013254	TANK-binding kinase 1
TBX3	NM_005996	T-box 3
TCF12	NM_003205	transcription factor 12
TCF24	NM_001193502	transcription factor 24
TCF4	NM_001083962	transcription factor 4
TDRD6	NM_001010870	tudor domain containing 6
TEDDM1	NM_172000	transmembrane epididymal protein 1
TESK1	NM_006285	testis-specific kinase 1
TFAP2B	NM_003221	transcription factor AP-2 beta (activating enhancer binding

		protein 2 beta)
TFDP2	NM_001178138	transcription factor Dp-2 (E2F dimerization partner 2)
TGFB2	NM_001135599	transforming growth factor, beta 2
TGIF2-C20ORF24	NM_001199535	TGIF2-C20orf24 readthrough
THRB	NM_000461	thyroid hormone receptor, beta
THSD7A	NM_015204	thrombospondin, type I, domain containing 7A
TLK2	NM_001112707	tousled-like kinase 2
TLL2	NM_012465	tolloid-like 2
TMED10	NM_006827	transmembrane emp24-like trafficking protein 10 (yeast)
TMEM132A	NM_017870	transmembrane protein 132A
TMEM136	NM_001198670	transmembrane protein 136
TMEM182	NM_144632	transmembrane protein 182
TMEM237	NM_001044385	transmembrane protein 237
TMEM33	NM_018126	transmembrane protein 33
TMOD2	NM_001142885	tropomodulin 2 (neuronal)
TNFRSF8	NM_001243	tumor necrosis factor receptor superfamily, member 8
TNFSF15	NM_001204344	tumor necrosis factor (ligand) superfamily, member 15
TNN	NM_022093	tenascin N
TNPO1	NM_002270	transportin 1
TNRC6B	NM_001024843	trinucleotide repeat containing 6B
TNRC6C	NM_001142640	trinucleotide repeat containing 6C
TOR1AIP2	NM_001199260	torsin A interacting protein 2
TOX3	NM_001080430	TOX high mobility group box family member 3
TP63	NM_001114978	tumor protein p63
TRA2B	NM_004593	transformer 2 beta homolog (Drosophila)
TRAM2	NM_012288	translocation associated membrane protein 2
TRAPPC6B	NM_001079537	trafficking protein particle complex 6B
TRERF1	NM_033502	transcriptional regulating factor 1
TRIM2	NM_001130067	tripartite motif containing 2
TRIM71	NM_001039111	tripartite motif containing 71
TRMT1L	NM_001202423	TRM1 tRNA methyltransferase 1-like
TRPS1	NM_014112	trichorhinophalangeal syndrome I
TRPV3	NM_145068	transient receptor potential cation channel, subfamily V, member 3
TRPV4	NM_001177428	transient receptor potential cation channel, subfamily V, member 4
TSHZ2	NM_001193421	teashirt zinc finger homeobox 2
TTC39A	NM_001080494	tetratricopeptide repeat domain 39A
TUSC2	NM_007275	tumor suppressor candidate 2
TWF1	NM_001242397	twinfilin, actin-binding protein, homolog 1 (Drosophila)

TXLNG	NM_001168683	taxilin gamma
TXNDC16	NM_001160047	thioredoxin domain containing 16
U2SURP	NM_001080415	U2 snRNP-associated SURP domain containing
UBASH3B	NM_032873	ubiquitin associated and SH3 domain containing B
UBE2I	NM_003345	ubiquitin-conjugating enzyme E2I
UBE2K	NM_001111112	ubiquitin-conjugating enzyme E2K
UBP1	NM_001128160	upstream binding protein 1 (LBP-1a)
UBR1	NM_174916	ubiquitin protein ligase E3 component n-recognin 1
UCHL5	NM_001199261	ubiquitin carboxyl-terminal hydrolase L5
UHRF1BP1	NM_017754	UHRF1 binding protein 1
UPF2	NM_015542	UPF2 regulator of nonsense transcripts homolog (yeast)
USP15	NM_006313	ubiquitin specific peptidase 15
VAMP1	NM_014231	vesicle-associated membrane protein 1 (synaptobrevin 1)
VAPA	NM_003574	VAMP (vesicle-associated membrane protein)-associated protein A
VASH2	NM_001136474	vasohibin 2
VAV3	NM_001079874	vav 3 guanine nucleotide exchange factor
VCPIP1	NM_025054	valosin containing protein (p97)/p47 complex interacting protein 1
VEGFA	NM_001025366	vascular endothelial growth factor A
VGLL4	NM_001128219	vestigial like 4 (Drosophila)
VPS37A	NM_001145152	vacuolar protein sorting 37 homolog A (S. cerevisiae)
VSNL1	NM_003385	visinin-like 1
VTI1A	NM_145206	vesicle transport through interaction with t-SNAREs homolog 1A
VWA3B	NM_144992	von Willebrand factor A domain containing 3B
WAC	NM_016628	WW domain containing adaptor with coiled-coil
WDFY3	NM_014991	WD repeat and FYVE domain containing 3
WDR3	NM_006784	WD repeat domain 3
WDR37	NM_014023	WD repeat domain 37
WDR52	NM_001164496	WD repeat domain 52
WRNIP1	NM_020135	Werner helicase interacting protein 1
WTAP	NM_152857	Wilms tumor 1 associated protein
WWC3	NM_015691	WWC family member 3
XKR6	NM_173683	XK, Kell blood group complex subunit-related family, member 6
XPO4	NM_022459	exportin 4
XYLT1	NM_022166	xylosyltransferase I
YPEL4	NM_145008	yippee-like 4 (Drosophila)
YWHAQ	NM_006826	tyrosine 3-monooxygenase/tryptophan 5-monooxygenase protein
ZAK	NM_133646	sterile alpha motif and leucine zipper containing kinase AZK
ZBTB44	NM_014155	zinc finger and BTB domain containing 44

ZBTB46	NM_025224	zinc finger and BTB domain containing 46
ZBTB7B	NM_015872	zinc finger and BTB domain containing 7B
ZC3H12D	NM_207360	zinc finger CCCH-type containing 12D
ZC3H13	NM_015070	zinc finger CCCH-type containing 13
ZC4H2	NM_001178032	zinc finger, C4H2 domain containing
ZCCHC14	NM_015144	zinc finger, CCHC domain containing 14
ZDHHC15	NM_001146257	zinc finger, DHHC-type containing 15
ZDHHC20	NM_153251	zinc finger, DHHC-type containing 20
ZEB1	NM_001128128	zinc finger E-box binding homeobox 1
ZFHX3	NM_001164766	zinc finger homeobox 3
ZFHX4	NM_024721	zinc finger homeobox 4
ZFP1	NM_153688	zinc finger protein 1 homolog (mouse)
ZFP106	NM_022473	zinc finger protein 106 homolog (mouse)
ZMIZ1	NM_020338	zinc finger, MIZ-type containing 1
ZMYM2	NM_001190964	zinc finger, MYM-type 2
ZMYM4	NM_005095	zinc finger, MYM-type 4
ZMYND11	NM_001202464	zinc finger, MYND-type containing 11
ZNF148	NM_021964	zinc finger protein 148
ZNF236	NM_007345	zinc finger protein 236
ZNF275	NM_001080485	zinc finger protein 275
ZNF281	NM_012482	zinc finger protein 281
ZNF292	NM_015021	zinc finger protein 292
ZNF532	NM_018181	zinc finger protein 532
ZNF592	NM_014630	zinc finger protein 592
ZNF608	NM_020747	zinc finger protein 608
ZNF652	NM_001145365	zinc finger protein 652
ZNF654	NM_018293	zinc finger protein 654
ZNF704	NM_001033723	zinc finger protein 704
ZNF831	NM_178457	zinc finger protein 831
ZNHIT6	NM_001170670	zinc finger, HIT-type containing 6
ZNRF3	NM_001206998	zinc and ring finger 3
ZRANB2	NM_005455	zinc finger, RAN-binding domain containing 2
ZSWIM4	NM_023072	zinc finger, SWIM-type containing 4
ZXDB	NM_007157	zinc finger, X-linked, duplicated B

Bibliography

The History of Cancer. ACS, 1-16.

Agarwal, V., Bell, G.W., Nam, J.W., and Bartel, D.P. (2015). Predicting effective microRNA target sites in mammalian mRNAs. Elife *4*.

Andres, A.-C., van der Valk, M.A., Sch6nenberger, C.-A., Fliickiger, F., LeMeur, M., Gerlinger, P., and Groner, B. (1988). Ha-ras and c-myc oncogene expression interferes with morphological and functional differentiation of mammary epithelial cells in single and double transgenic mice. . Genes Dev *2*, 1486-1495.

Aslakson, C.J., and Miller, F.R. (1992). Selective events in the metastatic process defined by analysis of the sequential dissemination of subpopulations of a mouse mammary tumor. Cancer Res *52*, 1399-1405.

Augoff, K., McCue, B., Plow, E.F., and Sossey-Alaoui, K. (2012). miR-31 and its host gene lncRNA LOC554202 are regulated by promoter hypermethylation in triple-negative breast cancer. Mol Cancer *11*, 1-12.

Azad, M.B., Chen, Y., Henson, E.S., Cizeau, J., McMillan-Ward, E., Israels, S.J., and Gibson, S.B. (2008). HYPOXIA INDUCES AUTOPHAGIC CELL DEATH IN APOPTOSIS- COMPETENT CELLS THROUGH A MECHANISM INVOLVING. Autophagy *4*, 195-204.

Bail, S., Swerdel, M., Liu, H., Jiao, X., Goff, L.A., Hart, R.P., and Kiledjian, M. (2010). Differential regulation of microRNA stability. RNA *16*, 1032-1039.

Barker, A.J., Gibson, K.H., Grundy, W., Godfrey, A.A., Barlow, J.J., Healy, M.P., Woodburn, J.R., Ashton, S.E., Curry, B.J., Scarlett, L.*, et al.* (2001). Studies leading to the identification of ZD1839 (IRESSA): an orally active, selective epidermal growth factor receptor tyrosine kinase inhibitor targeted to the treatment of cancer. Bioorg Med Chem Lett *11*, 1911-1914.

Benaich, N., Woodhouse, S., Goldie, S.J., Mishra, A., Quist, S.R., and Watt, F.M. (2014). Rewiring of an epithelial differentiation factor, miR-203, to inhibit human squamous cell carcinoma metastasis. Cell Rep *9*, 104-117.

Berezovskaya, O., Schimmer, A.D., Glinskii, A.B., Pinilla, C., Hoffman, R.M., Reed, J.C., and Glinsky, G.V. (2005). Increased Expression of Apoptosis Inhibitor Protein XIAP
Contributes to Anoikis Resistance of Circulating Human
Prostate Cancer Metastasis Precursor Cells. Cancer Res *65*, 2378-2386.

Beyer, S., Kristensen, M.M., Jensen, K.S., Johansen, J.V., and Staller, P. (2008). The histone demethylases JMJD1A and JMJD2B are transcriptional targets of hypoxia-inducible factor HIF. J Biol Chem *283*, 36542-36552.

Bhatnagar, S., Zhu, X., Ou, J., Lin, L., Chamberlain, L., Zhu, L.J., Wajapeyee, N., and Green, M.R. (2014). Genetic and pharmacological reactivation of the mammalian inactive X chromosome. Proc Natl Acad Sci U S A *111*, 12591-12598.

Bian, K., Fan, J., Zhang, X., Yang, X.W., Zhu, H.Y., Wang, L., Sun, J.Y., Meng, Y.L., Cui, P.C., Cheng, S.Y.*, et al.* (2012). MicroRNA-203 leads to G1 phase cell cycle arrest in laryngeal carcinoma cells by directly targeting survivin. FEBS Lett *586*, 804-809.

Bouchard, V., Demers, M.J., Thibodeau, S., Laquerre, V., Fujita, N., Tsuruo, T., Beaulieu, J.F., Gauthier, R., Vezina, A., Villeneuve, L.*, et al.* (2007). Fak/Src signaling in human intestinal epithelial cell survival and anoikis: differentiation state-specific uncoupling with the PI3-K/Akt-1 and MEK/Erk pathways. J Cell Physiol *212*, 717-728.

Boyd, J.M., Malstrom, S., Subramanian, T., Venkatesh, L.K., Schaeper, U., Elangovan, B., D'Sa-Eipper, C., and Chinnadurai, G. (1994). Adenovirus E1B 19 kDa and Bcl-2 proteins interact with a common set of cellular proteins. Cell *79*, 341-351.

Bracken, A.P., Pasini, D., Capra, M., Prosperini, E., Colli, E., and Helin, K. (2003). EZH2 is downstream of the pRB-E2F pathway, essential for proliferation and amplified in cancer. EMBO J *22*, 5323-5335.

Brassard, D.L., Maxwell, E., Malkowski, M., Nagabhushan, T.L., Kumar, C.C., and Armstrong, L. (1999). Integrin alpha-5-beta-3 Mediated Activation of Apoptosis. Exp Cell Res *251*, 33-45.

Bueno, M.J., Perez de Castro, I., Gomez de Cedron, M., Santos, J., Calin, G.A., Cigudosa, J.C., Croce, C.M., Fernandez-Piqueras, J., and Malumbres, M. (2008). Genetic and epigenetic silencing of microRNA-203 enhances ABL1 and BCR-ABL1 oncogene expression. Cancer Cell *13*, 496-506.

Calalb, M.B., Polte, T.R., and Hanks, S.K. (1995). Tyrosine Phosphorylation of Focal Adhesion Kinase at
Sites in the Catalytic Domain Regulates Kinase Activity:
a Role for Src Family Kinases. Mol Cell Biol *15*, 954-963.

Calin, G.A., Dumitru, C.D., Shimizu, M., Bichi, R., Zupo, S., Noch, E., Aldler, H., Rattan, S., Keating, M., Rai, K.*, et al.* (2002). Frequent deletions and down-regulation of micro- RNA genes miR15 and miR16 at 13q14 in chronic lymphocytic leukemia. Proc Natl Acad Sci U S A *99*, 15524-15529.

Cancer Genome Atlas, N. (2012). Comprehensive molecular portraits of human breast tumours. Nature *490*, 61-70.

Chambers, A.F., Groom, A.C., and MacDonald, I.C. (2002). Metastasis: Dissemination and growth of cancer cells in metastatic sites. Nature Reviews Cancer *2*, 563-572.

Chang, B., Chen, Y., Zhao, Y., and Bruick, R.K. (2007). JMJD6 is a Histone Arginine Demethylase. Science *318*, 444-449.

Cheang, M.C., Voduc, D., Bajdik, C., Leung, S., McKinney, S., Chia, S.K., Perou, C.M., and Nielsen, T.O. (2008). Basal-like breast cancer defined by five biomarkers has superior prognostic value than triple-negative phenotype. Clin Cancer Res *14*, 1368-1376.

Chen, T., Xu, C., Chen, J., Ding, C., Xu, Z., Li, C., and Zhao, J. (2015). MicroRNA-203 inhibits cellular proliferation and invasion by targeting Bmi1 in non-small cell lung cancer. Oncol Lett *9*, 2639-2646.

Collins, N.L., Reginato, M.J., Paulus, J.K., Sgroi, D.C., Labaer, J., and Brugge, J.S. (2005). G1/S cell cycle arrest provides anoikis resistance through Erk-mediated Bim suppression. Mol Cell Biol *25*, 5282-5291.

Colombano, S.P., and Reese, P.A. (1980). The Cascade Theory of Metastatic Spread: Are There Generalizing Sites? Cancer *46*, 2312-2314.

Consortium, I.H.G.S. (2001). Initial sequencing and analysis of the human genome. . Nature *409*, 860-921.

Consortium, T.G.O. (2000). Gene Ontology: tool for the unification of biology. Nat Genetics *25*, 25-29.

Dadiani, M., Bossel Ben-Moshe, N., Paluch-Shimon, S., Perry, G., Balint, N., Marin, I., Pavlovski, A., Morzaev, D., Kahana-Edwin, S., Yosepovich, A.*, et al.* (2016). Tumor Evolution Inferred by Patterns of microRNA Expression through the Course of Disease, Therapy, and Recurrence in Breast Cancer. Clinical Cancer Research *22*, 3651-3662.

Debnath, J., Mills, K.R., Collins, N.L., Reginato, M.J., Muthuswamy, S.K., and Brugge, J.S. (2002). The role of apoptosis in creating and maintaining luminal space within normal and oncogene-expressing mammary acini. Cell *111*, 29-40.

Decarlo, L., Mestel, C., Barcellos-Hoff, M.-H., and Schneider, R.J. (2015). Eukaryotic Translation Initiation Factor 4E Is a Feed-Forward Translational Coactivator of Transforming Growth Factor β Early Protransforming Events in Breast Epithelial Cells. Molecular and Cellular Biology *35*, 2597-2609.

Dhingra, R., Margulets, V., Chowdhury, S.R., Thliveris, J., Jassal, D., Fernyhough, P., Dorn, G.W., and Kirshenbaum, L.A. (2014). Bnip3 mediates doxorubicin-induced cardiac myocyte necrosis and mortality through changes in mitochondrial signaling. Proceedings of the National Academy of Sciences *111*, E5537-E5544.

Diao, Y., Guo, X., Jiang, L., Wang, G., Zhang, C., Wan, J., Jin, Y., and Wu, Z. (2014). miR-203, a tumor suppressor frequently down-regulated by promoter hypermethylation in rhabdomyosarcoma. J Biol Chem *289*, 529-539.

Dimri, G.P., Lee, X., Basile, G., Acosta, M., Scott, G., Roskelley, C., Medrano, E.E., Linskens, M., Rubelj, I., and Pereira-Smith, O. (1995). A biomarker that identifies senescent human cells in culture and in aging skin in vivo. . Proc Natl Acad Sci U S A *92*, 9363-9367.

Ding, X., Park, S.I., McCauley, L.K., and Wang, C.Y. (2013). Signaling between transforming growth factor beta (TGF-beta) and transcription factor SNAI2 represses expression of microRNA miR-203 to promote epithelial-mesenchymal transition and tumor metastasis. J Biol Chem *288*, 10241-10253.

Djuranovic, S., Nahvi, A., and Green, R. (2012). miRNA-mediated gene silencing by translational repression followed by mRNA deadenylation and decay. Science *336*, 237-240.

Douma, S., van Laar, T., Zevenhoven, J., Meuwissen, R., van Garderen, E., and Peeper, D.S. (2004). Suppression of anoikis and induction of metastasis by the neurotrophic receptor TrkB. Nature *430*, 1034-1040.

Du, Z.M., Hu, L.F., Wang, H.Y., Yan, L.X., Zeng, Y.X., Shao, J.Y., and Ernberg, I. (2011). Upregulation of MiR-155 in nasopharyngeal carcinoma is partly driven by LMP1 and LMP2A and downregulates a negative prognostic marker JMJD1A. PLoS One *6*, e19137.

Evan, G.I., Wyllie, A.H., Gilbert, C.S., Littlewood, T.D., Land, H., Brooks, M., Waters, C.M., Penn, L.Z., and Hancock, D.C. (1992). Induction of Apoptosis in Fibroblasts by c-myc Protein. Cell *69*, 119-128.

Fang, M., Ou, J., Hutchinson, L., and Green, M.R. (2014). The BRAF oncoprotein functions through the transcriptional repressor MAFG to mediate the CpG Island Methylator phenotype. Mol Cell *55*, 904-915.

Fang, M., Pak, M.L., Chamberlain, L., Xing, W., Yu, H., and Green, M.R. (2015). The CREB Coactivator CRTC2 Is a Lymphoma Tumor Suppressor that Preserves Genome Integrity through Transcription of DNA Mismatch Repair Genes. Cell Rep *11*, 1350-1357.

Fantozzi, A., and Christofori, G. (2006). Mouse models of breast cancer metastasis. Breast Cancer Research *8*, 212.

Fassan, M., Baffa, R., Palazzo, J.P., Lloyd, J., Crosariol, M., Liu, C.-G., Volinia, S., Alder, H., Rugge, M., Croce, C.M.*, et al.* (2009). MicroRNA expression profiling of male breast cancer. Breast Cancer Research *11*, R58.

Favata, M.F., Horiuchi, K.Y., Manos, E.J., Daulerio, A.J., Stradley, D.A., Feeser, W.S., Van Dyk, D.E., Pitts, W.J., Earl, R.A., Hobbs, F.*, et al.* (1998). Identification of a novel inhibitor of mitogen-activated protein kinase kinase. J Biol Chem *273*, 18623-18632.

Feng, Z., Yao, Y., Zhou, C., Chen, F., Wu, F., Wei, L., Liu, W., Dong, S., Redell, M., Mo, Q.*, et al.* (2016). Pharmacological inhibition of LSD1 for the treatment of MLL-rearranged leukemia. Journal of Hematology & Oncology *9*.

Fidler, I.J. (2003). The pathogenesis of cancer metastasis: the 'seed and soil' hypothesis revisited. . Nat Rev Cancer *3*, 1-6.

Finak, G., Bertos, N., Pepin, F., Sadekova, S., Souleimanova, M., Zhao, H., Chen, H., Omeroglu, G., Meterissian, S., Omeroglu, A.*, et al.* (2008). Stromal gene expression predicts clinical outcome in breast cancer. Nat Med *14*, 518-527.

Fire, A., Xu, S., Montgomery, M.K., Kostas, S.A., Driver, S.E., and Mello, C.C. (1998). Potent and specific
genetic interference by double-stranded RNA in Caenorhabditis elegans. Nature *391*, 806-811.

Franceschini, A., Meier, R., Casanova, A., Kreibich, S., Daga, N., Andritschke, D., Dilling, S., Ramo, P., Emmenlauer, M., Kaufmann, A.*, et al.* (2014). Specific inhibition of diverse pathogens in human cells by synthetic microRNA-like oligonucleotides inferred from RNAi screens. Proceedings of the National Academy of Sciences *111*, 4548-4553.

Frisch, S.M., and Francis, H. (1994a). Disruption of Epithelial Cell-Matrix Interactions Induces Apoptosis. J Cell Biol *124*, 619-626.

Frisch, S.M., and Francis, H. (1994b). Disruption of epithelial cell-matrix interactions induces apoptosis. The Journal of Cell Biology *124*, 619-626
.

Frisch, S.M., and Ruoslahti, E. (1997). Integrins and anoikis. Curr Opin Cell Biol *9*, 701-706.

Frisch, S.M., Vuori, K., Ruoslahti, E., and Chan-Hui, P.Y. (1996). Control of adhesion-dependent cell survival by focal adhesion kinase. J Cell Biol *134*, 793-799.

Furuta, M., Kozaki, K., Tanimoto, K., Tanaka, S., Arii, S., Shimamura, T., Niida, A., Miyano, S., and Inazawa, J. (2013). The tumor-suppressive miR-497-195 cluster targets multiple cell-cycle regulators in hepatocellular carcinoma. PLoS One *8*, e60155.

Furuta, M., Kozaki, K.I., Tanaka, S., Arii, S., Imoto, I., and Inazawa, J. (2010). miR-124 and miR-203 are epigenetically silenced tumor-suppressive microRNAs in hepatocellular carcinoma. Carcinogenesis *31*, 766-776.

Gargiulo, G., Serresi, M., Cesaroni, M., Hulsman, D., and van Lohuizen, M. (2014). In vivo shRNA screens in solid tumors. Nat Protoc *9*, 2880-2902.

Gazin, C., Wajapeyee, N., Gobeil, S., Virbasius, C.M., and Green, M.R. (2007). An elaborate pathway required for Ras-mediated epigenetic silencing. Nature *449*, 1073-1077.

Ghildiyal, M., Seitz, H., Horwich, M.D., Li, C., Du, T., Lee, S., Xu, J., Kittler, E.L., Zapp, M.L., Weng, Z.*, et al.* (2008). Endogenous siRNAs derived from transposons and mRNAs in Drosophila somatic cells. Science *320*, 1077-1081.

Gilley, J., Coffer, P.J., and Ham, J. (2003). FOXO transcription factors directly activatebimgene expression and promote apoptosis in sympathetic neurons. The Journal of Cell Biology *162*, 613-622.

Gligorijević, V., and Pržulj, N. (2015). Methods for biological data integration: perspectives and challenges. Journal of The Royal Society Interface *12*, 20150571.

Glinskii, A.B., Smith, B.A., Jiang, P., Li, X.-M., Yang, M., Hoffman, R.M., and Glinsky, G.V. (2003). Viable Circulating Metastatic Cell Produced in Orthotopic but not Ectopic Prostate Cancer Models. Cancer Res *63*, 4239-4243.

Griffiths-Jones, S., Saini, H.K., van Dongen, S., and Enright, A.J. (2008). miRBase: tools for microRNA genomics. Nucleic Acids Res *36*, D154-158.

Guo, H., Ingolia, N.T., Weissman, J.S., and Bartel, D.P. (2010). Mammalian microRNAs predominantly act to decrease target mRNA levels. Nature *466*, 835-840.

Hackenberg, M., Rodriguez-Ezpeleta, N., and Aransay, A.M. (2011). miRanalyzer: an update on the detection and analysis of microRNAs in high-throughput sequencing experiments. Nucleic Acids Res *39*, W132-138.

Hanahan, D., and Weinberg, R.A. (2000). The Hallmarks of Cancer. Cell *100*, 57-70.

Hanahan, D., and Weinberg, R.A. (2011). Hallmarks of cancer: the next generation. Cell *144*, 646-674.

Heo, I., Joo, C., Kim, Y.K., Ha, M., Yoon, M.J., Cho, J., Yeom, K.H., Han, J., and Kim, V.N. (2009). TUT4 in concert with Lin28 suppresses microRNA biogenesis through pre-microRNA uridylation. Cell *138*, 696-708.

Heravi-Moussavi, A., Anglesio, M.S., Cheng, S.W.G., Senz, J., Yang, W., Prentice, L., Fejes, A.P., Chow, C., Tone, A., Kalloger, S.E.*, et al.* (2012). Recurrent Somatic DICER1 Mutations in Nonepithelial Ovarian Cancers. N Engl J Med *366*, 234-242.

Hesse, J.E., Liu, L., Innes, C.L., Cui, Y., Palii, S.S., and Paules, R.S. (2013). Genome-wide small RNA sequencing and gene expression analysis reveals a microRNA profile of cancer susceptibility in ATM-deficient human mammary epithelial cells. PLoS One *8*, e64779.

Hofmann, U.B., Eggert, A.A.O., Blass, K., Bro¨cker, E.B., and Becker, J. (2003). Expression of Matrix Metalloproteinases in the Microenvironment of Spontaneous and Experimental Melanoma Metastases Reflects the Requirements for Tumor Formation. Cancer Res *63*, 8221-8225.

Horowitz, J.M., Park, S.H., Bogenmann, E., Cheng, J.C., Yandell, D.W., Kaye, F.J., Minna, J.D., Dryja, T.P., and Weinberg, R.A. (1990). Frequent inactivation of the retinoblastoma anti-oncogene is
restricted to a subset of human tumor cells. Proc Natl Acad Sci U S A *87*, 2775-2779
.

Howard, E.W., Leung, S.C., Yuen, H.F., Chua, C.W., Lee, D.T., Chan, K.W., Wang, X., and Wong, Y.C. (2008). Decreased adhesiveness, resistance to anoikis and suppression of GRP94 are integral to the survival of circulating tumor cells in prostate cancer. Clin Exp Metastasis *25*, 497-508.

Howe, E.N., Cochrane, D.R., Cittelly, D.M., and Richer, J.K. (2012). miR-200c targets a NF-kappaB up-regulated TrkB/NTF3 autocrine signaling loop to enhance anoikis sensitivity in triple negative breast cancer. PLoS One *7*, e49987.

Hsu, T.C., and Moorhead, P.S. (1956). CHROMOSOME ANOMALIES IN HUMAN NEOPLASMS WITH
SPECIAL REFERENCE TO THE MECHANISMS OF
POLYPL OID IZATION AND ANEUPLOIDIZATION
IN THE HELA STRAIN. Annals of the New York Academy of Sciences *1083-1094*.

Huang, W., Gonzalez, M.E., Toy, K.A., Banerjee, M., and Kleer, C.G. (2010). Blockade of CCN6 (WISP3) activates growth factor-independent survival and resistance to anoikis in human mammary epithelial cells. Cancer Res *70*, 3340-3350.

Ihaka, R., and Gentleman, R. (1996). R: A language for data analysis and graphics. J Comput Graph Stat *5*, 299-314.

Iorio, M.V., Visone, R., Di Leva, G., Donati, V., Petrocca, F., Casalini, P., Taccioli, C., Volinia, S., Liu, C.G., Alder, H.*, et al.* (2007). MicroRNA signatures in human ovarian cancer. Cancer Res *67*, 8699-8707.

Isobe, T., Hisamori, S., Hogan, D.J., Zabala, M., Hendrickson, D.G., Dalerba, P., Cai, S., Scheeren, F., Kuo, A.H., Sikandar, S.S.*, et al.* (2014). miR-142 regulates the tumorigenicity of human breast cancer stem cells through the canonical WNT signaling pathway. Elife *3*.

Jackson, A.L., Bartz, S.R., Schelter, J., Kobayashi, S.V., Burchard, J., Mao, M., Li, B., Cavet, G., and Linsley, P.S. (2003a). Expression profiling reveals off-target gene regulation by RNAi. Nature Biotechnology *21*, 635-637.

Jackson, A.L., Bartz, S.R., Schelter, J., Kobayashi, S.V., Burchard, J., Mao, M., Li, B., Cavet, G., and Linsley, P.S. (2003b). Expression profiling reveals off-target gene regulation by RNAi. Nat Biotech *21*, 635-638.

Kaur, A., Webster, M.R., Marchbank, K., Behera, R., Ndoye, A., Kugel, C.H., Dang, V.M., Appleton, J., O'Connell, M.P., Cheng, P.*, et al.* (2016). sFRP2 in the aged microenvironment drives melanoma metastasis and therapy resistance. Nature *532*, 250-254.

Kawahara, Y., Zinshteyn, B., Chendrimada, T.P., Shiekhattar, R., and Nishikura, K. (2007). RNA editing of the microRNA-151 precursor blocks cleavage by the Dicer-TRBP complex. EMBO Rep *8*, 763-769.

Kerr, J.F.R., Wyllie, A.H., and Currie, A.R. (1972). Apoptosis: a basic biological phenomenon with wide-ranging implications in tissue. Br J Cancer *26*, 239-257.

Kessler, J.D., Kahle, K.T., Sun, T., Meerbrey, K.L., Schlabach, M.R., Schmitt, E.M., Skinner, S.O., Xu, Q., Li, M.Z., Hartman, Z.C.*, et al.* (2012). A SUMOylation-dependent transcriptional subprogram is required for Myc-driven tumorigenesis. Science *335*, 348-353.

King, W.G., Mattaliano, M.D., Chan, T.O., Tsichlis, P.N., and Brugge, J.S. (1997). Phosphatidylinositol 3-kinase is required for integrin-stimulated AKT and Raf-1/mitogen-activated protein kinase pathway activation. Mol Cell Biol *17*, 4406-4418.

Knudson, A.G. (1971). Mutation and Cancer: Statistical study of retinoblastoma Proc Natl Acad Sci U S A *68*, 820-823.

Krieg, A.J., Rankin, E.B., Chan, D., Razorenova, O., Fernandez, S., and Giaccia, A.J. (2010). Regulation of the histone demethylase JMJD1A by hypoxia-inducible factor 1 alpha enhances hypoxic gene expression and tumor growth. Mol Cell Biol *30*, 344-353.

Kubicek, S., O'Sullivan, R.J., August, E.M., Hickey, E.R., Zhang, Q., Teodoro, Miguel L., Rea, S., Mechtler, K., Kowalski, J.A., Homon, C.A.*, et al.* (2007). Reversal of H3K9me2 by a Small-Molecule Inhibitor for the G9a Histone Methyltransferase. Molecular Cell *25*, 473-481.

Lee, L.C., Feinbaum, R.L., and Ambros, V. (1993
). The C. elegans Heterochronic Gene lin-4 Encodes Small RNAs with Antisense Complementarity to lin-14. Cell *75*, 843-854.

Lena, A.M., Shalom-Feuerstein, R., Rivetti di Val Cervo, P., Aberdam, D., Knight, R.A., Melino, G., and Candi, E. (2008). miR-203 represses 'stemness' by repressing DeltaNp63. Cell Death Differ *15*, 1187-1195.

Lienert, F., Mohn, F., Tiwari, V.K., Baubec, T., Roloff, T.C., Gaidatzis, D., Stadler, M.B., and Schubeler, D. (2011). Genomic prevalence of heterochromatic H3K9me2 and transcription do not discriminate pluripotent from terminally differentiated cells. PLoS Genet *7*, e1002090.

Lietha, D., Cai, X., Ceccarelli, D.F., Li, Y., Schaller, M.D., and Eck, M.J. (2007). Structural basis for the autoinhibition of focal adhesion kinase. Cell *129*, 1177-1187.

Lin, L., Chamberlain, L., Pak, M.L., Nagarajan, A., Gupta, R., Zhu, L.J., Wright, C.M., Fong, K.M., Wajapeyee, N., and Green, M.R. (2014). A large-scale RNAi-based mouse tumorigenesis screen identifies new lung cancer tumor suppressors that repress FGFR signaling. Cancer Discov *4*, 1168-1181.

Lin, X., and Nelson, W.G. (2003). Methyl-CpG-binding Domain Protein-2 Mediates Transcriptional Repression Associated with Hypermethylated GSTP1 CpG Islands in MCF-7
Breast Cancer Cells. Cancer Res *63*, 498-504.

Liu, C.G., Calin, G.A., Meloon, B., Gamliel, N., Sevignani, C., Ferracin, M., Dumitru, C.D., Shimizu, M., Zupo, S., Dono, M.*, et al.* (2004). An oligonucleotide microchip for genome-wide microRNA profiling in human and mouse tissues. Proc Natl Acad Sci U S A *101*, 9740-9744.

Liu, C.L., Kaplan, T., Kim, M., Buratowski, S., Schreiber, S.L., Friedman, N., and Rando, O.J. (2005). Single-nucleosome mapping of histone modifications in S. cerevisiae. PLoS Biol *3*, e328.

Lizotte, P.H., Jones, R.E., Keogh, L., Ivanova, E., Liu, H., Awad, M.M., Hammerman, P.S., Gill, R.R., Richards, W.G., Barbie, D.A.*, et al.* (2016). Fine needle aspirate flow cytometric phenotyping characterizes immunosuppressive nature of the mesothelioma microenvironment. Scientific Reports *6*, 31745.

Lomonosova, E., and Chinnadurai, G. (2008). BH3-only proteins in apoptosis and beyond: an overview. Oncogene *27 Suppl 1*, S2-19.

Lu, C., Kulkarni, K., Souret, F.F., MuthuValliappan, R., Tej, S.S., Poethig, R.S., Henderson, I.R., Jacobsen, S.E., Wang, W., Green, P.J.*, et al.* (2006). MicroRNAs and other small RNAs enriched in the Arabidopsis RNA-dependent RNA polymerase-2 mutant. Genome Res *16*, 1276-1288.

Luo, D., Wilson, J.M., Harvel, N., Liu, J., Pei, L., Huang, S., Hawthorn, L., and Shi, H. (2013). A systematic evaluation of miRNA:mRNA interactions involved in the migration and invasion of breast cancer cells. J Transl med *11*, 1-14.

Ma, L., Shan, Y., Bai, R., Xue, L., Eide, C.A., Ou, J., Zhu, L.J., Hutchinson, L., Cerny, J., Khoury, H.J.*, et al.* (2014). A therapeutically targetable mechanism of BCR-ABL-independent imatinib resistance in chronic myeloid leukemia. Sci Transl Med *6*, 252ra121.

Manka, D., Spicer, Z., and Millhorn, D.E. (2005). Bcl-2/adenovirus E1B 19 kDa interacting protein-3 knockdown enables growth of breast cancer metastases in the lung, liver, and bone. Cancer Res *65*, 11689-11693.

Matsushima, M., Fujiwara, T., Takahashi, E., Minaguchi, T., Eguchi, Y., Tsujimoto, Y., Suzumori, K., and Nakamura, Y. (1998). Isolation, mapping, and functional analysis of a novel human cDNA (BNIP3L) encoding a protein homologous to human NIP3. Genes Chromosomes Cancer *21*, 230-235.

Matter, M.L., Zhang, Z., Nordstedt, C., and Ruoslahti, E. (1998). The alpha-5-beta-1 Integrin Mediates Elimination of Amyloid-beta Peptide and Protects Against Apoptosis. J Cell Biol *141*, 1019-1030.

Meister, G., Landthaler, M., Patkaniowska, A., Dorsett, Y., Teng, G., and Tuschl, T. (2004). Human Argonaute2 mediates RNA cleavage targeted by miRNAs and siRNAs. Mol Cell *15*, 185-197.

Mi, S., Lu, J., Sun, M., Li, Z., Zhang, H., Neilly, M.B., Wang, Y., Qian, Z., Jin, J., Zhang, Y.*, et al.* (2007). MicroRNA expression signatures accurately discriminate acute lymphoblastic leukemia from acute myeloid leukemia. Proceedings of the National Academy of Sciences *104*, 19971-19976.

Mito, J.K., Min, H.D., Ma, Y., Carter, J.E., Brigman, B.E., Dodd, L., Dankort, D., McMahon, M., and Kirsch, D.G. (2013). Oncogene-dependent control of miRNA biogenesis and metastatic progression in a model of undifferentiated pleomorphic sarcoma. The Journal of Pathology *229*, 132-140.

Mitxelena, J., Apraiz, A., Vallejo-Rodriguez, J., Malumbres, M., and Zubiaga, A.M. (2016). E2F7 regulates transcription and maturation of multiple microRNAs to restrain cell proliferation. Nucleic Acids Res.

Moro, L., Venturino, M., Bozzo, C., Silengo, L., Altruda, F., Beguinot, L., Tarone, G., and Defilippi, P. (1998). Integrins induce activation of EGF receptor: role in MAP kinase induction and adhesion-dependent cell survival. EMBO J *17*, 6622-6632.

Musselman, C.A., Lalonde, M.E., Cote, J., and Kutateladze, T.G. (2012). Perceiving the epigenetic landscape through histone readers. Nat Struct Mol Biol *19*, 1218-1227.

Ng, T.I., Mo, H., Pilot-Matias, T., He, Y., Koev, G., Krishnan, P., Mondal, R., Pithawalla, R., He, W., Dekhtyar, T.*, et al.* (2007). Identification of host genes involved in hepatitis C virus replication by small interfering RNA technology. Hepatology *45*, 1413-1421.

Noguchi, S., Mori, T., Otsuka, Y., Yamada, N., Yasui, Y., Iwasaki, J., Kumazaki, M., Maruo, K., and Akao, Y. (2012). Anti-oncogenic microRNA-203 induces senescence by targeting E2F3 protein in human melanoma cells. J Biol Chem *287*, 11769-11777.

O'Brien, V., Frisch, S.M., and Juliano, R.L. (1996). Expression of the Integrin alpha-5 Subunit in HT29 Colon Carcinoma Cells Suppresses Apoptosis Triggered by Serum Deprivation. Exp Cell Res *224*, 208-213.

Paoli, P., Giannoni, E., and Chiarugi, P. (2013). Anoikis molecular pathways and its role in cancer progression. Biochim Biophys Acta *1833*, 3481-3498.

Pedanou, V.E., Gobeil, S., Tabaries, S., Simone, T.M., Zhu, L.J., Siegel, P.M., and Green, M.R. (2016). The histone H3K9 demethylase KDM3A promotes anoikis by transcriptionally activating pro-apoptotic genes BNIP3 and BNIP3L. Elife *5*.

Pokholok, D.K., Harbison, C.T., Levine, S., Cole, M., Hannett, N.M., Lee, T.I., Bell, G.W., Walker, K., Rolfe, P.A., Herbolsheimer, E.*, et al.* (2005). Genome-wide map of nucleosome acetylation and methylation in yeast. Cell *122*, 517-527.

Rakheja, D., Chen, K.S., Liu, Y., Shukla, A.A., Schmid, V., Chang, T.C., Khokhar, S., Wickiser, J.E., Karandikar, N.J., Malter, J.S.*, et al.* (2014). Somatic mutations in DROSHA and DICER1 impair microRNA biogenesis through distinct mechanisms in Wilms tumours. Nat Commun *2*, 4802.

Ramadoss, S., Guo, G., and Wang, C.Y. (2016). Lysine demethylase KDM3A regulates breast cancer cell invasion and apoptosis by targeting histone and the non-histone protein p53. Oncogene.

Raponi, M., Belly, R.T., Karp, J.E., Lancet, J.E., Atkins, D., and Wang, Y. (2004). Microarray analysis reveals genetic pathways modulated by tipifarnib in acute myeloid leukemia. BMC Cancer *4*.

Reginato, M.J., Mills, K.R., Paulus, J.K., Lynch, D.K., Sgroi, D.C., Debnath, J., Muthuswamy, S.K., and Brugge, J.S. (2003). Integrins and EGFR coordinately regulate the pro-apoptotic protein Bim to prevent anoikis. Nat Cell Biol *5*, 733-740.

Reid, G., Kao, S.C., Pavlakis, N., Brahmbhatt, H., MacDiarmid, J., Clarke, S., Boyer, M., and van Zandwijk, N. (2016). Clinical development of TargomiRs, a miRNA mimic-based treatment for patients with recurrent thoracic cancer. Epigenomics *8*, 1079-1085.

Ren, C., Morohashi, K., Plotnikov, Alexander N., Jakoncic, J., Smith, Steven G., Li, J., Zeng, L., Rodriguez, Y., Stojanoff, V., Walsh, M.*, et al.* (2015). Small-Molecule Modulators of Methyl-Lysine Binding for the CBX7 Chromodomain. Chemistry & Biology *22*, 161-168.

Rhodes, D.R., Kalyana-Sundaram, S., Mahavisno, V., Varambally, R., Yu, J., Briggs, B.B., Barrette, T.R., Anstet, M.J., Kincead-Beal, C., Kulkarni, P.*, et al.* (2007). Oncomine 3.0: genes, pathways, and networks in a collection of 18,000 cancer gene expression profiles. Neoplasia *9*, 166-180.

Ruby, J.G., Jan, C., Player, C., Axtell, M.J., Lee, W., Nusbaum, C., Ge, H., and Bartel, D.P. (2006). Large-scale sequencing reveals 21U-RNAs and additional microRNAs and endogenous siRNAs in C. elegans. Cell *127*, 1193-1207.

SAIKI, H.J., MCCREDIEM, K.B., VIETTI, M.,], HEWLETTM, D., § F. S. MORRISONM, D,"J. J. COSTANZIM, D,', W.J.STUCKEY, and EJ.WHITECAr, E.J.H., Dtt (1978). 5-AZACYTIDINE IN ACUTE LEUKEMIA. CAncer *42*, 2111-2114.

Saini, S., Majid, S., Yamamura, S., Tabatabai, L., Suh, S.O., Shahryari, V., Chen, Y., Deng, G., Tanaka, Y., and Dahiya, R. (2011). Regulatory Role of mir-203 in Prostate Cancer Progression and Metastasis. Clin Cancer Res *17*, 5287-5298.

Santra, M.K., Wajapeyee, N., and Green, M.R. (2009). F-box protein FBXO31 mediates cyclin D1 degradation to induce G1 arrest after DNA damage. Nature *459*, 722-725.

Sato, N., Maitra, A., Fukushima, N., van Heek, N.T., Matsubayashi, H., Iacobuzio-Donahue, C.A., Rosty, C., and Goggin, M. (2003). Frequent Hypomethylation of Multiple Genes Overexpressed in Pancreatic Ductal Adenocarcinoma. Cancer Res *63*, 4158-4166.

Schmelzle, T., Mailleux, A.A., Overholtzer, M., Carroll, J.S., Solimini, N.L., Lightcap, E.S., Veiby, O.P., and Brugge, J.S. (2007). Functional role and oncogene-regulated expression of the BH3-only factor Bmf in mammary epithelial anoikis and morphogenesis. Proc Natl Acad Sci U S A *104*, 3787-3792.

Schwartz, M.A. (1997). Integrins, oncogenes, and anchorage independence. J Cell Biol *139*, 575-578.

Seluanov, A., Gorbunova, V., Falcovitz, A., Sigal, A., Milyavsky, M., Zurer, I., Shohat, G., Goldfinger, N., and Rotter, V. (2001). Change of the Death Pathway in Senescent Human Fibroblasts in Response to DNA Damage Is Caused by an Inability To Stabilize p53. Molecular and Cellular Biology *21*, 1552-1564.

Shaw, L.M., Rabinovitz, I., Wang, H.H.-F., Toker, A., and Mercurio, A.M. (1997). Activation of Phosphoinositide 3-OH by the alpha6beta4 integrin promotes carcinoma invasion. . Cell *91*, 949-960.

Sheng, Z., Li, L., Zhu, L.J., Smith, T.W., Demers, A., Ross, A.H., Moser, R.P., and Green, M.R. (2010). A genome-wide RNA interference screen reveals an essential CREB3L2-ATF5-MCL1 survival pathway in malignant glioma with therapeutic implications. Nat Med *16*, 671-677.

Shi, Y., Lan, F., Matson, C., Mulligan, P., Whetstine, J.R., Cole, P.A., Casero, R.A., and Shi, Y. (2004). Histone demethylation mediated by the nuclear amine oxidase homolog LSD1. Cell *119*, 941-953.

Silva, J., Mak, W., Zvetkova, I., Appanah, R., Nesterova, T.B., Webster, Z., Peters, A.H., Jenuwein, T., Otte, A.P., and Brockdorff, N. (2003). Establishment of histone h3 methylation on the inactive X chromosome requires transient recruitment of Eed-Enx1 polycomb group complexes. Dev Cell *4*, 481-495.

Silva, J.M., Li, M.Z., Chang, K., Ge, W., Golding, M.C., Rickles, R.J., Siolas, D., Hu, G., Paddison, P.J., Schlabach, M.R.*, et al.* (2005). Second-generation shRNA libraries covering the mouse and human genomes. Nat Genet *37*, 1281-1288.

Simpson, C.D., Anyiwe, K., and Schimmer, A.D. (2008). Anoikis resistance and tumor metastasis. Cancer Lett *272*, 177-185.

Simpson, C.D., Hurren, R., Kasimer, D., MacLean, N., Eberhard, Y., Ketela, T., Moffat, J., and Schimmer, A.D. (2012). A genome wide shRNA screen identifies alpha/beta hydrolase domain containing 4 (ABHD4) as a novel regulator of anoikis resistance. Apoptosis *17*, 666-678.

Snowden, A.W., Gregory, P.D., Case, C.C., and Pabo, C.O. (2002). Gene-Specific Targeting of H3K9 Methylation Is Sufficient for Initiating Repression In Vivo. Curr Biol *12*, 2159-2166.

Sorlie, T., Perou, C.M., Tibshirani, R., Aas, T., Geisler, S., Johnsen, H., Hastie, T., Eisen, M.B., van de Rijn, M., Jeffrey, S.S.*, et al.* (2001). Gene expression patterns of breast carcinomas distinguish tumor subclasses with clinical implications. Proc Natl Acad Sci U S A *98*, 10869-10874.

Sowter, H.M., Ratcliffe, P.J., Watson, P., Greenberg, A.H., and Harris, A.L. (2001). HIF-1-dependent regulation of hypoxic induction of the cell death factors BNIP3 and NIX in human tumors. Cancer Res *61*, 6669-6673.

Stich, H.F., and Emson, H.E. (1959). Aneuploid deoxyribonucleic acid content of human carcinomas. . Nature *184*, 290-291.

Tabaries, S., Dong, Z., Annis, M.G., Omeroglu, A., Pepin, F., Ouellet, V., Russo, C., Hassanain, M., Metrakos, P., Diaz, Z.*, et al.* (2011). Claudin-2 is selectively enriched in and promotes the formation of breast cancer liver metastases through engagement of integrin complexes. Oncogene *30*, 1318-1328.

Taipaleenmaki, H., Browne, G., Akech, J., Zustin, J., van Wijnen, A.J., Stein, J.L., Hesse, E., Stein, G.S., and Lian, J.B. (2015). Targeting of Runx2 by miR-135 and miR-203 Impairs Progression of Breast Cancer and Metastatic Bone Disease. Cancer Res *75*, 1433-1444.

Taube, M.E., Liu, X.W., Fridman, R., and Kim, H.R. (2006). TIMP-1 regulation of cell cycle in human breast epithelial cells via stabilization of p27(KIP1) protein. Oncogene *25*, 3041-3048.

TCGA (2011). The Cancer Genome Atlas - Invasive Breast Carcinoma Gene Expression Data (http://tcga-data.nci.nih.gov/tcga/).

Tomlinson, I.P.M., Roylance, R., and Houlston, R.S. (2001). Two hits revisited again. J Med Genet *38*, 81-85.

Trapnell, C., Roberts, A., Goff, L., Pertea, G., Kim, D., Kelley, D.R., Pimentel, H., Salzberg, S.L., Rinn, J.L., and Pachter, L. (2012). Differential gene and transcript expression analysis of RNA-seq experiments with TopHat and Cufflinks. Nat Protoc *7*, 562-578.

Tsukada, Y., Fang, J., Erdjument-Bromage, H., Warren, M.E., Borchers, C.H., Tempst, P., and Zhang, Y. (2006). Histone demethylation by a family of JmjC domain-containing proteins. Nature *439*, 811-816.

Vakoc, C.R., Mandat, S.A., Olenchock, B.A., and Blobel, G.A. (2005). Histone H3 lysine 9 methylation and HP1gamma are associated with transcription elongation through mammalian chromatin. Mol Cell *19*, 381-391.

Valentinis, B., Morrione, A., Peruzzi, F., Prisco, M., Reiss, K., and Baserga, R. (1999). Anti-apoptotic signaling of the IGF-1 receptor in fibroblasts following loss of matrix adhesion. Oncogene *18*, 1827-1836
.

van Groeningen, C.J., Levya, A., O'Brien, A.M.P., Gall, H.E., and Pinedo, H.M. (1986). Phase I and Pharmacokinetic Study of 5-Aza-2'-deoxycytidine (NSC 127716) in Cancer Patients. Cancer Res
46, 4831-4836.

Van Rechem, C., Black, J.C., Boukhali, M., Aryee, M.J., Graslund, S., Haas, W., Benes, C.H., and Whetstine, J.R. (2015). Lysine demethylase KDM4A associates with translation machinery and regulates protein synthesis. Cancer Discov *5*, 255-263.

Viticchie, G., Lena, A.M., Latina, A., Formosa, A., Gregersen, L.H., Lund, A.H., Bernardini, S., Mauriello, A., Miano, R., Spagnoli, L.G.*, et al.* (2011). MiR-203 controls proliferation, migration and invasive potential of prostate cancer cell lines. Cell Cycle *10*, 1121-1131.

Voisin, L., Julien, C., Duhamel, S., Gopalbhai, K., Claveau, I., Saba-El-Leil, M.K., Rodrigue-Gervais, I.G., Gaboury, L., Lamarre, D., Basik, M.*, et al.* (2008). Activation of MEK1 or MEK2 isoform is sufficient to fully transform intestinal epithelial cells and induce the formation of metastatic tumors. BMC Cancer *8*, 337.

Wajapeyee, N., Serra, R.W., Zhu, X., Mahalingam, M., and Green, M.R. (2008). Oncogenic BRAF induces senescence and apoptosis through pathways mediated by the secreted protein IGFBP7. Cell *132*, 363-374.

Wang, C., Wang, X., Liang, H., Wang, T., Yan, X., Cao, M., Wang, N., Zhang, S., Zen, K., Zhang, C.*, et al.* (2013). miR-203 inhibits cell proliferation and migration of lung cancer cells by targeting PKCalpha. PLoS One *8*, e73985.

Wang, C., Zheng, X., Shen, C., and Shi, Y. (2012). MicroRNA-203 suppresses cell proliferation and migration by targeting BIRC5 and LASP1 in human triple-negative breast cancer cells. J Exp Clin Cancer Res *31*, 58.

Wang, L., and Wang, J. (2012). MicroRNA-mediated breast cancer metastasis: from primary site to distant organs. Oncogene *31*, 2499-2511.

Ward, W.H., Cook, P.N., Slater, A.M., Davies, D.H., Holdgate, G.A., and Green, L.R. (1994). Epidermal growth factor receptor tyrosine kinase. Investigation of catalytic mechanism, structure-based searching and discovery of a potent inhibitor. Biochem Pharmacol *48*, 659-666.

Wee, E.J., Peters, K., Nair, S.S., Hulf, T., Stein, S., Wagner, S., Bailey, P., Lee, S.Y., Qu, W.J., Brewster, B.*, et al.* (2012). Mapping the regulatory sequences controlling 93 breast cancer-associated miRNA genes leads to the identification of two functional promoters of the Hsa-mir-200b cluster, methylation of which is associated with metastasis or hormone receptor status in advanced breast cancer. Oncogene *31*, 4182-4195.

Whelan, K.A., and Reginato, M.J. (2014). Surviving without oxygen: Hypoxia regulation of mammary morphogenesis and anoikis. Cell Cycle *10*, 2287-2294.

Willis, S.N.J., Fletcher, J.I., Kaufmann, T., van Delft, M.F., Chen, L., Czabotar, P.E., Ierino, H., Lee, E.F., Fairlie, W.D., Bouillet, P.*, et al.* (2007). Apoptosis initiated when BH3 ligands engage multiple Bcl-2 homologs, not Bax or Bak. Science *315*.

Wölfl, S., Han, Y., Chen, J., Zhao, X., Liang, C., Wang, Y., Sun, L., Jiang, Z., Zhang, Z., Yang, R.*, et al.* (2011). MicroRNA Expression Signatures of Bladder Cancer Revealed by Deep Sequencing. PLoS ONE *6*, e18286.

Xiang, Y., Zhu, Z., Han, G., Ye, X., Xu, B., Peng, Z., Ma, Y., Yu, Y., Lin, H., Chen, A.P.*, et al.* (2007). JARID1B is a histone H3 lysine 4 demethylase up-regulated in prostate cancer. Proc Natl Acad Sci U S A *104*, 19226-19231.

Xie, L., Gazin, C., Park, S.M., Zhu, L.J., Debily, M., Kittler, E.L.W., Zapp, M.L., Lapointe, D., Gobeil, S., Virbasius, C.M.*, et al.* (2012). A synthetic interaction screen identifies factors selectively required for proliferation and TERT transcription in p53-deficient human cancer cells. PLoS Genet.

XU, H.-S., ZONG, H.-L., SHANG, M., MING, X., ZHAO, J.-P., MA, C., and CAO, L. (2014). MiR-324-5p inhibits proliferation of glioma by target regulation of GLI1. Eur Rev Med Pharmacol Sci *18*, 828-832.

Yamane, K., Tateishi, K., Klose, R.J., Fang, J., Fabrizio, L.A., Erdjument-Bromage, H., Taylor-Papadimitriou, J., Tempst, P., and Zhang, Y. (2007). PLU-1 is an H3K4 demethylase involved in transcriptional repression and breast cancer cell proliferation. Mol Cell *25*, 801-812.

Yamane, K., Toumazou, C., Tsukada, Y., Erdjument-Bromage, H., Tempst, P., Wong, J., and Zhang, Y. (2006). JHDM2A, a JmjC-containing H3K9 demethylase, facilitates transcription activation by androgen receptor. Cell *125*, 483-495.

Yang, Y., Li, F., Saha, M.N., Abdi, J., Qiu, L., and Chang, H. (2015). miR-137 and miR-197 Induce Apoptosis and Suppress Tumorigenicity by Targeting MCL-1 in Multiple Myeloma. Clin Cancer Res *21*, 2399-2411.

Yi, R., Poy, M.N., Stoffel, M., and Fuchs, E. (2008). A skin microRNA promotes differentiation by repressing 'stemness'. Nature *452*, 225-229.

Yin, H., Song, P., Su, R., Yang, G., Dong, L., Luo, M., Wang, B., Gong, B., Liu, C., Song, W.*, et al.* (2016). DNA Methylation mediated down-regulating of MicroRNA-33b and its role in gastric cancer. Sci Rep *6*, 18824.

Yu, S.J., Hu, J.Y., Kuang, X.Y., Luo, J.M., Hou, Y.F., Di, G.H., Wu, J., Shen, Z.Z., Song, H.Y., and Shao, Z.M. (2013). MicroRNA-200a promotes anoikis resistance and metastasis by targeting YAP1 in human breast cancer. Clin Cancer Res *19*, 1389-1399.

Yu, X., Zhang, X., Dhakal, I.B., Beggs, M., Kadlubar, S., and Luo, D. (2012). Induction of cell proliferation and survival genes by estradiol-repressed microRNAs in breast cancer cells. . BMC Cancer *12*.

Yuan, Y., Zeng, Z.Y., Liu, X.H., Gong, D.J., Tao, J., Cheng, H.Z., and Huang, S.D. (2011). MicroRNA-203 inhibits cell proliferation by repressing deltaNp63 expression in human esophageal squamous cell carcinoma. BMC Cancer *11*, 1-10.

Zeng, Y., Yi, R., and Cullen, B.R. (2005). Recognition and cleavage of primary microRNA precursors by the nuclear processing enzyme Drosha. EMBO J *24*, 138-148.

Zhang, H., Kolb, F.A., Brondani, V., Billy, E., and Filipowicz, W. (2002). Human Dicer preferentially cleaves dsRNAs at their termini without a requirement for ATP. . EMBO J *21*, 5875-5885.

Zhang, L., Huang, J., Yang, N., Greshock, J., Megraw, M.S., Giannakakis, A., Liang, S., Naylor, T.L., Barchetti, A., Ward, M.R.*, et al.* (2006). microRNAs exhibit high frequency genomic alterations in human cancer. Proc Natl Acad Sci U S A *103*, 9136-9141.

Zhang, Y.F., Zhang, A.R., Zhang, B.C., Rao, Z.G., Gao, J.F., Lv, M.H., Wu, Y.Y., Wang, S.M., Wang, R.Q., and Fang, D.C. (2013). MiR-26a regulates cell cycle and anoikis of human esophageal adenocarcinoma cells through Rb1-E2F1 signaling pathway. Mol Biol Rep *40*, 1711-1720.

Zhang, Z., Vuori, K., Reed, J.C., and Ruoslahti, E. (1995). The alpha-5-beta-1 integrin supports survival of cells of fibronectin and up-regulates Bcl-2 expression. . Proc Natl Acad Sci U S A *92*, 6161-6165.

Zhang, Z., Zhang, B., Li, W., Fu, L., Fu, L., Zhu, Z., and Dong, J.T. (2011). Epigenetic Silencing of miR-203 Upregulates SNAI2 and Contributes to the Invasiveness of Malignant Breast Cancer Cells. Genes Cancer *2*, 782-791.

Zhao, H., Langerod, A., Ji, Y., Nowels, K.W., Nesland, J.M., Tibshirani, R., Bukholm, I.K., Karesen, R., Botstein, D., Borresen-Dale, A.L.*, et al.* (2004).

Different gene expression patterns in invasive lobular and ductal carcinomas of the breast. Mol Biol Cell *15*, 2523-2536.

Zhu, P., Tan, M.J., Huang, R.L., Tan, C.K., Chong, H.C., Pal, M., Lam, C.R., Boukamp, P., Pan, J.Y., Tan, S.H.*, et al.* (2011). Angiopoietin-like 4 protein elevates the prosurvival intracellular O2(-):H2O2 ratio and confers anoikis resistance to tumors. Cancer Cell *19*, 401-415.

Zhu, Z., Sanchez-Sweatman, O., Huang, X., Wiltrout, R., Khokha, R., Zhao, Q., and Gorelik, E. (2001). Anoikis and metastatic potential of cloudman S91 melanoma cells. Cancer Res *61*, 1707-1716.